Design and Development of a Novel Electrohydraulic Servovalve Configuration

Amit M. Limaye

A Thesis

in

The Department

of

Mechanical Engineering

Presented in Partial Fulfillment of the Requirements
for the Degree of Master of Engineering at
Concordia University
Montréal, Québec, Canada

February 1985

ABSTRACT

Design and Development of a Novel Electrohydraulic Servovalve Configuration

Amit M. Limaye

In this thesis, a novel electrohydraulic servovalve configuration is presented. In this configuration, the drain line is connected to the tank through a direction control valve, a metering valve and a relief valve, which allows external control over the drain orifice and the back pressure.

The servosystems with the conventional servovalve and the new servovalve configuration are modelled and simulated for step inputs for various values of parameters. The simulation results showed that the servosystem with this new configuration exhibits a higher steady state velocity, a lower percent overshoot and a lower settling time than the servosystem with the conventional servovalve, if the orifice opening and the back pressure are properly tuned.

A test bench basically consisting of a hydraulic power supply, a linear actuator, a loading table and a

velocity feedback transducer is developed and fully instrumented to test both the servovalve configurations. The servosystems with these two configurations are tested under same conditions, as in simulation. The experimental results confirmed that the new servovalve configuration offers better steady state and transient performance if the back pressure and the orifice opening are properly adjusted.

The mathematical models of the servosystems are used to evaluate the performance of both the servovalve configurations for four sets of system parameters. From these results, it is seen that for all the four sets, the new servovalve configuration offers a higher steady state velocity, lower percent overshoot and a lower settling time, if the ratio of the orifice opening to the steady state servovalve opening ranges from 1.5 to 3 and the ratio of the back pressure to the supply pressure is less than 0.2. This zone is termed as an 'operating zone'. A design procedure is provided to compute the values of the parameters for the new servovalve to operate in this 'operating zone'.

ACKNOWLEDGEMENTS

The author would like to express his gratitude and deep appreciation to his supervisors Dr. R.M.H. Cheng and Dr. S.LeQuoc for initiating this project, their guidance and encouragement in all phases of this research work.

The author also highly appreciates the technical assistance and numerous suggestions given by Mr. Wesley Fitch throughout this research work. Special thanks to Mr. K. Leung who was of invaluable assistance in the final phase of this thesis work.

The technical support of Mr. E.Heasman, Mr. J.Elliot and other technical staff is also highly appreciated. Special thanks to Mr. J.Seeger, who helped in developing the hydraulic test rig.

The technical advice and help of Mr. N.Krouglicof and Mr. P.Favreau is highly appreciated. The cooperation given by the colleagues in the Center for Industrial Controls is also appreciated.

Thanks also go to Mrs. C.Nadeau and Mrs. L. Palazzo for their help in typing.

The facilities provided by the Center for Industrial Controls of Concordia University to carry out this work are

also acknowledged.

The funding for this project was provided by Natural Sciences and Engineering Research Council of Canada under operating grants A 8662 and A 1718.

TABLE OF CONTENTS

PAGE

PAGE

LIST OF TABLES

LIST OF FIGURES

PAGE

NOMENCLATURE

A	=	piston are, double ended piston	,in^2
$A_{1,2}$	=	piston areas, single ended piston	,in^2
A_0	=	orifice opening	,in^2
A_v	=	servovalve opening	,in^2
A^*	=	normalized area ratio	,-
B	=	viscous damping coefficient	,lbf/in/sec
C_d	=	flow discahrge coefficient	,-
C_l	=	leakage coefficient	,in^5/lbf sec
C_t	=	total leakage coefficient	,in^5/lbf sec
F_c	=	coulomb friction	,lbf
F_s	=	coulomb friction when stationary	,lbf
F_d	=	coulomb friction when in motion	,lbf
F_v	=	viscous friction	,lbf sec/in
F_f	=	frictional force	,lbf
F	=	actuator force	,lbf
F_{max}	=	maximum actuator force	,lbf
I	=	servovalve current	,mA
K	=	spring stiffness	,lbf/in
K_a	=	servovalve amplifier gain	,mA/V
K_f	=	feedback gain	,V sec/in
K_v	=	servovalve area constant	,in^2/in
K_x	=	servovalve torque motor constant	,m/mA
$P_{1,2}$	=	pressures in actuator chambers	,psi
P_s	=	supply pressure	,psi

P_r	=	relief valve setting pressure	,psi
$Q_{1,2}$	=	flow rate in/out of the actuator	,in^3/sec
Q_s	=	maximum supply flow	,in^3/sec
Q_l	=	leakage flow	,in^3/sec
s	=	Laplace operator	,-
t	=	time	,sec
t_d	=	delay of direction control valve	,sec
T^*	=	Normalised settling time	,-
T_c	=	Settling time using the conventional servovalve	,sec
T_n	=	Settling time using the new servovalve	,sec
$v_{1,2}$	=	volume of oil under compression	,in^3
V^*	=	Normalised steady state velocity	,-
V_c	=	Steady state velocity using the conventional servovalve	,in/sec
V_n	=	Steady state velocity using the new servovalve	,in/sec
V_i	=	input command	,V
$V_{i1,2}$	=	input commands	,V
V_f	=	feedback voltage	,V
$V_{1,2}$	=	supply voltages	,V
V_{ref}	=	reference input command	,V
V	=	load velocity	,in/sec
V_{max}	=	maximum load velocity	,in/sec
V_0	=	reference velocity	,in/sec
X	=	load displacement	,in

β	=	bulk modulus of fluid	,psi
δ^*	=	normalized percentage overshoot	,-
δ_n	=	percentage overshoot using the new servovalve	,-
δ_c	=	percentage overshoot using the conventional servovalve	,-
ξ	=	system damping	,-
τ_v	=	servovalve time constant	,sec
ω	=	frequency of input command	,rad/sec
ω_n	=	system natural frequency	,rad/sec

DIMENSIONLESS QUANTITIES

z_0	=	restrictor opening
z_v	=	Servovalve opening
z_i	=	Servovalve opening (i=1,4)
p_r	=	pressure relief valve setting
$p_{1,2}$	=	pressure in actuator chambers
$q_{1,2}$	=	flow rate in/out of actuator
λ	=	actuator force
ϕ	=	actuator velocity

CHAPTER 1

INTRODUCTION

1.1 GENERAL

Fluid power control is the transmission and control of energy by means of a pressurised fluid. The growth of fluid power control has accelerated where precise control of motion is desired and weight and space are limited. The high power to weight ratio makes hydraulic servomechanisms the most ideal means of control. The demand to achieve more accurate and faster controls at higher power levels is achieved by using hydraulic servomechanisms along with the electrical signal processing which led to electrohydraulic servomechanisms. These electrohydraulic servomechanisms employing valve controlled ram have found a widespread use in systems of automation, aircraft and missile controls, earth moving equipment control, simulation and training systems etc. The key element in the system is the electrohydraulic servovalve. With a power gain of 10^4 to 10^6, the servovalve serves as a very effective forward loop amplifier as well as an electrical to hydraulic transducer.

1.2 HISTORICAL DEVELOPMENT OF SERVOVALVE [1]

The earliest contribution to hydraulics dates back to early Greek and Roman civilizations. During the 18th century industrial revolution many inventions were made which are the essential components of the present electrohydraulic servovlave. During the 19th century and the begining of the 20th century, the technology of servomechanisms was limited to mechanical and hydromechanical devices. During the period prior and later to world war II, several significant developments were made in controls and in signal transmission. These led to the development of a valve using jet pipe principle.

By the year 1945, a servovalve was essentially a sliding spool moving inside a sleeve to meter the flow. The spool was driven by a direct acting motor usually a DC solenoid. Proportional control was achieved by causing the solenoid to act against a spring and varying the motor current to cause a change in position, forming a single stage valve. Single stage valves have limitations such as limited power and flow capability. They also pose stability problems in some applications. Two stage valves have a first stage which works as a hydraulic preamplifier and the second as a metering device. Because the function of power amplification and flow control is done in two different stages, they eliminate both the limitations of single stage

valves. By 1946, Tinsley of England patented the first two stage valve, which used a direct acting solenoid to drive the spool in first stage and differential pressure to drive the second stage. This was improved by Raytheon of Bell aircraft who developed two stage valves that implemented direct mechanical feedback from second to first stage. About the same time, two important developments were done at Massachusetts Institute of Technology. The first was a use of a torque motor instead of solenoid, which resulted in significant power saving and improvement in linearity. The second was an introduction of electrical feedback between two stages, which improved the valve static characteristics by reducing friction in the first stage.

In 1950, W.C.Moog developed the first two stage servevalve using frictionless pilot stage. He used a flapper-nozzle variable orifice in conjunction with a fixed orifice to drive the second stage. The flapper-nozzle valve was driven by a torque motor and spool position was achieved by a spring acting directly on the spool. Such arrangement gave an appreciable reduction in valve threshold and a high dynamic response because of the lower mass at the first stage. The use of mechanical force feedback in a two stage valve was pioneered by Carson in 1953. By combining the frictionless first stage with mechanical feedback from the second stage, he was able to improve threshold and dynamic response. By introducing a double symmetrical orifice bridge, Moog was able to reduce the null offset caused by enviromental

changes. These were the major developments achieved till late 1950's which led to the present form of electrohydraulic servovalve configuration.

Throughout this period, a number of other devices were developed. Some of these include: servovalves with dynamically shaped pressure feedback, three stage servovalves etc. Presently the efforts are directed to meet the demands of industry. The demand to automate a high power process control, such as die casting, has necessitated replacement of present servovalve by a servovalve with higher flow and pressure capacities. Also the need for better response in radar drives and laser pointers have also posed greater challange in developing servovalve with superior frequency response.

1.3 TYPES OF SERVOVALVES

There are different types [2] of servovalves available in practice. The types, their principle of operation and typical characteristics are explained below. The nomenclature used to describe the transfer functions of these types of valves is valid only for this section.

1) Flow control servovalve:

This is a very basic servovalve in which the control

flow at constant load is proportional to the input current. Flow from these servovalves is influenced by changing load pressure as indicated in Fig. 1.1 [2].

For the null stability considerations, the region shown in the plot is very critical. The change in flow gain at null can cause poor positioning accuracy and system instability at low amplitude input signals. This situation can be improved by providing a nominal underlap between the spool and the sleeve. The dynamic response of flow control

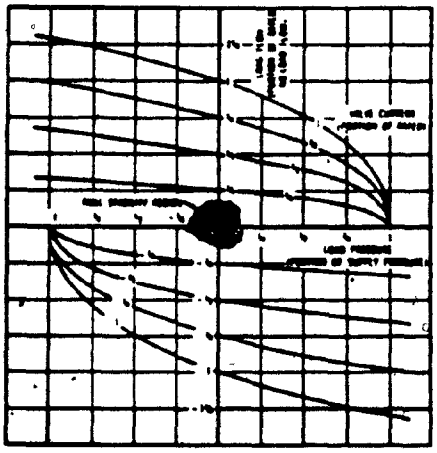

Fig. 1.1. Flow-Pressure Characteristics of Flow Control Servovalves [2]

servovalves is generally expressed by a second order transfer function as given below.

$$\frac{Q}{I} = K\left[\frac{1}{1 + \left(\frac{2\xi}{\omega_n}\right)s + \left(\frac{s}{\omega_n}\right)^2}\right] \qquad (1.1)$$

where,

K = servovalve static flow gain at zero load pressure drop, $in^3/sec/mA$

ξ = dampingratio, non dimensional

ω_n = natural frequency, rad/sec

Q = output load flow, in^3/sec

I = input current, mA

2)Pressure control servovalves

These servovalves provide a differential pressure output in response to the electric input current. The static flow-pressure curves for a typical pressure control servovalve are shown in Fig. 1.2 [2]. It can be seen from this Figure that the reduction in controlled pressure with the load flow is small.The second order transfer function of pressure control servovalves is given by,

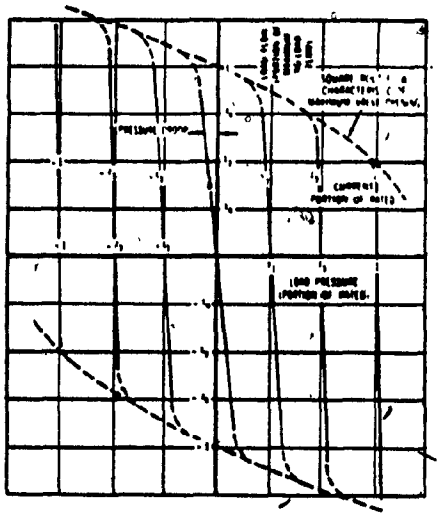

Fig. 1.2. Flow-Pressure Characteristics of Pressure Control Servovalves [2]

$$\frac{P}{I} = K_1 \left[\frac{1}{1 + \left(\frac{2\xi}{\omega_n}\right) s + \left(\frac{s}{\omega_n}\right)^2} \right] \qquad (1.2)$$

where,

K_1 = pressure control servovalve static gain, $in^3/sec/mA$

P = servovalve differential output, psi

3) Pressure-flow control servovalves:

These servovalves combine the functions of the pressure and flow control giving effective damping in highly resonant loaded servo systems. The flow from these valves is determined by the electrical input signal and the load pressure. This types of valves exhibit a linear relationship between flow, current and pressure as shown Fig. 1.3 [2]. The applications of this type of valves are limited to the cases which require this particular flow-pressure characteristics.

The dynamic performance of these valves can be expressed as

$$Q = (K_1 I - K_2 P) \left[\frac{1}{1 + \frac{s}{\omega_n}} \right]^2 \qquad (1.3)$$

where,

K_1 = servovalve sensitivity to input current,

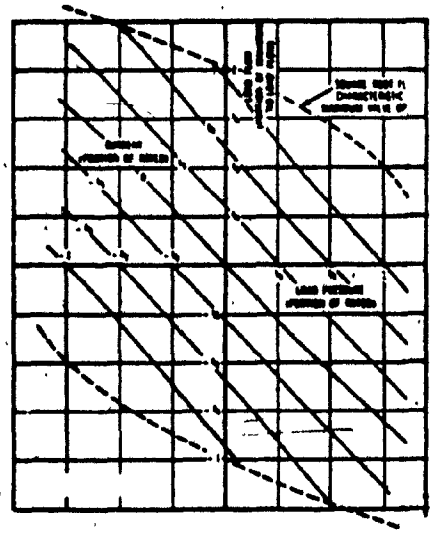

Fig. 1.3. Flow-Pressure Characteristics of Pressure-Flow Control Servovalves [2]

$in^3/sec/mA$

K_2 = servovalve sensitivity to load pressure, $in^3/sec/psi$

ω_n = natural frequency, rad/sec

4) Dynamic pressure feedback servovalves:

This type of servovalves function as the pressure control servovalves under dynamic conditions and as the flow control servovalves under steady state conditions. Therefore, in dynamic conditions, they provide a high damping for resonant loads and in steady state they provide a high resolution and stiffness. These servovalves are used in applications where increase in damping of the valve actuator combination is desired.

The dynamic performance of this type of servovalves is represented by

$$Q = \left[K_1 I - K_2 \left(\frac{\tau s}{1+\tau s}\right) P\right] \left[\frac{1}{1 + \frac{s}{\omega_n}}\right]^2 \qquad (1.4)$$

where,

τ = time constant of the built-in dynamic pressure feedback filter, sec

ω_n = equivalent natural frequency, rad/sec

It can be seen that the term $\left[\frac{\tau s}{1+\tau s}\right]$

associated with the pressure term gives the dynamic pressure feedback. A longer time constant τ, gives more effective pressure feedback and hence more system damping.

5) Static load error washout servovalves:

This type basically is an extension of the pressure feedback type technique. In pressure-flow servovalves, the pressure feedback is proportional to the load pressure and therefore it acts for static as well as dynamic load forces. This causes variation of actuator position proportional to the load force in steady state. In static load error washout servovalves, an additional positive pressure feedback with a low pass filter is used to correct for postion error in static conditions.

The transfer function for this type is given by

$$Q = \left[K_1 I - \left(K_2 - \frac{K_3}{1+\tau s}\right) P\right] \left[\frac{1}{1 + \frac{s}{\omega_n}}\right]^2 \qquad (1.5)$$

where,

K_1 = flow sensitivity to current $in^3/sec/mA$

K_2 = proportional pressure feedback sensitivity, $in^3/sec/psi$

K_3 = positive pressure feedback sensitivity,

$in^3/sec/psi$

τ = time constant of the low pass built-in dynamic pressure feedback filter, sec

ω_n = equivalent natural frequency of the servovalve, rad/sec.

As can be seen from the above relation, the term K_2P provides the negative pressure feedback and thus the damping and the term $\left[\frac{K_3}{1+\tau s}\right] P$, gives the positive pressure feedback acting as a low pass filter. Normally K_2 is set to give desired load damping and K_3 is set in order to correct for load position errors.

6) Acceleration switching servovalves:

In this type of servovalves, the proportional input current is replaced by an alternating switching action. This technique is also known as pulse width modulation. The net flow is produced by control of relative on and off time durations. The transfer function for this type of servovalves is given by,

$$\left(\frac{Q}{I_t}\right) = \left(\frac{K}{s}\right) \qquad (1.6)$$

where,

K = acceleration switching servovalve gain,

in^3/sec/time imbalance

I_t = time imbalance of the current input, dimensionless.

The net flow Q through the servovalve depends on the time unbalance of the current. The advantages of this type of servovalves are relaxed tolerance, higher reliability in adverse enviroments and low cost. However, their use in practice is limited because of the fact that they are succeptible to exhibit limit cycle oscillations [3] which may not be accepted in most of the cases.

1.4 APPLICATIONS OF ELECTROHYDRAULIC SERVOVALVES

Electrohydraulic servovalves are used in a wide range of applications. In aerospace, they are used in radar drives, control for missile launchers, flight controls because of their high power to weight ratio and accuracy. In industrial applications, they are extensively used in NC and CNC machines because of the rigidity and accuracy of these drives. Fig. 1.4a,b [1] gives the spectrum of the industrial and aerospace applications.

Many authors have used electrohydraulic servosystems for their research applications. Kearney et al [4] used electrohydraulic servosystem to test the reflex of human vertibulospinal system which is thought to influence the postural control. In a recent design of 4 wheel drive

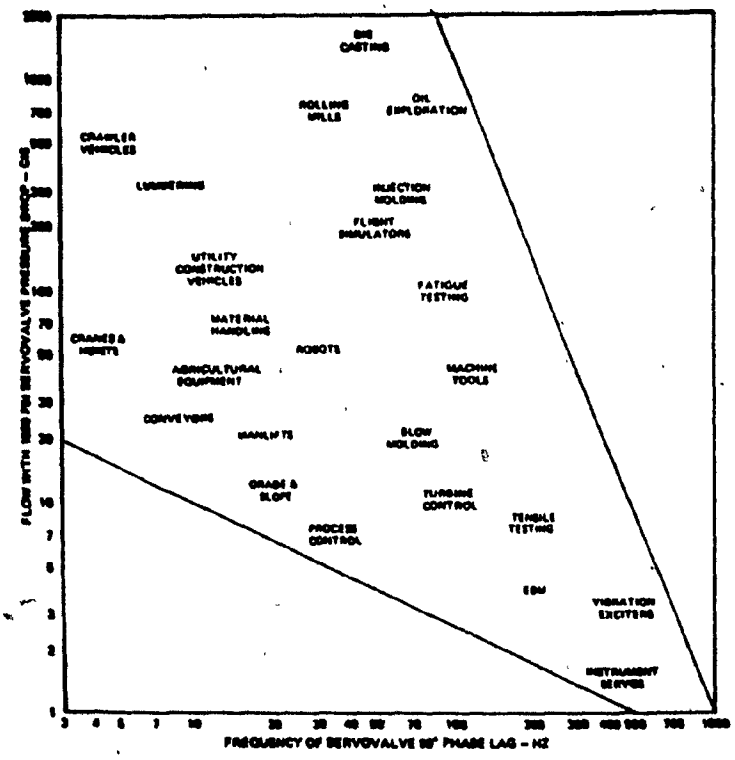

(a) Industrial

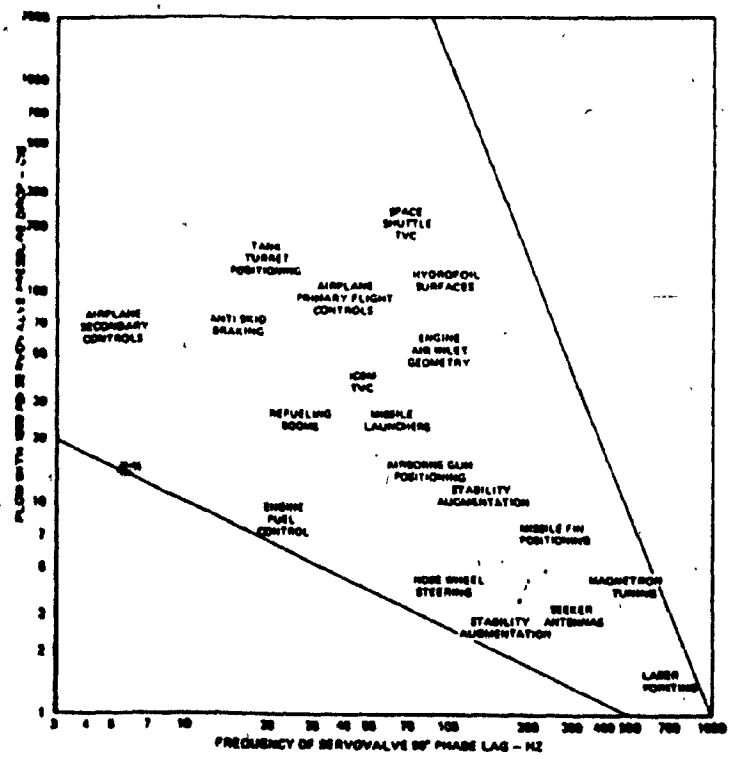

(b) Aerospace

Fig. 1.4. Applications of Hydraulic Servomechanisms

tractors, Lourigan [5] has proposed electrohydraulic servosystem for smooth and accurate response. Stikeleather and Suggs [6] have proposed the use of electrohydraulics for their active suspension system. In order to study the prosthetic arm, Broome [7] used a hydraulic servo to achieve quick response of flexibly coupled loads. Lu et al [8] successfully developed an electrohydraulic servosystem to evaluate the dynamic behaviour of piles under cyclic loads. For a high speed train, the problem of current collection from an overhead contact wire through pantograph was effectively solved by Vinayagalingam [9] using hydraulic servo.

1.5 LITERATURE SURVEY

1.5.1 On the characteristics of the valves

Various researchers have studied the basic flow control servovalve characteristics from different aspects. Vilenius and Vivaldo [10] studied the effect of nonlinearities on the dynamic characteristics of electrohydraulic servovalves. They included the nonlinearities in flow rate and flow force characterictics and simulated the mathematical model. By carrying out experiments, they proved the validity of the model. Martin and Burroughs [11] modelled the servovalve in two different ways and simulated an electrohydraulic position control system to compare the simulation with the experimental

results. They proved that the second order valve model provides a good correlation with the experimental system upto 35 Hz. Montgomery and Lichtarowicz [12] used nondimensionlised model to examine the effect of spool valve lap on operation of hydraulic servosystems.The analytical and experimental results showed that underlap improves valve stability and the most stable system is obtained with exhaust underlap and supply zero lap; or exhaust zero lap and supply underlap; whereas zero lap is the worst in relation to stability. Kaneko [13] studied pressure control servovalves and successfully established a method of designing these valves. Cheng, LeQuoc and Limaye [14], [15] presented an entirely new concept of electrohydraulic servovalve. The new electrohydraulic servovalve combines a metering valve, a relief valve and a direction control valve in addition to the conventional servovalve. The novelty lies in the fact that the metering orifice and the back pressure could be tuned to give a higher steady state velocity and higher damping than the conventional servovalve.

1.5.2 On the characteristics of servosystems

Considerable amount of work has been done to determine the performance of the servosystems . Asymmetric or single rod actuators which are widely used in open loop systems have the advantage of being more compact and less expensive. Watton [16] studied the effect of this asymmetric

condition on the system response. He concluded that under certain conditions the transient response in either direction is same. In some cases, however, he observed severe oscillations in velocity response. Leburn and Scavarda [17] considered the nonlinearities such as hysteresis at the torque motor and coulomb friction in the actuator in their design of electrohydraulic exciter. They showed that the model considering these nonlinearities favourably agrees with the experimental results. Shearer [18] and Parnaby [19] studied the effect of coulomb friction in hydraulic servosystems. Shearer modelled valve controlled ram including coulomb friction and showed a close correlation between experimental and analytical results. He found that alternate ramp input reveals the best picture of the system behaviour with high coulomb friction. However, at high feedback gains he observed violent limit cycle oscillations. Paranby used describing function technique to analyse the coulomb friction and predicted stability boundaries analytically which compared favourably with the experimental results. He showed that reduction in loop gain, increase in system damping and application of dither are the effective means to avoid limit cycle oscillations.

A technique of sensitivity analysis was applied to position control system by Vilenius [20]. He proved, both analytically and experimentally, that the parameter sensitivity of position control system depends strongly on deadband nonlinearity of servovalve whereas viscous

friction and leakage are quite insensitive. Young and Saggs [21] employed a lead compensating network to improve the resonant frequency for a position control system. Houzong [22] used a PID network to improve the stability of electro hydraulic servosystem used for revolving arm of an industrial robot.

1.5.3 Present techniques of simulation of servosystems:

As the need for steady state as well as dynamic simulation of hydraulic system performance is realised before developing a system, many computer packages have been developed. Bowns et al [23], [24] have developed a Fortran based General Hydraulic Simulation Program package (G.H.S.P) which allows an engineer to simulate a hydraulic system with little knowledge of computers. It provides a library of models with a facility to change the models whenever necessary. This package uses Gear's method which is especially used for solution of stiff differential equations. However, because of the limitations of the Gear's method, this package can not effectively solve the discontinuities such as direction change of a direction control valve, cracking of a relief valve etc.

Kinoglu et al [25] have described an integrated approach in designing and analysing hydraulic systems using

CD/2000 Computer Aided Design and drafting software and the Advanced Fluid System Simulation (AFSS) codes. The AFSS programs contain Steady State (SSFAN), Transient (HYTRAN), Frequency (HSFR) and Thermal (HYTTHA) response programs which were originally developed by McDonell Douglas Corp. This integrated approach provides a symbol library, graphics programs and engineering data base in addition to the AFSS codes.

An interactive graphics program for Computer Aided Design of electrohydraulic control systems, has been developed by General Motors Research Laboratory [26]. A designer is required to input system constants such as load, damping coefficient etc. and the PID controller gains. The transient response can either be seen on the screen or plotted on a printer. The controller setting and other parameters can be adjusted till the desired response is achieved.

I.5.4 Use of microprocessors in servosystems

In many applications, control strategy is required to be changed as the output requirement is changed. Since the microprocessors are extremely flexible in terms of programming and therefore, in change of control strategy, they are extensively used as a controller in many applications. Maskrey [27] has proposed the use of microprocessors in electrohydraulic servosystems as an

element in closing the loop, as a pre loop processor or as an adaptive controller. He has also proposed its use in redundant controls which are common in space vehicles and aircrafts. Shetty and Copeland [28] have recommended the use of microprocessors in electrohydraulic copying systems, since use of microprocessors simplifies the programming job.

1.5.5 On the velocity control requirement of machine tools

Bell and Cowan [29] examined the requirements of machine tool feed drives which need good dynamic response, dynamic and static stiffness, fast traversing speed etc. They found that severe step conditions as in case of high speed motors pose danger of cavitation in both sides of the motor ports. They also showed that the stabilization of velocity loop is achieved by using a transitional lag in the network.

1.5.6 Work done on relief valves

Some work is also done on relief valve static and dynamic characteristics, its effect on the response of a hydraulic control system etc. Steber [30] made an attempt to simulate a pressure relief valve on an analog computer. He noted that it is difficult to analyse the transient fluid flow situations e.g. when a relief valve cracks open.

Iyengar [31] studied the effect of fluid contamination on the static and dynamic characteristics on different makes of compound relief valves. He deduced that the valves show some hysteresis and exhibit limit cycle oscillations in some cases. He also proved that uniform wear of poppets does not affect the performance of the valves but the pitting of the pilot or main poppet leads to undesirable characteristics. Chong and Dransfield [32] investigated the dynamic response of an inertia loaded system using different pressure relief valves. By experimental investigations, they showed that the variation in system response because of choice of relief valve is more prominent at low pressure settings only and that the relief valve can be represented by steady state flow-pressure characteristics if its dynamics is approximately 50 times faster than the system dynamics.

1.6 OBJECTIVE OF THE RESEARCH WORK

This research work is devoted to the development of a new servovalve configuration. First, based on the steady state and transient velocity characteristics of a test data [34], a new servovalve block is thought of. An experimental rig is designed and developed in the Center for Industrial Controls at Concordia University to carry out experiments on the conventional and the new servovalve. The servosystems with the conventional and new servovalve configurations are mathematically modelled and simulated using VAX 11/780

digital computer and the behaviour of the two configurations is predicted. Experiments are carried out in order to prove the validity of the model. Then, based on some simulation results, an operating zone is established in which the new servovalve configuration gives a higher steady state velocity, lower % overshoot and lower settling time than the conventional servovalve.

The thesis is divided into eight chapters. The first chapter briefly describes historical development of hydraulic servomechanisms and their applications. It reviews the previous work that has been done on different aspects of the electrohydraulic servo systems.

The second chapter gives description of a typical servosystem used in practice. Further it gives the classification and development of a new circuit. Finally it suggests a modular servovalve block consisting of direction control valve, metering valve and relief valve in addition to the conventional servovalve.

In the third chapter, dimensionless parameters are defined. A steady state analysis of servosystems with both the configurations is done. From these characteristics, a condition is derived for the new servovalve to achieve higher steady state velocity than the conventional servovalve. The effects of back pressure and orifice area on the steady state velocity are studied and some conclusions

are drawn.

The fourth chapter covers mathematical modelling of the two servosystems and depicts simulation results for two-step and square wave input for different gains and inertial loads in case of the conventional servovalve. For the same conditions of inputs, the circuit with the new servovalve is simulated for various metering areas and back pressures. Finally, comparison of these results is done and conclusions are drawn.

The fifth chapter describes the design and working of the test rig. It includes the experimental results carried under same set of input and test conditions used in simulation. Finally experimental results of the two servovalves are compared and conclusions are drawn.

In the sixth chapter, the simulation and experimental results are compared in order to see the validity of the mathematical model.

In the seventh chapter, the performance of the two servovalves is tested for four sets of system parameters. Based on these simulation results, an operating zone is established in which the new servovalve offers higher steady state velocity, lower % overshoot and lower settling time than the conventional servovalve.

The eighth chapter gives the highlights of the research work and some suggestions for the future work.

CHAPTER 2

ELECTROHYDRAULIC SERVOSYSTEMS

2.1 INTRODUCTION

In the previous chapter, the historical development of the electrohydraulic servovalves and their applications have been discussed. The work done by several researchers covering different aspects of servosystems has been included. Later, the objective of the research has been stated.

In this chapter, section (2.2) describes the operation of a typical servomechanism which is used in power steering of an automobile. Then, based on the number and the type of control elements used, the hydraulic servosystems are classified in different classes and groups in section (2.3). Section (2.4) covers the development of a new type of circuit in which the back pressure and the return orifice can be tuned. Finally in section (2.5), the modular form of new servovalve configuration consisting of a direction control valve, a metering valve, and a relief valve in addition to the conventional servovalve is discussed.

2.2 OPERATION OF A TYPICAL HYDRAULIC SERVOMECHANISM

The principle of operation of hydraulic servomechanism can be explained by referring to Fig. 2.1 [33] which shows a schematic diagram of an automobile power steering system. The basic components used in servosystems are a servovalve, a pump, an actuator and a feedback element.

The rotation of the steering wheel 1 drives a screw which displaces the spool 2 with respect to the sleeve. This alters the amount of port opening of the valve in such a way that a net quantity of oil is delivered to the actuator 3, thus moving the piston against the external load at the wheels 4. The feedback link 5 transmits the motion of the piston rod to the sleeve of the valve and ensures that the displacement of actuator accurately matches with that of the valve spool. A small force is required to move the spool with respect to the sleeve but a large force is developed at the actuator to overcome the load.

In the previous example of the positional servomechanism, the feedback element is mechanical and the feedback ratio is one. However, different input-output and feedback forms are possible. In a mechanical system, the input or feedback could be amplified by introducing a lever mechanism thus, giving a certain leverage ratio. In an electrohydraulic servosystem, the input has to be electrical. The output element could either be a linear or a

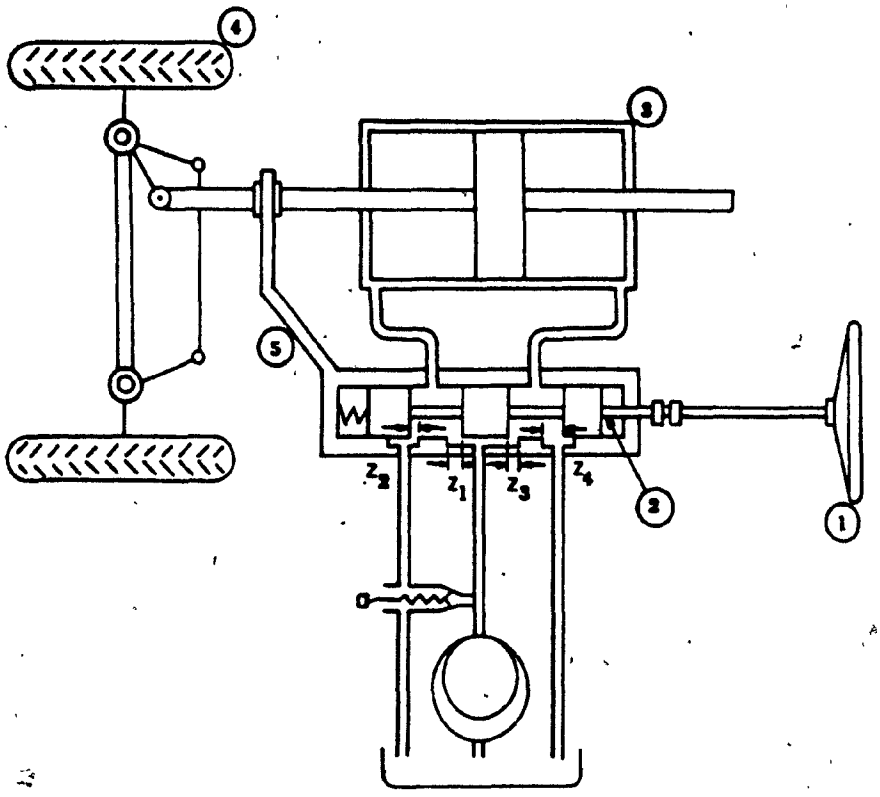

Fig. 2.1. A Schematic of an Automobile Power Steering System

rotary actuator. Also depending upon the type of servocontrol desired, the feedback element could be a position, a velocity, an acceleration or a force transducer.

2.3 STRUCTURAL CLASSIFICATION OF SERVOMECHANISMS

Tumarkin [33] studied the hydraulic servomechanisms on the basis of structural analysis. The objective of this analysis was to ascertain possible connections between elements so as to predict new circuits with special properties and characteristics. He used a technique of nondimensional analysis to compare the steady state velocity characteristics of different circuits. However, he did not cover the transient analysis of the different circuits under investigation.

The servomechanism as shown in Fig. 2.1 having apertures Z_1-Z_4 can be represented by Fig.2.2 [33] where all the four apertures are varied as the spool is moved. The ports Z_1 and Z_3 are connected to the supply side and the ports Z_2 and Z_4 are connected to the drain side. Depending on the nature of control used, basically 3 types of connections can be defined viz. controlled, constant and variable. Controlled connections are operated or varied by the input signal, e.g. opening of a servovalve is a controlled connection since it changes with the input signal. Constant connections are provided by elements such as a flow control valve whose opening does not change with

the input signal but has to be set externally. Variable connections can alter their opening with some of the system parameters (such as pressure on one side of actuator) but are not directly varied by the the input signal. Considering the controlled elements, basically 3 types of circuits are possible. Figs.2.3 a,b,c [33] respectively show these possible circuits with uncontrolled supply, uncontrolled discharge and uncontrolled actuator chambers.

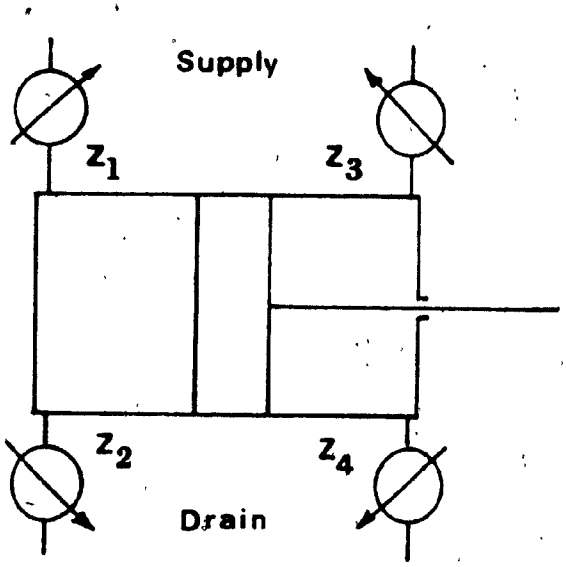

Fig. 2.2. Structural Form of Automobile Power Steering

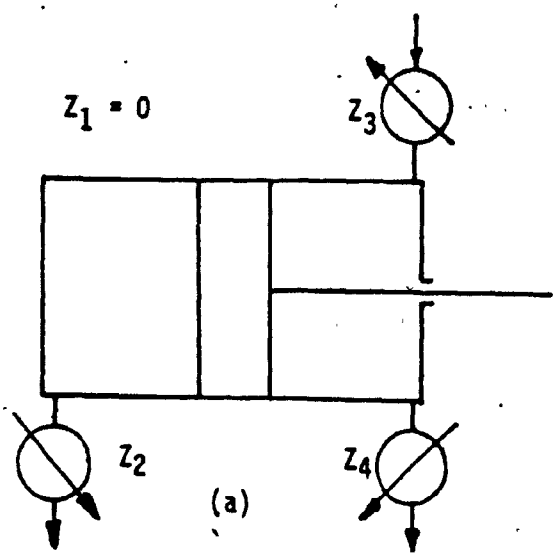

Uncontrolled Supply

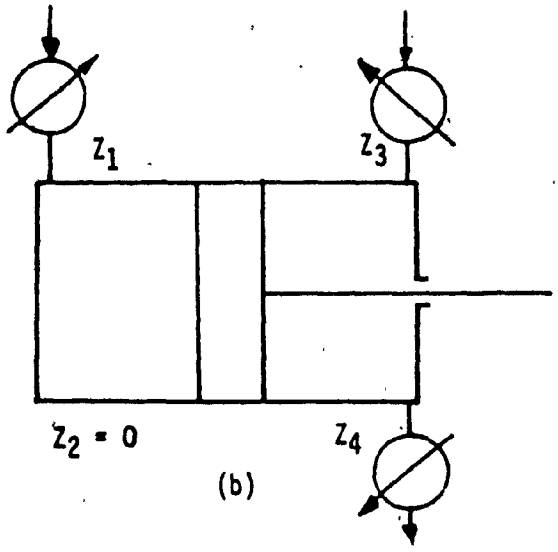

Uncontrolled Discharge

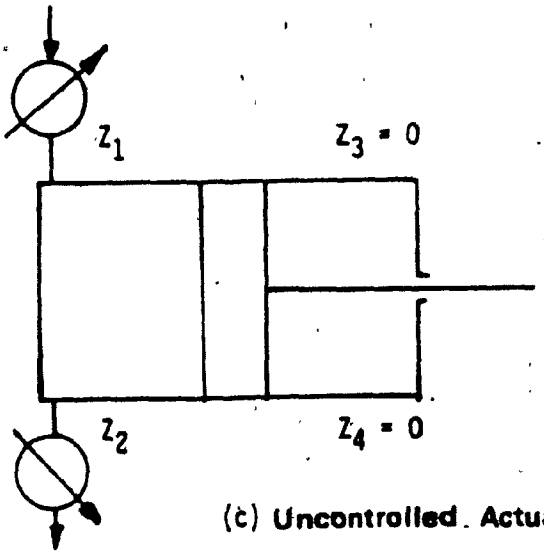

(c) Uncontrolled Actuator Chamber

Fig. 2.3. Methods of System Synthesis

Depending on the number of controlled elements, the circuits can be divided into 9 classes as shown in Table 2.1

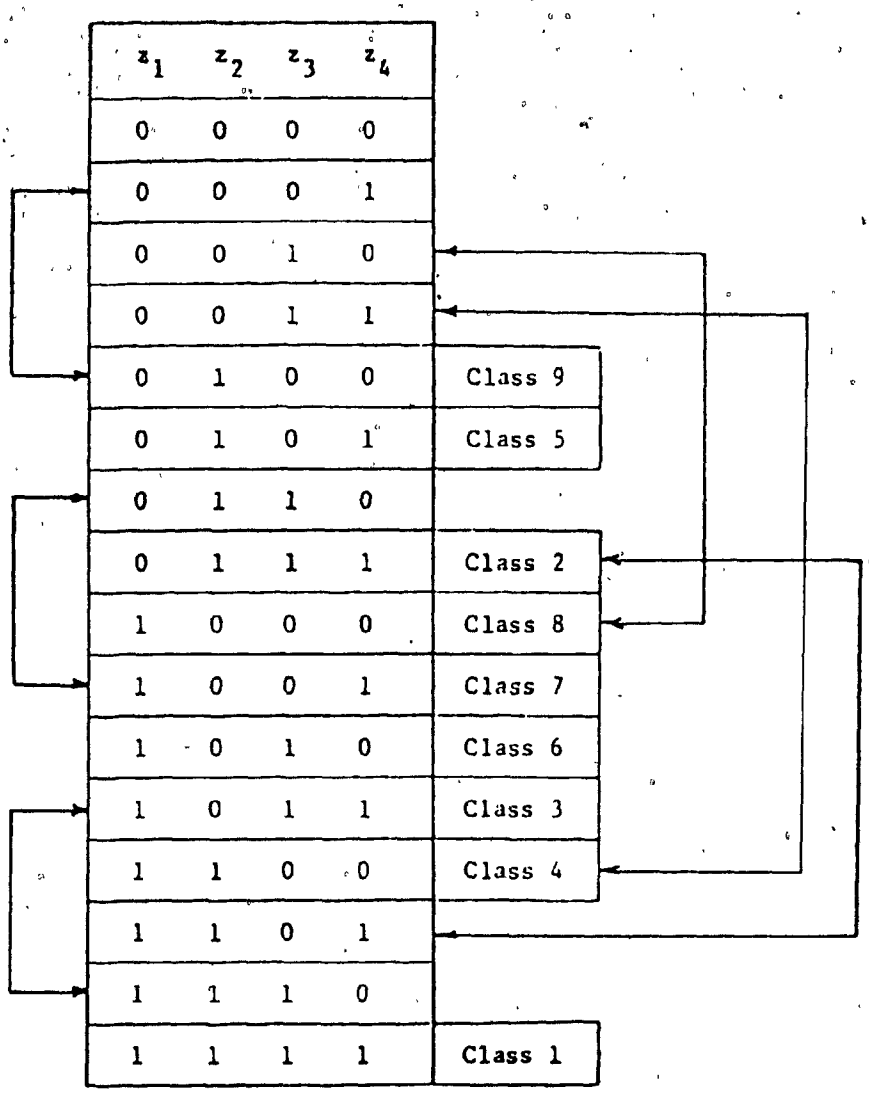

z_1	z_2	z_3	z_4	
0	0	0	0	
0	0	0	1	
0	0	1	0	
0	0	1	1	
0	1	0	0	Class 9
0	1	0	1	Class 5
0	1	1	0	
0	1	1	1	Class 2
1	0	0	0	Class 8
1	0	0	1	Class 7
1	0	1	0	Class 6
1	0	1	1	Class 3
1	1	0	0	Class 4
1	1	0	1	
1	1	1	0	
1	1	1	1	Class 1

Table 2.1. Formation of Different Classes of Hydraulic Servomechanisms

As already explained, Z_1 and Z_3 are connected to pressure side and Z_2 and Z_4 are connected to drain side.

A '0' (zero) entry in the table implies that it is not a controlled element and a '1' (one) entry implies that it is a controlled element, e.g. class 2 is represented by ' 0,1,1,1 ' (or ' 1,1,0,1 ') and the notation ' 0,1,1,1 ' against Z_1, Z_2, Z_3 and Z_4, respectively means that Z_1 is controlled whereas Z_2, Z_3 and Z_4 are not controlled.

The description of the individual class is given in table 2.2. Circuits which are shown in class 8 and class 9 have only one controlled element and therefore, are not feasible unless some more elements are added. Depending upon the type of constant or variable connection introduced, in all 5 groups can be formed as stated in Table 2.3

Class 1	Control of both sides of actuator
Class 2	Control of only one supply and control of discharge
Class 3	Control of supply and control of only one discharge
Class 4	Control of only one side
Class 5	Control of discharge only
Class 6	Control of supply only
Class 7	Control of supply to and discharge from one side
Class 8	Control of only one side
Class 9	Control of only one discharge

Table 2.2 Description of Individual Class

Group 1	Independent supply source
Group 2	Constant connection such as a flow control valve
Group3	Variable connection such as a slide valve
Group4	Variable connection such as a relief valve
Group 5	Differential acting actuator

Table 2.3 Description of Individual Groups.

Based on the 9 classes and 5 groups, the hydraulic servomechanisms can be classified as shown in the Fig.2.4 [33].

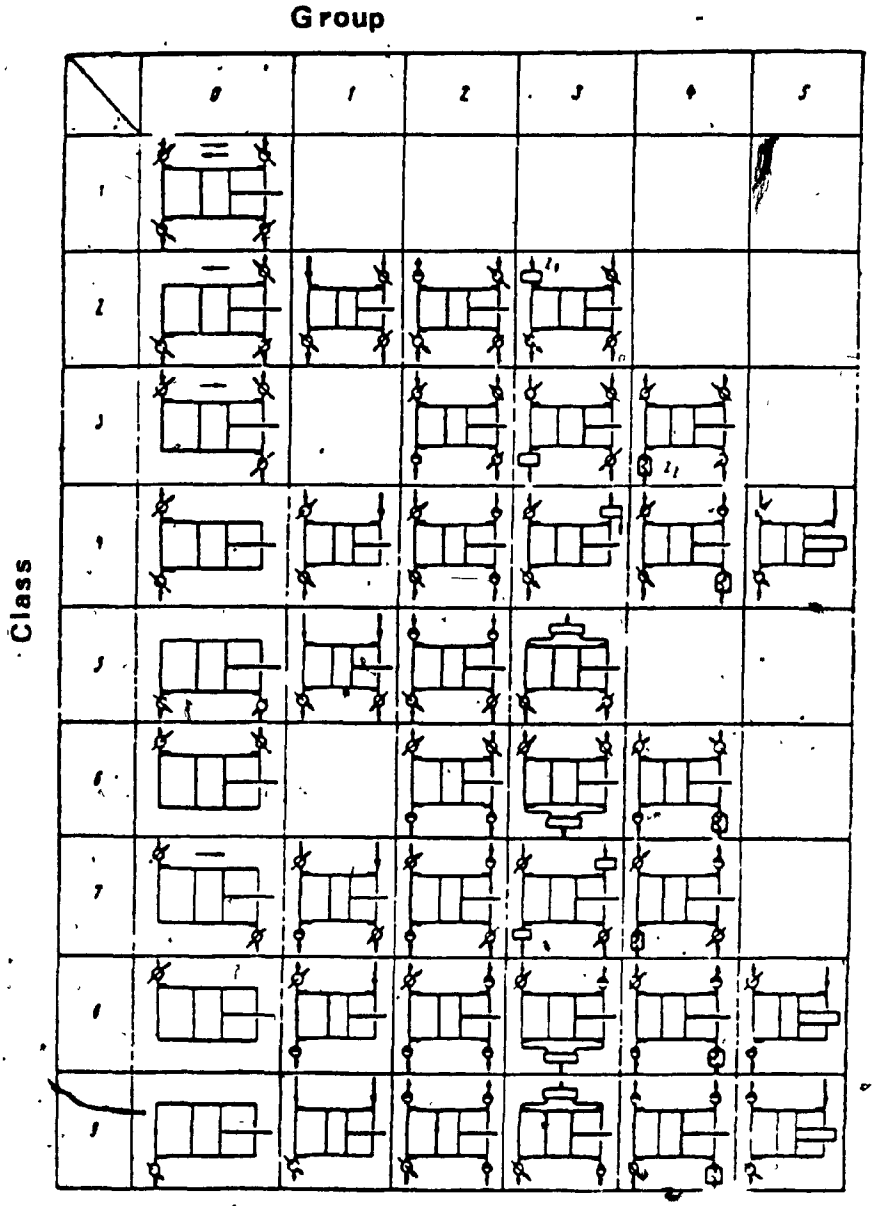

Fig. 2.4. Structural Classification of Hydraulic Servomechanisms [33]

2.4 DEVELOPMENT OF A NEW HYDRAULIC SERVOCIRCUIT

The servocircuit as shown in class 4-group 1 has an uncontrolled discharge port and it is assumed to offer a constant back pressure. Instead of the constant backpressure P_r, a relief valve was introduced in the drain line. The conventional circuit and the circuit with a relief valve in the drain line are depicted in Figs.2.5 a,b respectively. However, with the drain orifice very large (of the order of normal pipe diameter), the transient response of the circuit was found to be extremely undesirable. Therefore use of a fine metering valve in the drain line was considered. The schematic diagram of a circuit with a metering and a relief valve in the drain line is shown in Fig. 2.6 . Transient response of this circuit was seen to be superior than the conventional circuit if the backpressure and the metering diameters are properly tuned. However, as seen in Fig. 2.6, one side of the actuator is always connected to pressure port and the other to drain port. Therefore, this circuit is operable only in one direction. In order to achieve similar characteristics in both the directions, a direction control valve was introduced between the servovalve and the actuator as shown in the Fig.2.7.

For the circuit as shown in the Fig.2.5 a, the servovalve spool is driven by current (I) in the torque motor and the pressure and drain ports are switched depending upon the sign of this current. Also, when the

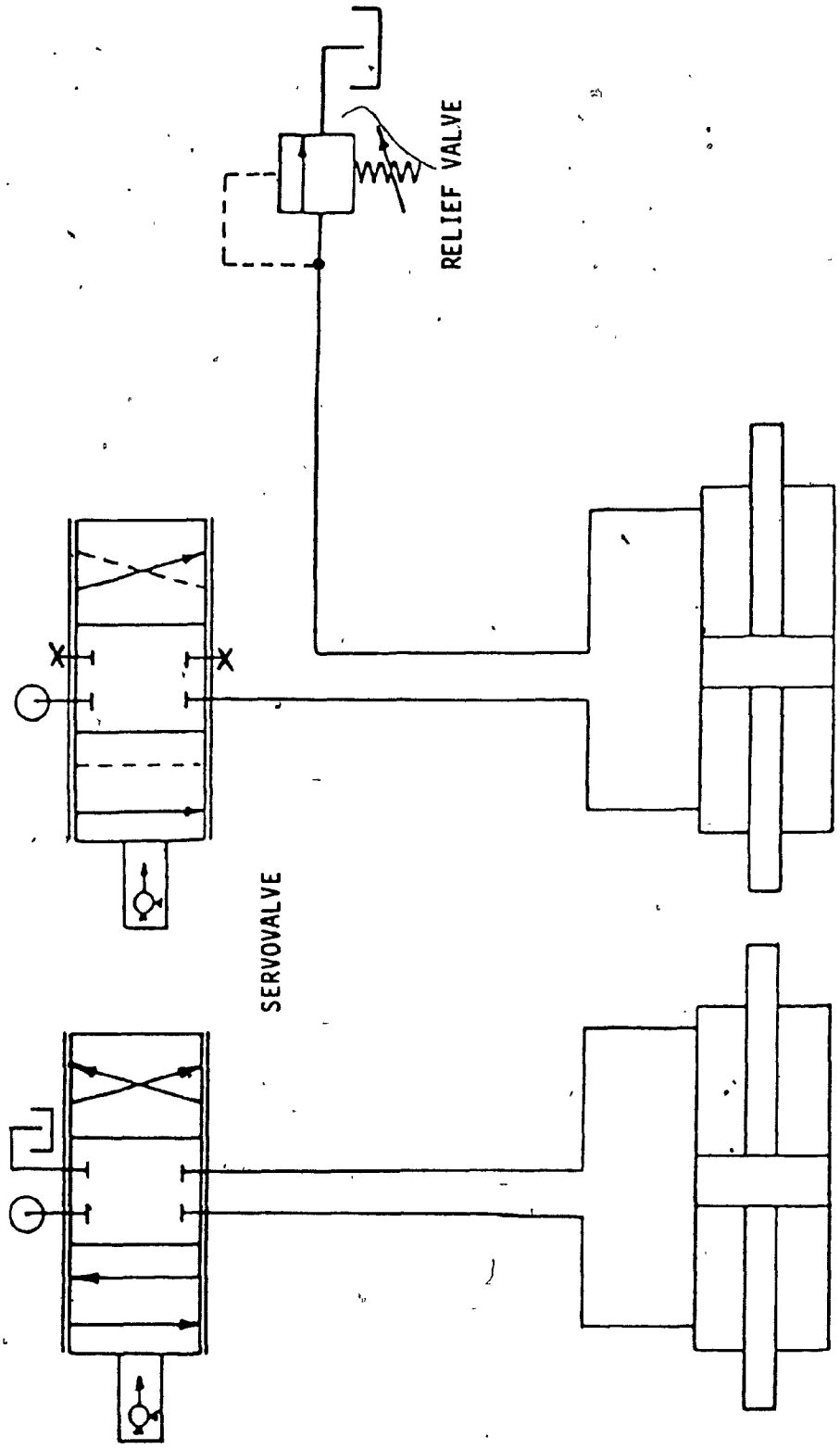

(a) Conventional Circuit (b) Circuit with Relief Valve in the Drain Line

Fig. 2.5. Schematic Diagram of Servo Circuits

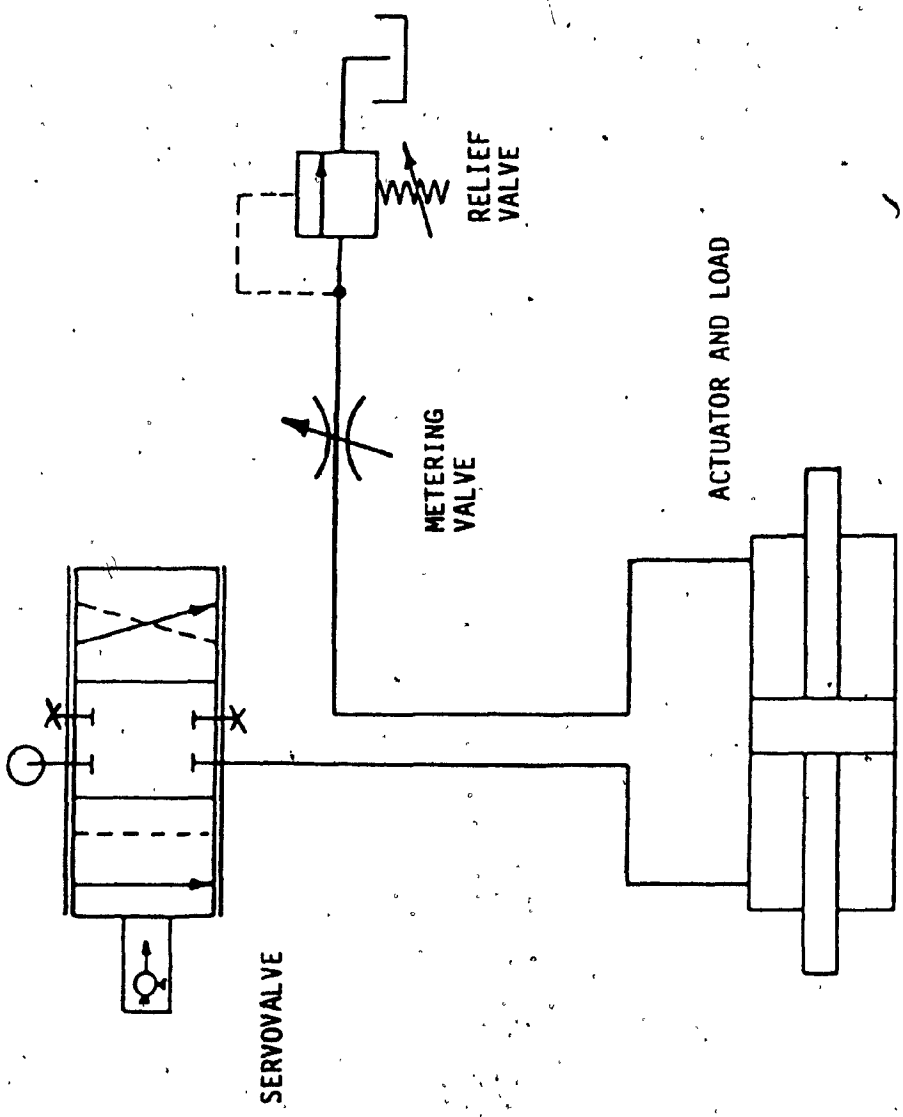

Fig. 2.6. A Circuit with Needle Valve and Relief Valve in Drain Line

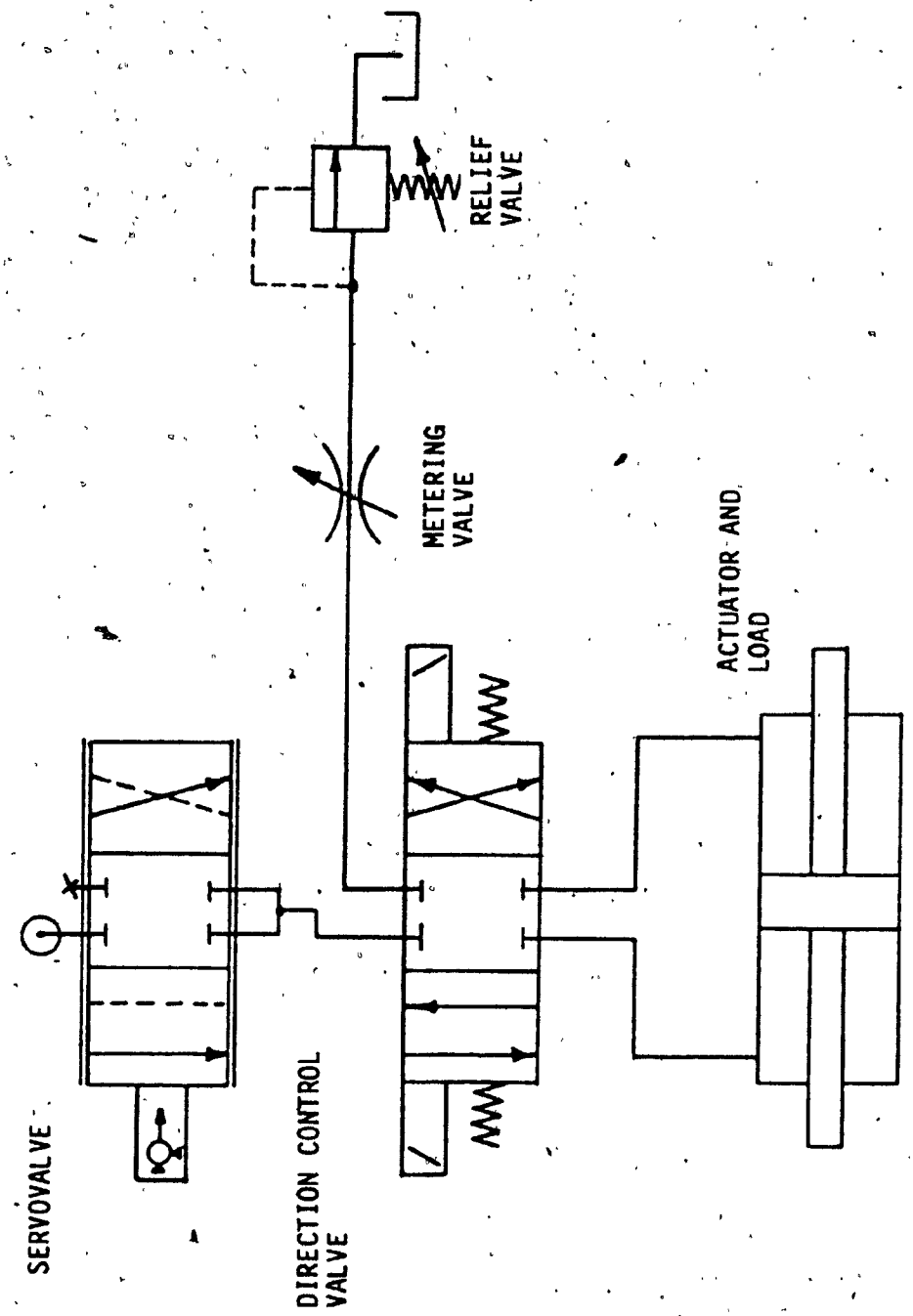

Fig. 2.7. A New Servovalve Circuit

when the current is zero, ideally, the actuator ports are blocked. The function of switching the pressure and the drain ports for the circuit as shown in Fig. 2.7, is performed by the direction control valve, which is a 4 way 3 position (center blocked) 2 solenoids and spring centered. The direction control valve is driven by an on-off controller which switches appropriate solenoid depending upon the sign of the error, $(V_i - V_f)$.

2.5 A NEW MODULAR SERVOVALVE

The steady state and transient response of the circuit described in the previous section is found to be superior [14]. Therefore, the different components viz. direction control valve, metering valve , and relief valve can be assembled together with the conventional servovalve to form a new modular servovalve configuration. Fig.2.8 shows the design concept of this modular servovalve. Henceforth, this modular form of servovalve has been termed as ' new servovalve ' or ' new servovalve configuration ' in this thesis.

The various functions performed by different sections of the new servovalve viz. inlet flow control, return pressure control, return flow control and direction control are indicated by chain dotted lines. The spool valve or the inlet flow control section receives a constant pressure supply P_s. Depending upon the magnitude of the input current, the spool is displaced and the inlet flow is

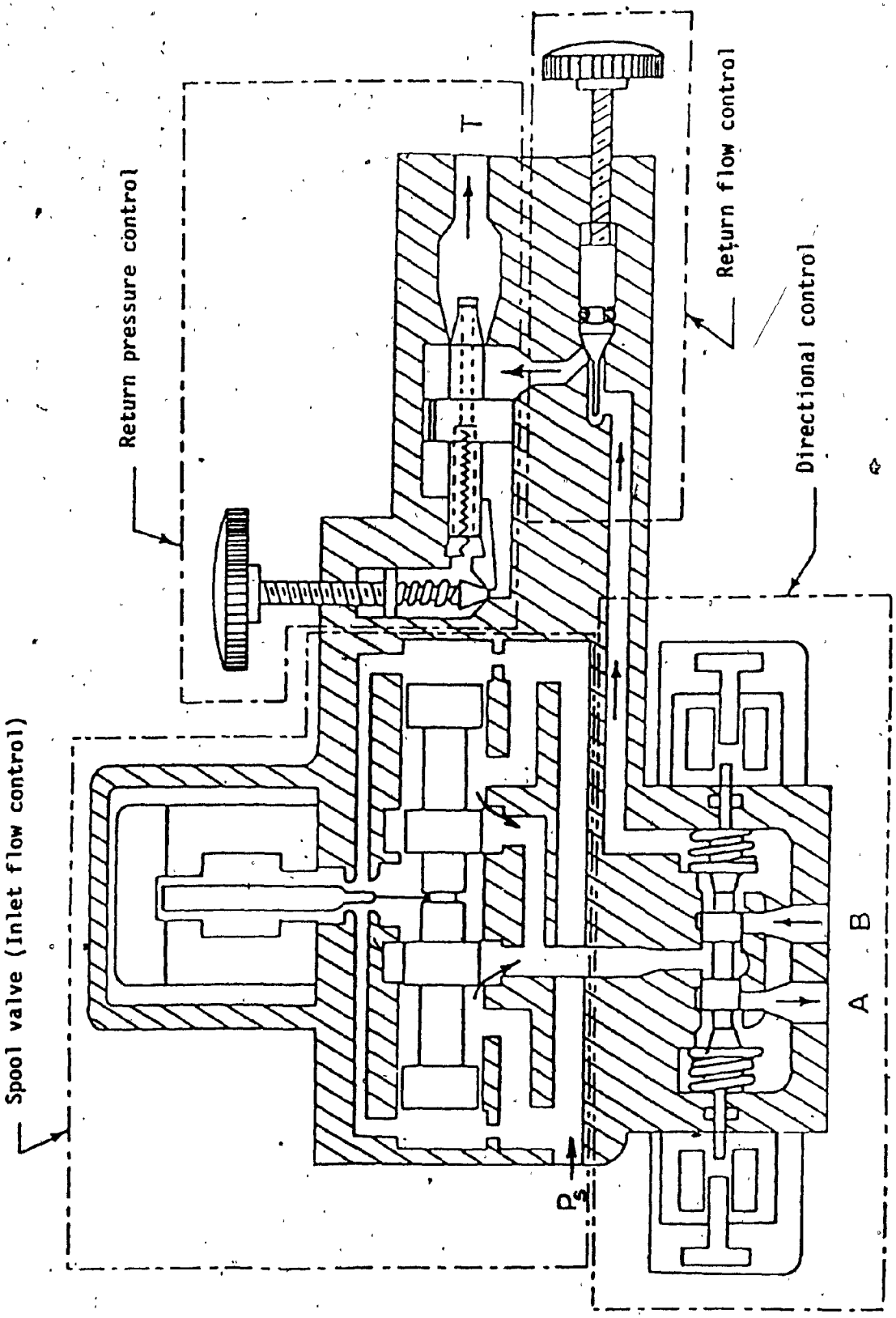

Fig. 2.8. A New Modular Servovalve Configuration

controlled. The two output ports of the spool valve section are joined to form a common pressure port to the direction control section. The two output ports of the direction control section should to be connected to the two actuator chambers. The pressure and the drain ports to the actuator are changed depending on the sign of the input to the direction control valve. The return port of the direction control section is connected to the tank through the return flow control and pressure control sections.

Some efforts have been made to design a valve module incorporating relief, flow control and direction control valve to achieve savings in space and cost [35] and also implemating a brake valve in actuator line to avoid unintentional adjustment of the motor caused by an exterior load [36]. Funk and Pecan [37] demonstrated feasibility of a dual input (hydraulic and electric) servovalve using fluidic amplifiers and positive derivative feedback whose damping can be adjusted to optimize the system performance.

2.6 SUMMARY

In this chapter, working of a typical hydraulic servosystem has been described. The structural classification of servosystem based on the number and the type of (controlled, constant and variable) connections has been done. The circuit in class 4- group 1 is modified by

adding direction control valve, metering valve and relief valve to form a new circuit. Then a novel modular servovalve has been designed in which the orifice size and the back pressure could be adjusted to get desired characteristics.

CHAPTER 3

STEADY STATE ANALYSIS OF SERVOCIRCUITS

3.1 INTRODUCTION

In the previous chapter, structural classification of hydraulic servomechanism has been done. Based on this classification, various other possible circuits have been developed. Then a new circuit consisting of a direction control valve, a metering valve and a relief valve in addition to the conventional servovalve has been thought of. Finally, a new servovalve block has been designed which can be tuned to give desired transient and steady state velocity characteristics. This chapter includes steady state analysis of conventional and new servovalve using dimensionless parameters.

Section (3.2) defines the non-dimensional parameters used for the steady state analysis. Section (3.3) contains the steady state velocity analysis of the two servovalve configurations. In section (3.4) the characteristics are compared and conclusions are drawn. Finally, the results of the analysis are summarized in section (3.5).

3.2 NON DIMENSIONAL PARAMETERS

Consider the servomechanism with conventional servovalve as shown in Fig. 3.1. In order to compare velocity characteristics of different servomechanisms, following non-dimensional parameters [33] are defined.

- Servovalve opening (Z_v): The dimensionless servovalve opening is defined as

$$Z_v = \frac{C_d A_v \sqrt{\frac{2}{\rho} P_s}}{Q_s} \tag{3.1}$$

where P_s is the constant supply pressure and Q_s is the maximum supply flow.

- Pressures in actuator chambers (p_1,p_2):The non dimensional pressures are defined as

$$p_i = \frac{P_i}{P_s} \qquad i=1,2 \tag{3.2}$$

These values of pressures actually give the fraction of supply pressure in the actuator chambers.

- Flow rate in and out of the actuator chamber (q_1,q_2): The non dimensional flows are defined as

$$q_i = \frac{Q_i}{Q_s} \qquad i=1,2 \tag{3.3}$$

which represent the fraction of maximum supply flow being used.

- Actuator force (λ): The actuator force is defined as

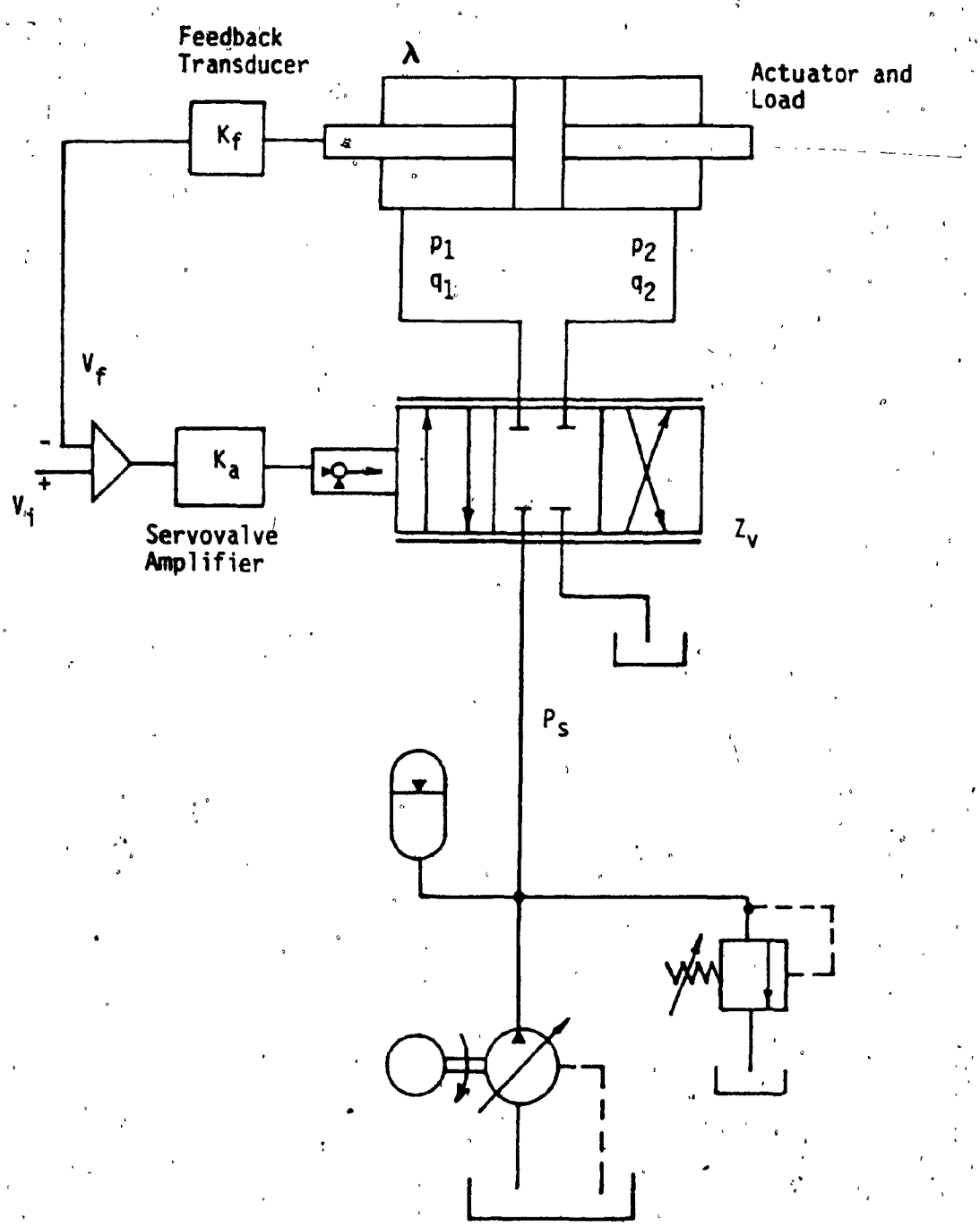

Fig. 3.1. Schematic of Servomechanism with Conventional Servovalve

$$\lambda = \frac{F}{F_{max}} \qquad (3.4)$$

where, F is the force developed by the actuator and F_{max} is the maximum force that can be developed. When a single ended piston is used, the non dimensional force is given as,

$$\lambda = \frac{P_1A_1 - P_2A_2}{P_sA_1} \quad ; (A_1 > A_2) \qquad (3.5)$$

$$= P_1 - P_2\left(\frac{A_2}{A_1}\right) \qquad (3.5a)$$

For a double ended piston, this expression reduces to

$$\lambda = \frac{[P_1 - P_2]\,A}{P_sA} \qquad (3.6)$$

$$\lambda = P_1 - P_2 \qquad (3.6a)$$

- Actuator velocity (ϕ): The dimensionless actuator velocity is defined as

$$\phi = \frac{V}{V_{max}} \qquad (3.7)$$

Thus, ϕ represents fraction of the maximum velocity that is attained.

For servomechanism with new servovalve as shown in Fig. 3.2 , the following dimensionless quantities are defined.

- Metering valve opening (Z_0):

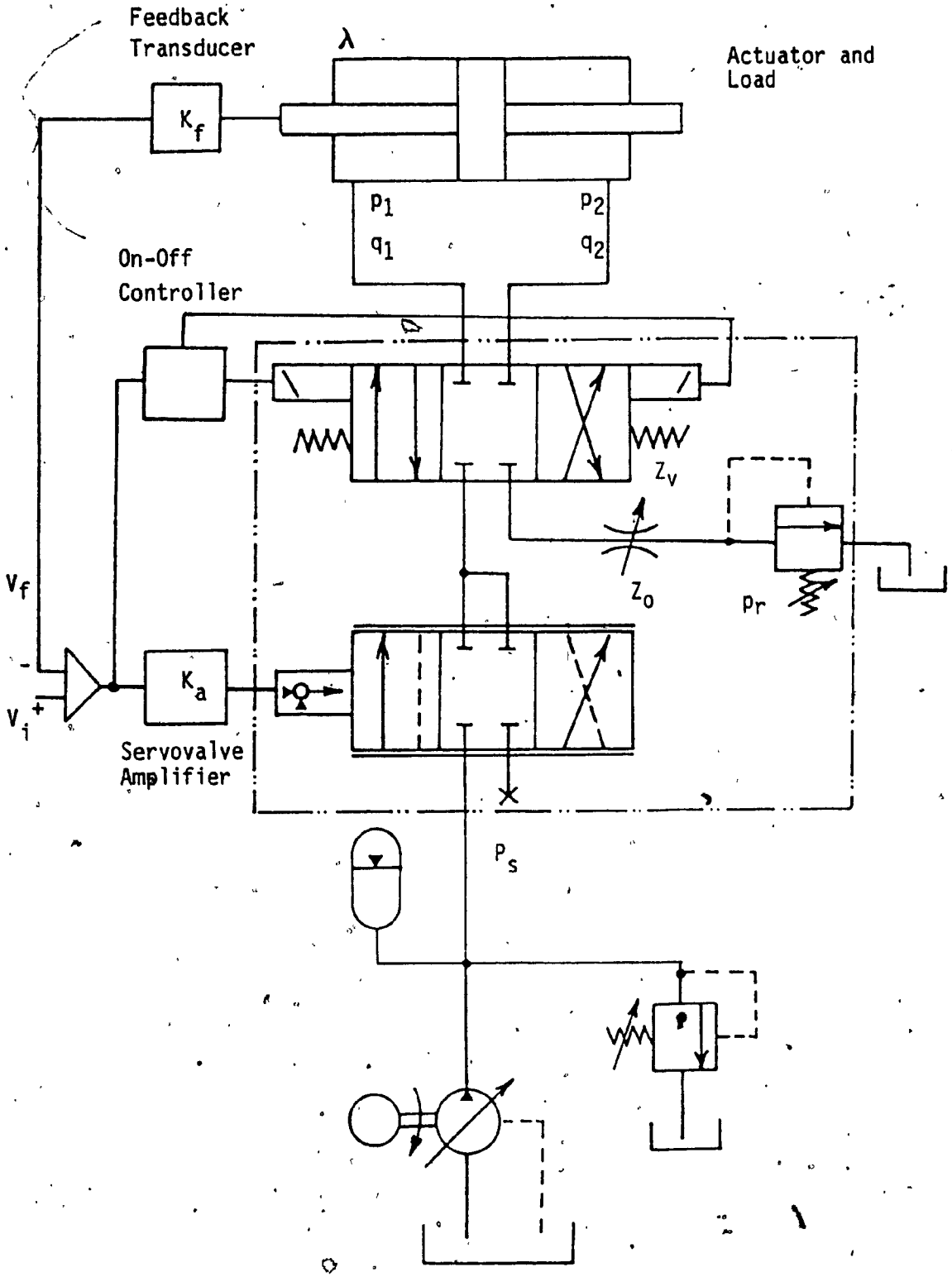

Fig. 3.2. Schematic of Servomechanism with New Servovalve Configuration

$$Z_0 = \frac{C_d A_0 \sqrt{\frac{2}{\rho} P_s}}{Q_s} \qquad (3.8)$$

- Relief valve setting (p_r):

$$p_r = \frac{P_r}{P_s} \qquad (3.9)$$

3.3 STEADY STATE ANALYSIS

Referring to Fig. 3.1, and assuming that the P_1 is the pressure side,

$$q_1 = \frac{C_d A_v \sqrt{\frac{2}{\rho} (P_s - P_1)}}{Q_s} \qquad (3.10)$$

multiplying and dividing the term under the square root sign by $\sqrt{P_s}$,

$$q_1 = \frac{C_d A_v \sqrt{\frac{2}{\rho} P_s}}{Q_s} \left[\sqrt{\frac{P_s - P_1}{P_s}}\right] \qquad (3.10a)$$

therefore, as per the definitions stated above,

$$q_1 = Z_v \left[\sqrt{1 - p_1}\right] \qquad (3.10b)$$

similarly, q_2 can be simplified as

$$q_2 = \frac{C_d A_v \sqrt{\frac{2}{\rho} P_2}}{Q_s} \qquad (3.11)$$

$$= \frac{C_d A_v \sqrt{\frac{2}{\rho} P_s}}{Q_s} \sqrt{\frac{P_2}{P_s}} \qquad (3.11a)$$

$$= Z_v \sqrt{p_2} \qquad (3.11b)$$

The equations (3.10b) and (3.11b) represent the actuator inlet and outlet flows in dimensionless form in terms of other dimensionless quantities. Assuming that the external leakage is neglegible; in steady state, the inlet and the outlet flow rates will be equal.

Therefore,

$$q_1 = q_2 \qquad (3.12)$$

or,

$$Z_v \sqrt{1-p_1} = Z_v \sqrt{p_2} \qquad (3.12a)$$

For a double ended piston, from equations (3.6a) and (3.12b),

$$Z_v \sqrt{1-p_1} = Z_v \sqrt{p_1-\lambda} \qquad (3.13)$$

Simplifying (3.13), we get,

$$p_1 = \frac{1+\lambda}{2} \qquad (3.13a)$$

Therefore, substituting (3.13a) in (3.10b),

$$q_1 = 0.71\, Z_v \sqrt{1-\lambda} \qquad (3.14)$$

Assuming that the internal leakage i.e. the leakage

from the high pressure side to the low pressure side is neglegible,

$$\phi = \frac{V}{V_{max}} = \frac{A\,V}{A\,V_{max}} \tag{3.15}$$

but $AV=Q_l$ and $AV_{max}=Q_s$, therefore,

$$\phi = \frac{Q_l}{Q_s} \tag{3.15a}$$

from (3.14) and (3.15a),

$$\phi = 0.71\ Z_v \sqrt{1-\lambda} \tag{3.16}$$

In steady state, λ can be considered to be constant. Therefore, according to equation (3.16),the actuator velocity varies linearly with the servovalve opening for a given load, λ.

For the servomechanism shown in Fig. 3.2, definitions (3.1) to (3.7) are still valid and for P_l connected to pressure side, the equation (3.10b) for the flow is the same. But the flow out of the actuator is given by

$$q_2 = \frac{C_d A_0 \sqrt{\frac{2}{\rho}(P_2-P_r)}}{Q_s} \tag{3.17}$$

$$= \frac{C_d A_0 \sqrt{\frac{2}{\rho}(P_s)}}{Q_s} \sqrt{\frac{P_2-P_r}{P_s}} \tag{3.17a}$$

Therefore, using (3.2) and (3.8), eqn. (3.17a) reduces to

$$q_2 = Z_0 \sqrt{p_2 - p_r} \qquad (3.18)$$

Now, for a double ended piston,

$\lambda = p_1 - p_2$ same as (3.6a)

Let the pressure drop across the orifice Z_0 be p

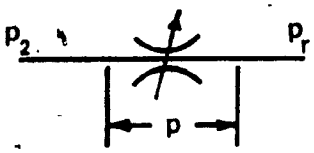

which gives

$$p_2 = p + p_r \qquad (3.19)$$

Therefore, equation (3.18) reduces to

$$q_2 = Z_0 \sqrt{p} \qquad (3.20)$$

substituting the equation (3.19) in equation (3.6a),

$$\lambda = p_1 - p - p_r \qquad (3.21)$$

or,

$$p_1 = \lambda + p + p_r \qquad (3.21a)$$

Therefore, from equation (3.10b),

$$q_1 = Z_v \sqrt{1 - \lambda - p - p_r} \qquad (3.22)$$

Now, as stated previously, in steady state,

$q_1 = q_2$ same as (3.12)

Tthereforе, from equations (3.20) and (3.22), this reduces to

$$Z_v \sqrt{1-\lambda-p-p_r} = Z_0 \sqrt{p} \qquad (3.23)$$

solving for p, we get,

$$p = \left(\frac{Z_v^2}{Z_v^2+Z_0^2}\right)(1-\lambda-p_r) \qquad (3.24)$$

substituting (3.24) in (3.20),

$$q_2 = Z_0 \sqrt{(1-\lambda-p_r)\left(\frac{Z_v^2}{Z_v^2+Z_0^2}\right)} \qquad (3.25)$$

$$\phi = Z_0 \sqrt{(1-\lambda-p_r)\frac{Z_v^2}{Z_v^2+Z_0^2}} \qquad (3.26)$$

Therefore for a given load λ, fixed relief valve setting p_r, and fixed orifice diameter Z_0, the actuator velocity varies with the square root of $(Z_0^2 Z_v^2)/(Z_v^2+Z_0^2)$.

3.4 COMPARISON OF STEADY STATE VELOCITY CHARACTERISTICS AND CONCLUSIONS

Equations (3.16) and (3.26) respectively represent steady state velocity characteristics of the servosystems with the conventional and the new servovalve.

Fig. (3.3) (a),(b),(c) and (d) plot the velocity characteristics for the following conditions.

λ	p_r
0.1	0.1
0.1	0.2
0.2	0.1
0.2	0.2

Each case is tested for Z_0 = 0.1,0.2,0.3 and 0.4 as Z_v is varied from 0.1 to 0.5.

From these graphs, following conclusions can be drawn.

i) The steady state velocity for the conventional servovalve varies linearly with the valve opening (till the physical limitation of the valve). On the other hand for a given orifice size Z_0 and back pressure p_r, the slope of the graph is initially high but reduces as Z_v is increased. Therefore, for each combination of λ , p_r and Z_0, there exists a crossing point upto which the new servovalve offers higher velocity.

ii) The region upto the crossing point, in which the new servovalve offers higher steady state velocity, becomes larger as the metering orifice area Z_0 is increased and the back pressure p_r is reduced e.g. consider points 1 and 2 in Fig. 3.3a and points 1 in Fig. 3.3a and 3 in Fig. 3.3b. For points 1 and 2; as Z_0 is increased from 0.1 to 0.2, the crossing point is increased from Z_v=0.8 to Z_v=1.8. For points 3 and 1; as p_r is reduced from 0.2 to 0.1, the crossing point is increased from Z_v=0.65 to Z_v=0.8.

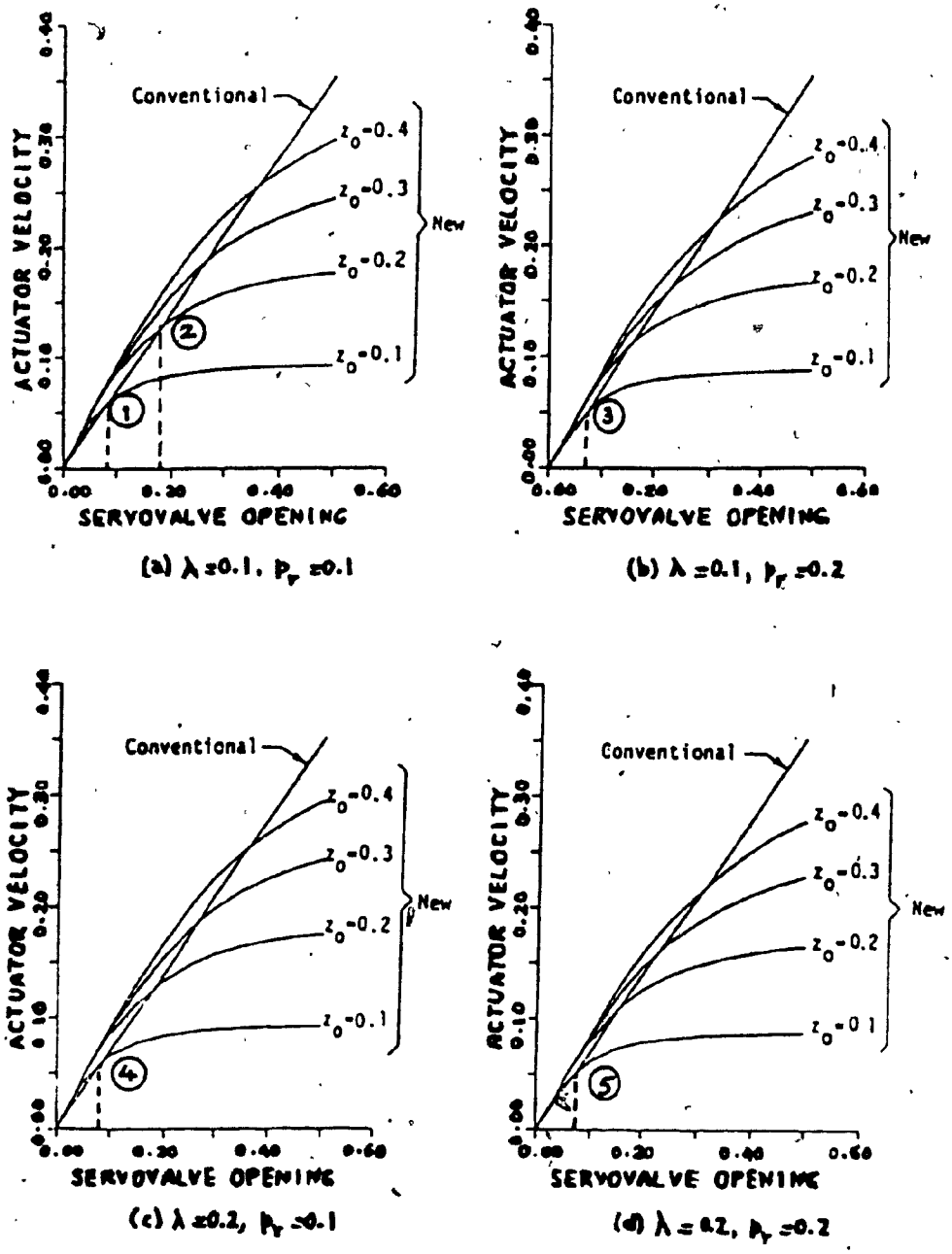

(a) λ =0.1, p_r =0.1

(b) λ =0.1, p_r =0.2

(c) λ =0.2, p_r =0.1

(d) λ = 0.2, p_r =0.2

Fig. 3.3. Steady State Velocity Characteristics

iii) Increase in load from 0.1 to 0.2 reduces the crossing point marginally (points 1 and 4 or 3 and 5).

Some deductions can be drawn from this analysis.

i) The crossing point is achieved when velocities for both the configurations are same. i.e.,

$$0.71\, Z_v \sqrt{1-\lambda} = Z_0 \sqrt{(1-\lambda-p_r)\,\frac{Z_v^2}{Z_v^2+Z_0^2}} \qquad (3.27)$$

therefore, squaring both sides,

$$\frac{1-\lambda}{2} = (1-\lambda-p_r)\left(\frac{Z_0^2}{Z_v^2+Z_0^2}\right) \qquad (3.27a)$$

$$\frac{Z_0^2+Z_v^2}{Z_0^2} = \frac{2(1-\lambda-p_r)}{(1-\lambda)} \qquad (3.27b)$$

$$\frac{Z_v^2}{Z_0^2} = \frac{(1-\lambda-2p_r)}{(1-\lambda)} \qquad (3.27c)$$

Now if $\lambda \ll 1$, then $1-\lambda \simeq 1$

$$Z_v^2 = Z_0^2\,(1-2p_r) \qquad (3.27d)$$

$$Z_v = Z_0 \sqrt{(1-2p_r)} \qquad (3.27e)$$

Expanding the quantity under square root sign using Binomial theorem and neglecting the higher order terms,

$$Z_v = Z_0\,(1-p_r) \qquad (3.27f)$$

Fig.3.4 shows a 3 dimensional plot of the locus of the crossing point. The plot is based on the assumption that the Z_0 and Z_v could be varied from 0 to 1.5 (since by definition, Z_0 and Z_v could be greater than 1).

The condition to get higher steady state velocity in case of the new servovalve configuration is that,

$$Z_0 (1-p_r) \geqslant Z_v \qquad (3.28)$$

The boundary of the 3-D curve represents a limiting case where

$$Z_v = Z_0 (1-p_r) \qquad \text{same as (3.27f)}$$

All the points which are inside the envelope will give higher steady state velocity. Rest of the points either give same velocity (points on the boundary) or lower velocity (points outside the envelope) than the conventional servovalve.

It can be also seen that the operating region is reduced as the back pressure is increased and at $p_r=1$, the curve becomes a straight line and lies in Z_0-p_r plane.

ii) If $Z_0 = Z_v$ and $p_r = 0$, then eqn. (3.26) becomes

$$= Z_v^2 \sqrt{(1-\lambda)\frac{1}{2Z_v^2}} \qquad (3.29)$$

$$= 0.71\ Z_v \sqrt{(1-\lambda)} \qquad (3.29a)$$

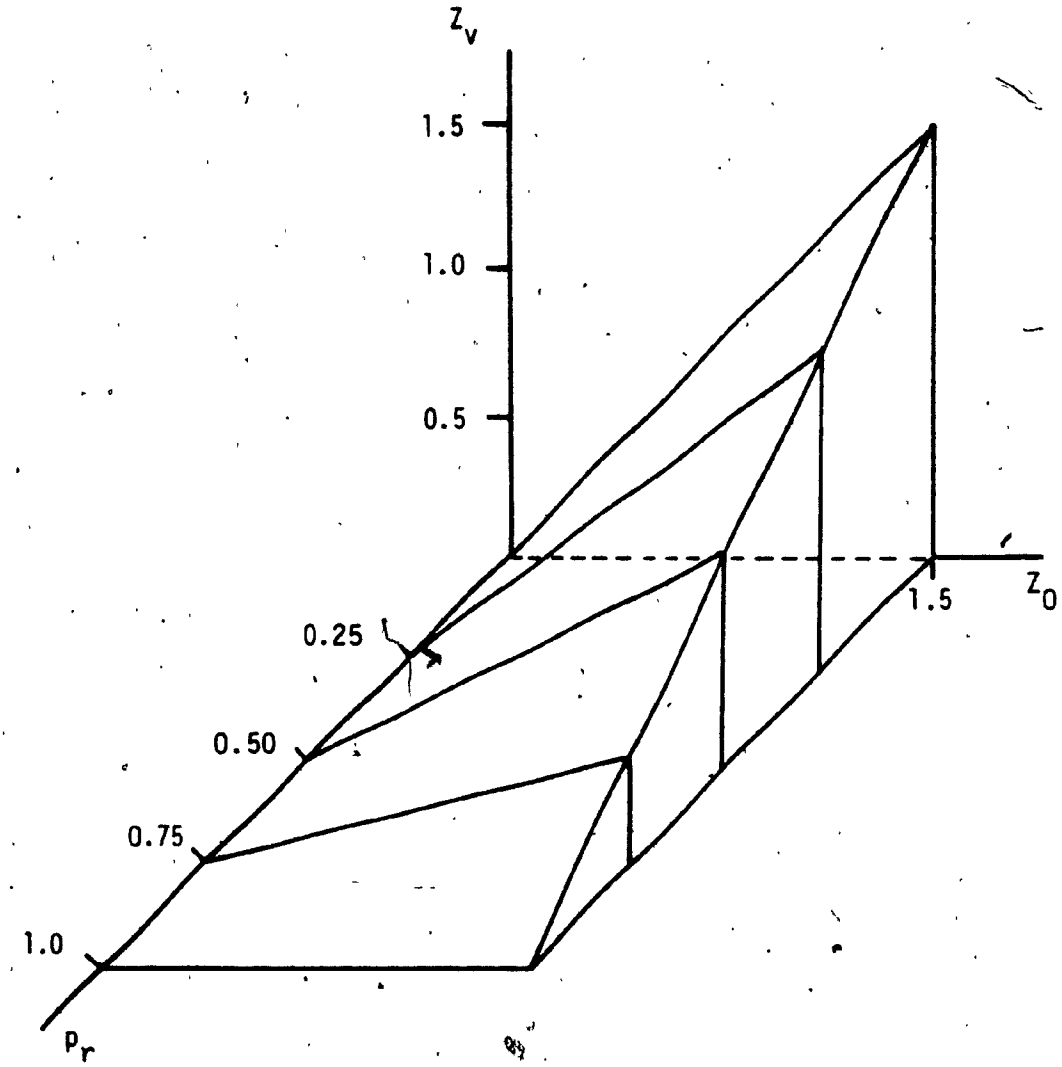

Fig. 3.4 Locus of Crossing Point

Which is same as equation (3.16), which gives velocity for the conventional servovalve.

iii) If $Z_0 = Z_v$ then for the new servovalve,

$$\phi = Z_v^2 \sqrt{(1-\lambda-p_r)\frac{1}{2Z_v^2}} \qquad (3.30)$$

therefore at the crossing point, the following equality should be satisfied.

$$0.71\ Z_v \sqrt{(1-\lambda)} = 0.71\ Z_v \sqrt{(1-\lambda-p_r)} \qquad (3.31)$$

or,

$$p_r = 0 \qquad (3.31a)$$

which is the same condition as that for the conventional servovalve.

iv) If $Z_0 >> Z_v$,

$$Z_0^2+Z_v^2 \simeq Z_0^2 \qquad (3.32)$$

therefore,

$$\phi = Z_0 Z_v \sqrt{\frac{(1-\lambda-p_r)}{Z_0^2}} \qquad (3.32a)$$

$$\phi = Z_v \sqrt{(1-\lambda-p_r)} \qquad (3.32b)$$

therefore, for crossing point,

$$0.71\ Z_v \sqrt{(1-\lambda)} = Z_v \sqrt{(1-\lambda-p_r)} \qquad (3.33)$$

$$p_r = \frac{1-\lambda}{2} \tag{3.33a}$$

or in other words, the velocity for the new configuration will be greater than the conventional if,

$$p_r < \frac{1-\lambda}{2} \tag{3.33b}$$

3.5 SUMMARY

In this chapter, first non dimensional parameters are defined. Using these parameters, both the servovalve configurations are analysed. From the analysis the different conclusions are drawn which are summarized below. The steady state velocity of the conventional servovalve varies linearly with the servovalve opening whereas the new servovalve exhibits a non linear relationship for given orifice area and back pressure. Hence, there exists a crossing point upto which the new servovalve gives higher velocity. The zone upto the crossing point in which the new servovalve has higher velocity than the conventional servovalve, increases as the orifice area is increased and the back pressure is reduced.

CHAPTER 4

TRANSIENT ANALYSIS OF TWO SERVOVALVES

4.1 INTRODUCTION

In the previous chapter, non-dimensional parameters have been defined. Later, steady state velocity analysis of servosystems with conventional servovalve and new servovalve has been presented. From the analysis, it has been shown that the new servovalve configuration gives higher steady state velocity under certain conditions. This chapter contains transient analysis of the servosystems.

Section (4.2) describes features of different methods used for transient analysis. In section (4.3), individual components such as servovalve, actuator etc., which are used in servosystems are modelled and a total system model is developed. Simulation results for various input conditions employing the two configurations of servovalve are included in section (4.4). The comparison of these results is presented in section (4.5) and some conclusions are drawn.

4.2 GENERAL

The design of any hydraulic control system basically involves 3 steps viz. circuit design, static sizing and dynamic analysis. For a simple on-off type of hydraulic system, dynamic analysis is often not required. However, for a complicated control system such as electrohydraulic servosystem, dynamic analysis is extremely important in order to determine the stability and response characteristics under different input conditions. The dynamic analysis could be done in one of the following ways.

i) Transfer function technique

ii) State space technique

or

iii) A set of informal equations.

The transfer function technique is the most classical method which gives a frequency dependent relationship between the output and the input. However, this method is applicable only for linear differential equations with constant coefficients. The method of state space equation allows concise representation of dynamic relationship between the system variables and simultaneous inputs in the form of a matrix model. While this method can

inputs in the form of a matrix model. While this method can

include non linear entries, most subsequent formal vector-matrix analysis applies only to linear situations. The dynamic model may also be in the form of a set of simultaneous linear and nonlinear, algebraic and differential equations describing the relationship between the system variables and the inputs. This method is very useful as it can be directly applied for simulation using analog or digital computers.

4.3 DEVELOPMENT OF MATHEMATICAL MODEL

The servosystems with conventional and new servovalve configurations are modelled using the method of informal equations, i.e. individual components are modelled separately and a total model is developed. The various components in the system with the conventional servovalve can be modelled as follows.

- Input to the servovalve:

Step response characteristics of both the servovalve configurations are investigated. Two different types of step inputs viz. a two-step input and a square wave input are chosen. The selection of two-step input is based on the following reason. Experimentally, it was observed that the system with new servovalve shows a very high pressure and velocity transient when it starts from stationary conditions. This transient was not seen to be

severe in case of square wave input. Since the model is not intended to take into account the pressure transient occuring when the piston starts moving, only the response of the second step is used for comparison. The square wave input i.e alternate positive and negative input is selected to take into account the pure time delay involved in the switching of the direction control valve.

The two-step input is modelled as,

$$V_i \begin{cases} = & 0.0 & t = 0.0 \\ = & V_{i1} & t \geq 0.1 \\ = & V_{i1}+V_{i2} & t \geq 0.2 \end{cases} \quad (4.1)$$

The square wave input is modelled as,

$$V_{ref} = \sin \omega t \quad (4.2)$$

$$V_i \begin{cases} = & V_{i1} & V_{ref} > 0.0 \\ = & -V_{i1} & V_{ref} < 0.0 \end{cases} \quad (4.3)$$

- Servocontroller

A proportional type servocontroller is used. Since the range of the interest of input frequency is low (5-10 Hz), the servocontroller dynamics is neglected. Therefore, the actual current fed into servovalve coils tan be modelled as

$$I = K_a (V_i - V_f) \quad (4.4)$$

- Electrohydraulic servovalve:

(a) Servovalve transfer function: Servovalve transfer function is difficult to derive analytically [2]. The relationship between servovalve area available for flow, A_V and the input current is usually expressed as first or second order transfer function depending upon the input frequency range. The values for equivalent first order time constant or second order equivalent natural frequency and damping can be obtained from the valve manufacturers or they may be established by curve fitting. Again, since the input frequency range is low, the servovalve is modelled as a first order system. The equivalent time constant is determined from the specifications provided by the manufacturer [Appendix D]. Therefore, the servovalve can be modelled as

$$\frac{A_V}{I} = \frac{K_X K_V}{(\tau_V s+1)} \qquad (4.5)$$

or,

$$\tau_V \frac{dA_V}{dt} = K_X K_V (I) - A_V \qquad (4.5a)$$

$$\frac{dA_V}{dt} = \frac{1}{\tau_V}\left[K_X K_V (I) - A_V\right] \qquad (4.5b)$$

The constant $K_X K_V$ i.e. product of servovalve torque motor constant (K_X) and the servovalve area constant (K_V) is

determined experimentally as explained in Appendix A.1.

(b) Flow equations: The output stage of the servovalve is the four way spool valve. It is assumed [37], [38], [39], that the valve has symmetrical porting and zero lap. Further, it is assumed that the radial clearance between the valve body and the sleeve is zero, the metering edges are sharp and the flow rate through the valve is described by orifice flow equation [40] for incompressible flow. Therefore, the flow equations can be stated as

$$\left.\begin{aligned} Q_1 &= C_d A_v \sqrt{\frac{2}{\rho}(P_s - P_1)} \\ Q_2 &= C_d A_v \sqrt{\frac{2}{\rho}(P_2)} \end{aligned}\right\} \quad A_v > 0.0$$

$$\left.\begin{aligned} Q_1 &= C_d A_v \sqrt{\frac{2}{\rho}(P_1)} \\ Q_2 &= C_d A_v \sqrt{\frac{2}{\rho}(P_s - P_2)} \end{aligned}\right\} \quad A_v < 0.0 \qquad (4.6)$$

$$\left.\begin{aligned} Q_1 &= 0.0 \\ Q_2 &= 0.0 \end{aligned}\right\} \quad A_v = 0.0$$

- Conduits:

The pictorial view of the test stand, Fig.5.1, shows that there are number of bends leading to the actuator. A calculation for pressure losses due to the friction and bends was done which showed that these losses are negligible compared to the operating pressure for the range of the

actuator velocity (less than 5 % of the operating pressure). Therefore, these losses are neglected. The oil temperature and the density are assumed to be constant. The effects of oil under compression are included. Therefore, applying the continuity equation to each actuator chamber [37], we get,

$$\left.\begin{aligned} \frac{dP_1}{dt} &= \frac{\beta}{v_1}(Q_1 - Q_l) \\ \frac{dP_2}{dt} &= \frac{\beta}{v_2}(-Q_2 + Q_l) \end{aligned}\right\} \qquad (4.7)$$

- **Actuator:**

(a) Leakage flow: The leakage coefficient is determined experimentally as explained in the Appendix A.5 and is seen to be proportional to the pressure difference across the actuator. Hence, the leakage flow can be expressed as

$$Q_l = C_l(P_1 - P_2) \qquad (4.8)$$

(b) Force equations: The net force developed by the actuator is used to overcome the inertial force and the coulomb friction. The frictional force between the bearings mounted on the loading table and the shaft is assumed to be zero and the viscous damping force is found to be negligible [Appendix A.4]. The supply pressure is assumed to be constant and the losses in the filter are neglected. Hence, the force equation can be expressed as,

$$(P_1-P_2)A = M \frac{d^2X}{dt^2} + F_c \qquad (4.9)$$

The coulomb force F_c can be represented as follows.

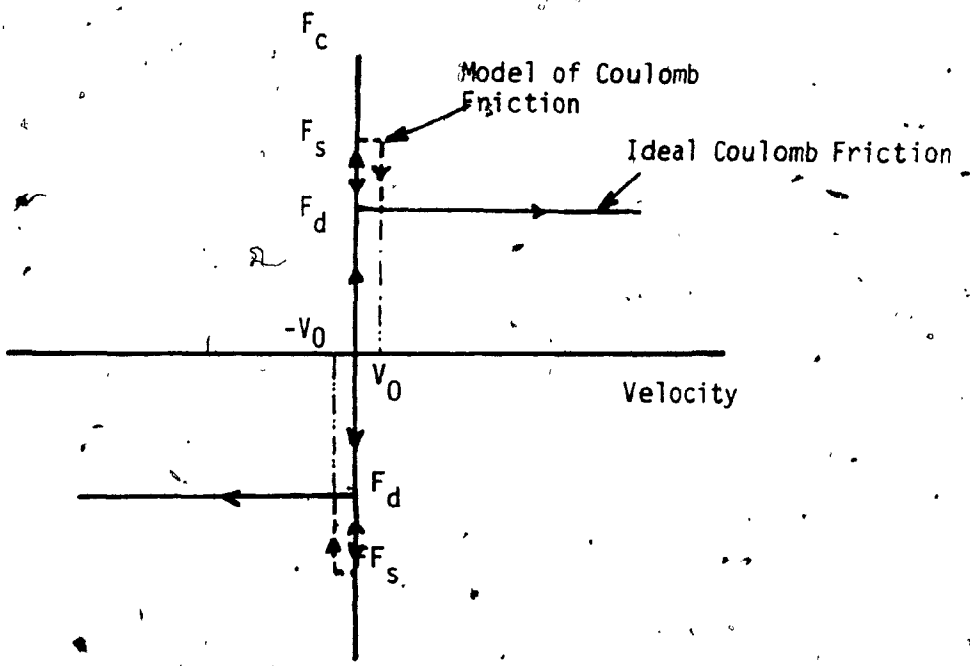

Ideally, the switchover from the static (F_s) to dynamic friction (F_d) is considered to occur at $|V| = 0^+$. However, this causes some instability [18] when the model is to be solved by numerical techniques. Therefore, the switchover is assumed to take place at certain velocity (not equal to zero) V_0, which is chosen in order to give sufficient numerical stability.

Therefore, the coulomb friction could be modelled as

follows [18].

$$F_{sum} = (P_1 - P_2)A$$

$$\left.\begin{aligned} F_c &= F_{sum} && |F_{sum}| < F_s \,,\ |V| \leq V_0 \\ F_c &= F_s \frac{F_{sum}}{|F_{sum}|} && |F_{sum}| > F_s,\ |V| \leq V_0 \\ F_c &= F_d \frac{V}{|V|} && |V| > V_0 \end{aligned}\right\} \quad (4.10)$$

The value of V_0 is chosen to be $4.33*10^{-4}$ in/sec ($1.0*10^{-4}$ m/sec) which is 0.15% of the steady state velocity (3.0 in/sec).

- Output actuator velocity:

The velocity of the actuator is measured using a moving magnet type transducer which is also used as a feedback device. The sensitivity of the transducer (K_f) is determined experimentally as explained in Appendix A.3. Therefore, the output voltage corresponding to the actuator velocity can be expressed as,

$$V_f = K_f \left(\frac{dX}{dt}\right) \quad (4.11)$$

For the servo system with new servovalve, the above mathematical model holds good except for the flow equations. In the case of new servovalve configuration, it is assumed that the relief valve offers a constant back pressure Pr and its dynamics is neglected. The

direction control valve introduces a pure time delay in the actuation. Expermentally, it was seen that this time delay is 8 ms and sometimes varies form 3-10 ms [Appendix B.2]. The losses in the direction control valve are assumed to be negligible.

As explained in section (2.5), in case of the new servovalve configuration, the switching of pressure and drain ports is done by the directon control valve, which is controlled by an on-off controller. Depending upon the sign of the input error voltage $(V_i - V_f)$, the on-off controller performs switching of the ports and if the feedback voltage V_f is never greater than the input voltage, the switching depends on the sign of input voltage V_i. However, the switching action is delayed by t_d sec, which is the pure time delay of the direction control valve. This can be explained further referring to the following figure.

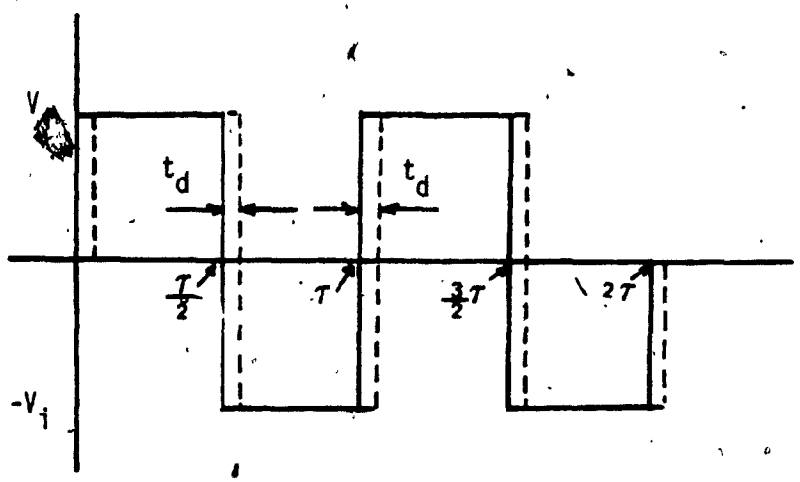

As shown in the figure, the sign of the voltage input changes at 0.5 sec. However, because of the time delay of t_d sec, the switching of the pressure and the drain ports occurs at $0.5 + t_d$ sec. Same delay is shown in case of other switching. Therefore, the flow model for the new servovalve can be written as,

For $t_d \leq t < 0.5\tau + t_d$ or $\tau + t_d \leq t < 1.5\tau + t_d$

$$Q_1 = C_d |A_v| \sqrt{\frac{2}{\rho}(P_s - P_1)}$$

$$Q_2 = C_d A_0 \sqrt{\frac{2}{\rho}(P_2 - P_r)} \quad ; P_2 \geq P_r,$$

$$Q_2 = 0.0 \quad ; P_2 < P_r,$$

For $0.5\tau + t_d \leq t < \tau + t_d$ or $1.5\tau + t_d \leq t < 2\tau + t_d$

$$Q_1 = -C_d A_0 \sqrt{\frac{2}{\rho}(P_1 - P_r)} \quad ; P_1 \geq P_r,$$

$$Q_1 = 0.0 \quad ; P_1 < P_r,$$

$$Q_2 = -C_d |A_v| \sqrt{\frac{2}{\rho}(P_s - P_2)}$$

(4.12)

4.4 SIMULATION RESULTS

The system of equations (4.1-4.12) are solved by Runge-Kutta order IV method using Fortran 77 on VAX 11/780 minicomputer. The program listing is given in Appendix C.

The systems with conventional and new servovalve are simulated for two-step under input and test conditions as stated in Table 4.1. Figs. 4.1 and 4.2 respectively show the effects of gain and inertial load on the system with conventional servovalve.

As seen from the response of the conventional servovalve for different gains (Fig.4.1), it can be stated that increase in gain from 6.67 mA/V to 7.46 mA/V, increases the steady state velocity from 2.36 in/sec (0.06 m/sec) to 2.51 in/sec (0.064 m/sec).There is no significant difference in dynamic response for this increment in gain.

Theoretically, the relationships between the system natural frequency ω_n and system damping ξ for a second order system are given as follows [37].

$$\left.\begin{aligned} \omega_n &= \sqrt{\frac{4\beta A^2}{(v_1+v_2)\,M}} \\ \xi &= \frac{C_t}{A}\sqrt{\frac{\beta M}{(v_1+v_2)}} \end{aligned}\right\} \qquad (4.13)$$

i.e the natural frequency varies inversely with the square root of load and the system damping varies directly with the square root of load, other quantities being constant.

Type	V_{i1} V	V_{i2} V	K_a mA/V	M Slugs	A_0 in^2 (m^2)	P_r psi (N/m^2)
Conventional	-0.8	1.2	6.67	653	--	--
				938	--	--
			7.46	653	--	--
				938	--	--
New	0.8	1.2	6.67	938	$3.2*10^{-2}$ ($2.066*10^{-5}$)	80 ($4.83*10^5$)
						180 ($1.24*10^6$)
					$8.77*10^{-3}$ ($5.66*10^{-6}$)	80 ($4.83*10^5$)
						180 ($1.24*10^6$)
					$4.38*10^{-3}$ ($2.83*10^{-6}$)	80 ($4.83*10^5$)
						180 ($1.24*10^6$)
			7.46	653	$3.2*10^{-2}$ ($2.066*10^{-5}$)	80 ($4.83*10^5$)
						180 ($1.24*10^6$)
					$8.77*10^{-3}$ ($5.66*10^{-6}$)	80 ($4.83*10^5$)
						180 ($1.24*10^6$)
					$4.38*10^{-3}$ ($2.83*10^{-6}$)	80 ($4.83*10^5$)
						180 ($1.24*10^6$)

Table 4.1 Input and Test Conditions : 2-step Input

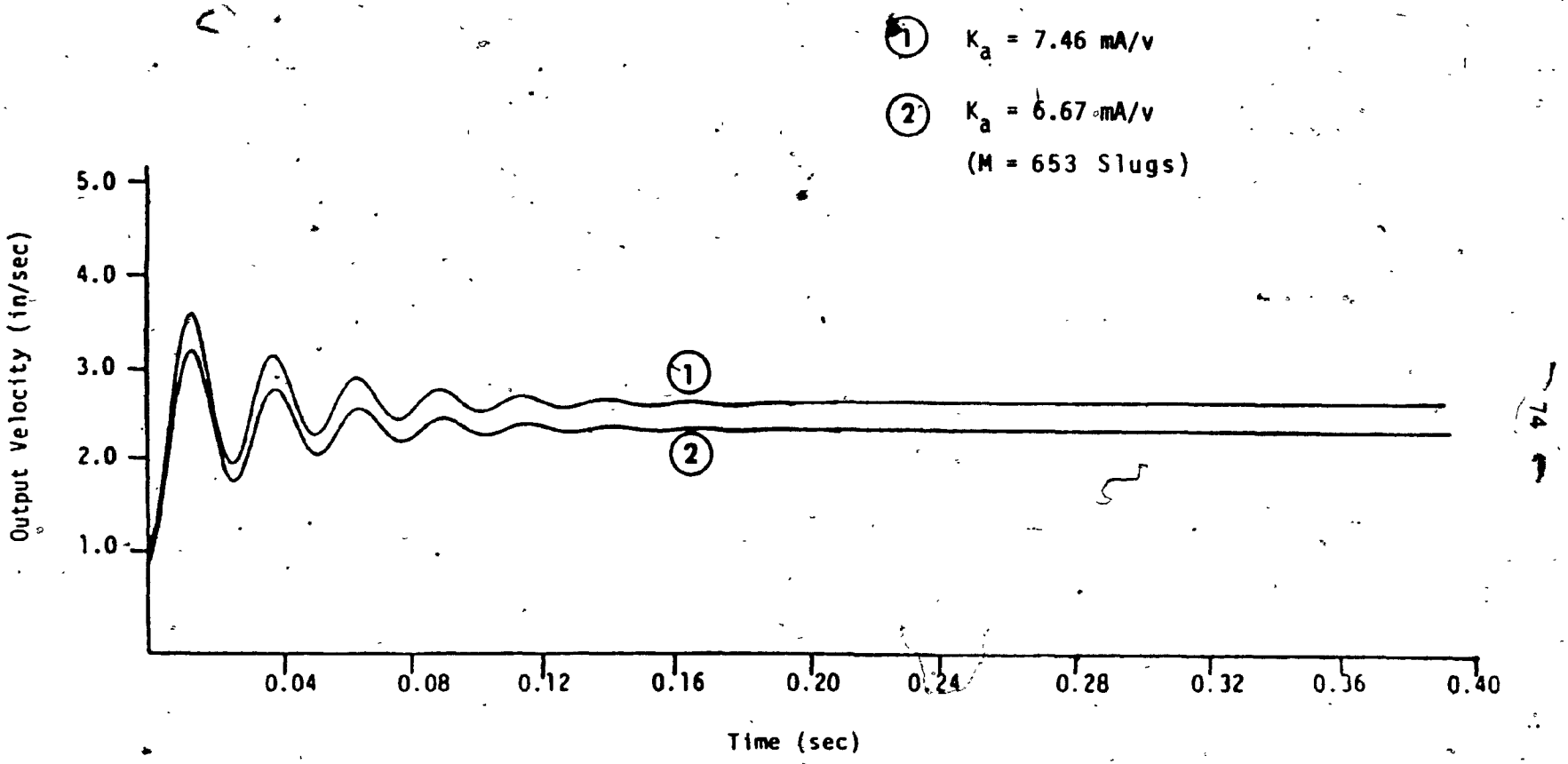

Fig. 4.1: Effect of Gain on Conventional Servovalve: 2-Step Input (Simulation)

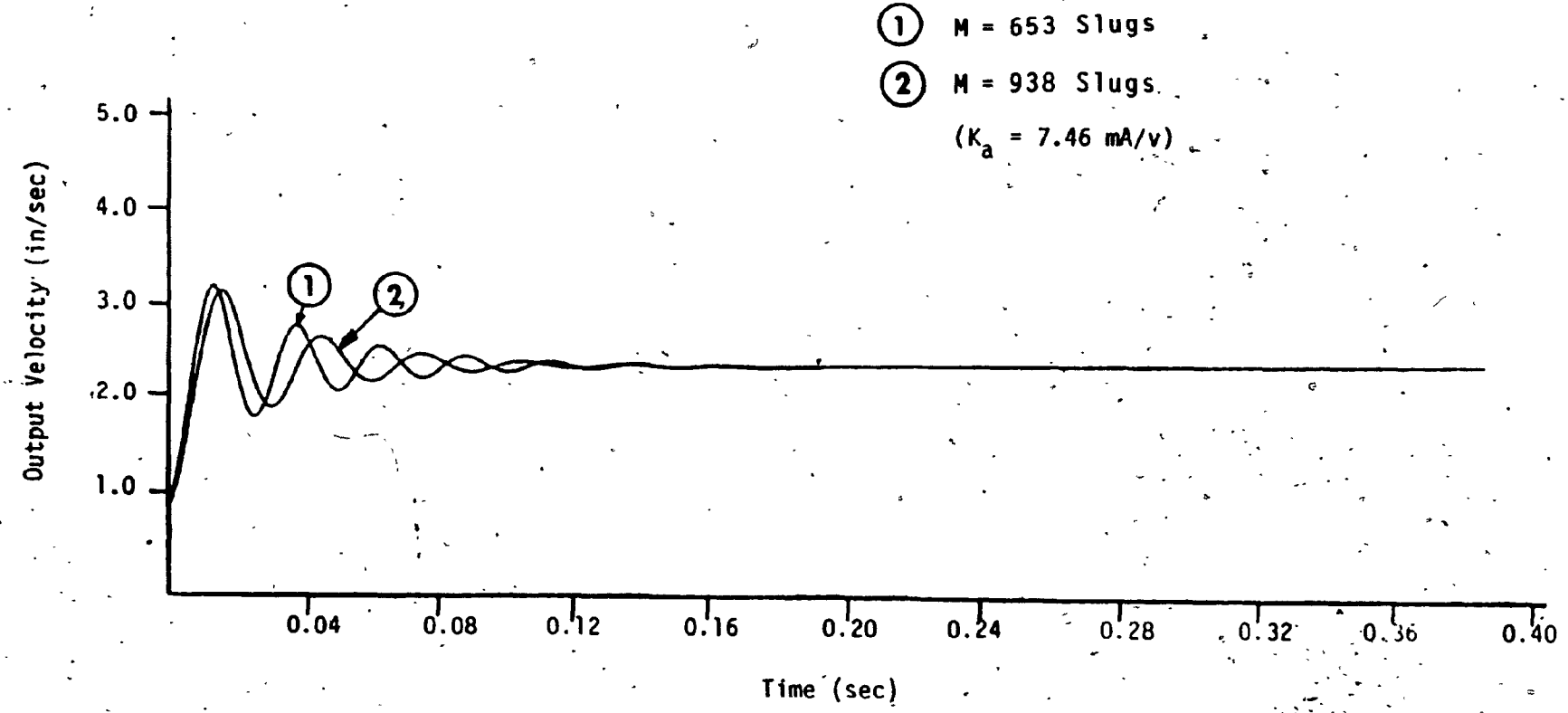

Fig. 4.2: Effect of Mass on Conventional Servovalve: 2-Step Input (Simulation)

From simulation results it can be seen that, as mass M is increased from 653 to 938 Slugs, the damped natural frequency is reduced from 262 rad/sec to 207 rad/sec and the damping is increased.

Figs.4.3 and 4.4 respectively show the effect of metering orifice and back pressure on the new servovalve configuration. Fig.4.5 shows the comparison of the new and conventional servovalve under same set of input conditions.

From Fig.4.3, the metering orifice is seen to have the following effect. As the orifice size is reduced from $3.2*10^{-2}$ in^2 ($2.067*10^{-5}$ m^2) to $8.77*10^{-3}$ in^2 ($5.66*10^{-6}$ m^2) to $4.38*10^{-3}$ in^2 ($2.83*10^{-6}$),

i) there is no significant change in the rise time (and is approx. equal to 9 ms).

ii) the damped natural frequency also does not change (and is approx. equal to 150 rad/sec).

iii) the damping is increased and therefore the settling time is reduced.

iv) the steady state velocity is reduced from 2.64 in/sec (0.067 m/sec) to 2.55 in/sec (0.065 m/sec) to 2.48 in/sec (0.063 m/sec). This can be explained by steady state characteristics of the new servovalve as shown in Fig. 3.3, which indicates that as Z_0 is reduced, steady state velocity is reduced (e.g. points 2 and 1 in Fig. 3.3a).

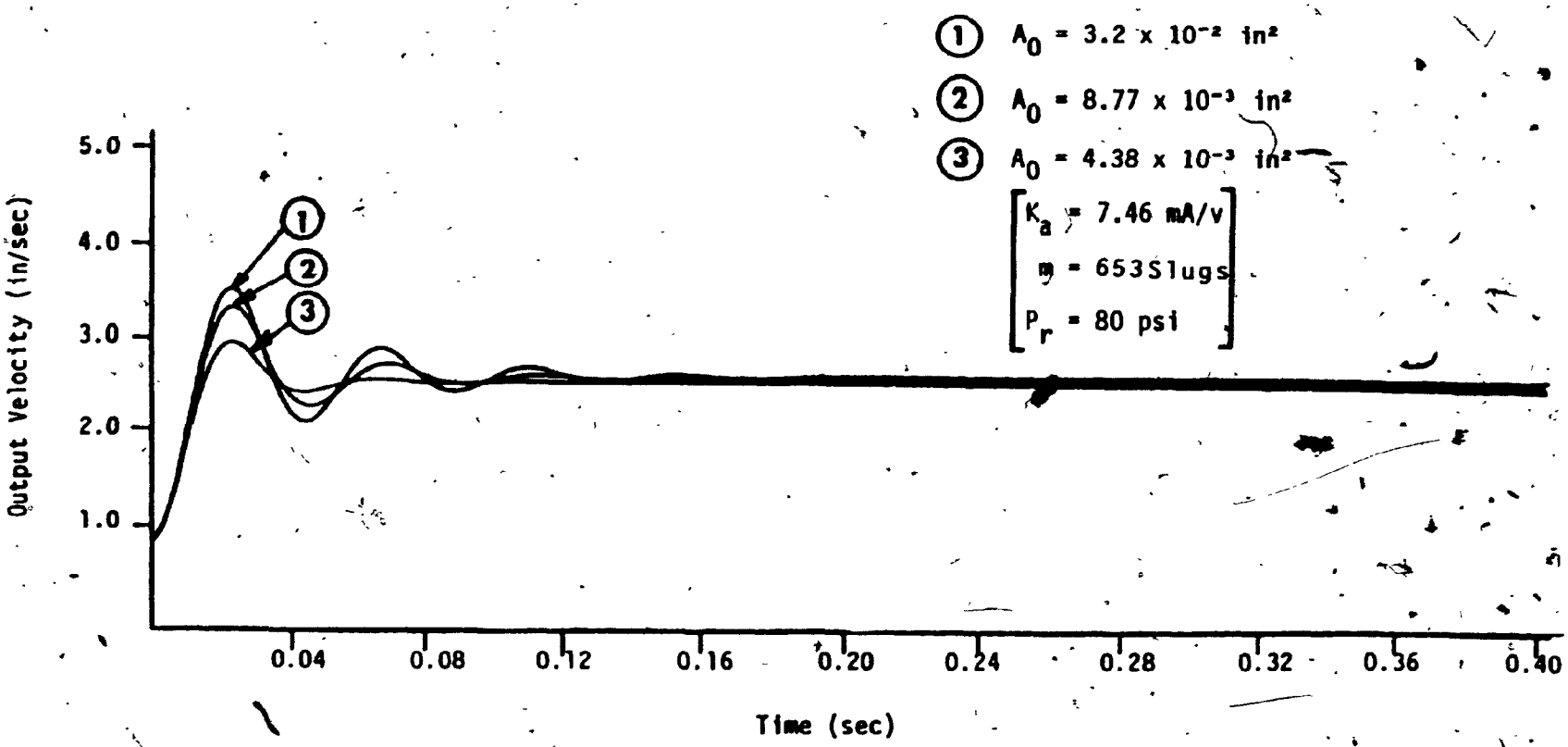

Fig. 4.3: Effect of Metering Orifice on New Servovalve: 2-Step Input (Simulation)

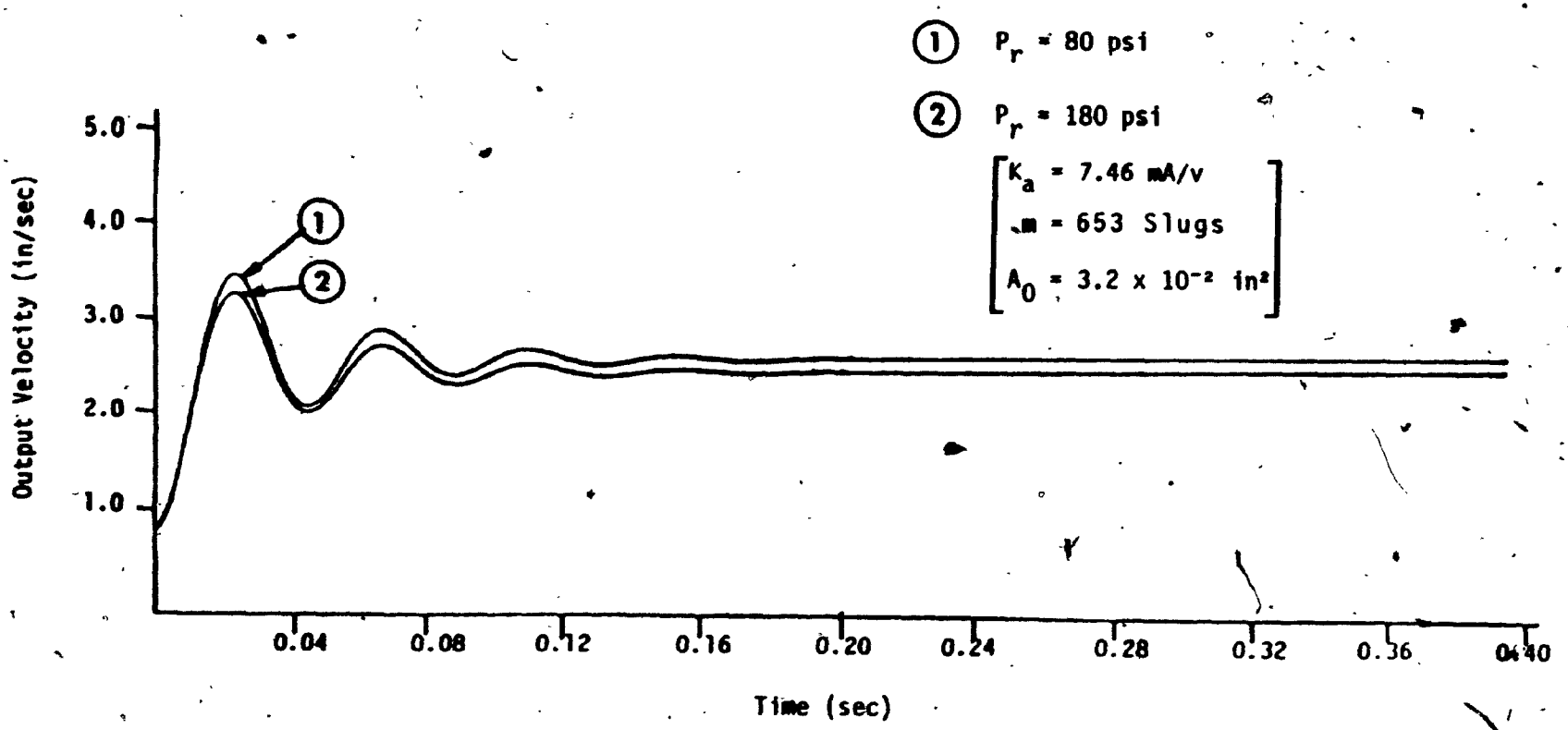

Fig. 4.4: Effect of Back Pressure on New Servovalve: 2-Step Input (Simulation)

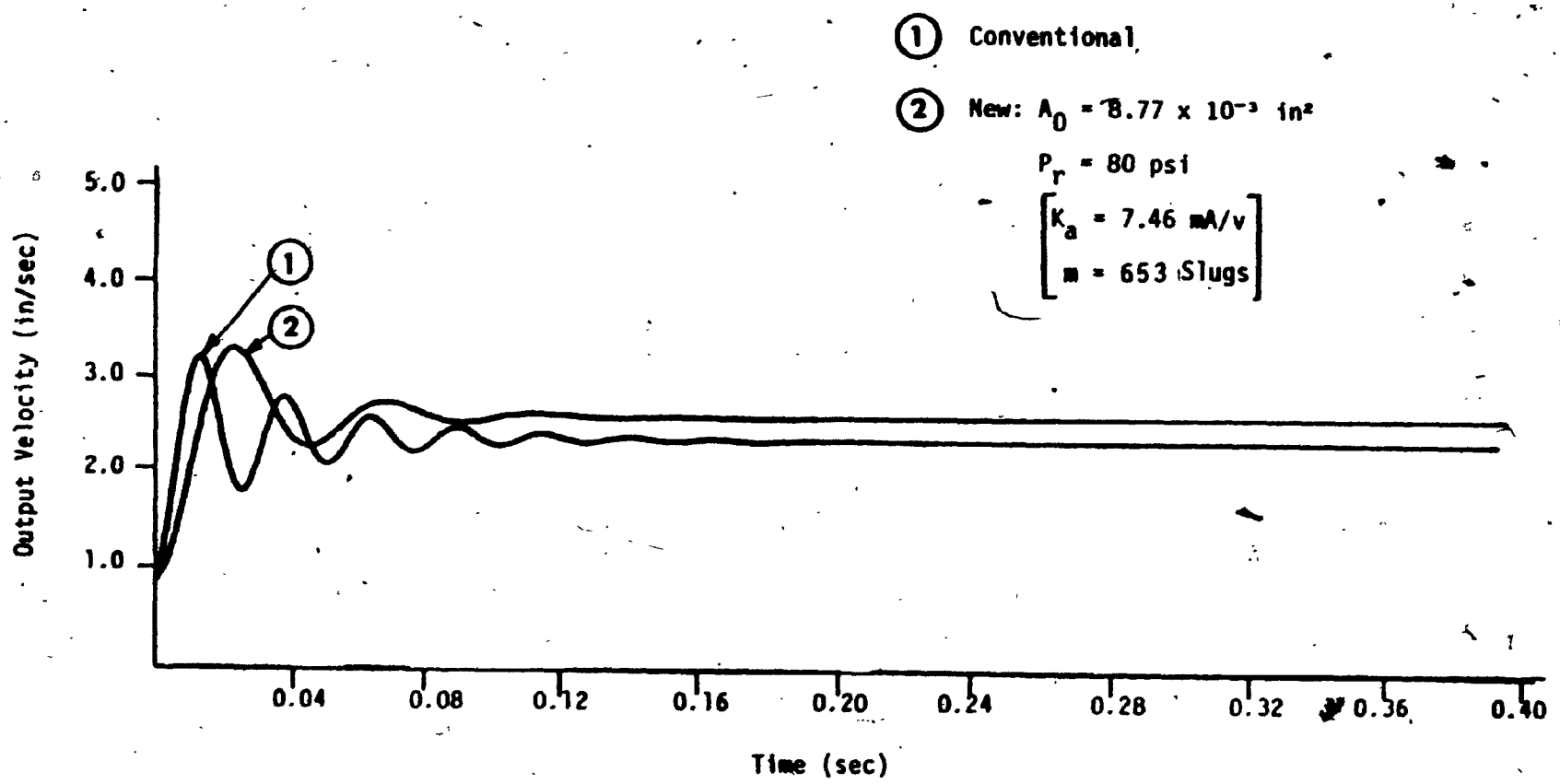

Fig. 4.5: Comparison of Conventional and New Servovalve: 2-Step Input (Simulation)

From Fig.4.4, the following conclusions can be drawn. As the back pressure is increased form 80 psi ($4.83*10^5$ N/m^2) to 180 psi ($1.24*10^6$ N/m^2) ,

i) the % overshoot is reduced from 48% to 44% but there is no significant change in settling time.

ii) the steady state velocity is reduced from 2.64 in/sec (0.067 m/sec) to 2.46 in/sec (0.0625 m/sec). This can be explained by equation 3.26 which shows that the steady state velocity is proportional to square root of $(1- \lambda - p_r)$.

Fig. 4.5 shows the comparison of transient and steady state response for the conventional and the new servovalve which are tested under same input conditions. In case of the new servovalve configuration, the orifice size A_0 and the back pressure P_r are adjusted so as to get better characteristics than the conventional servovalve. Following conclusions can be drawn.

i) the steady state velocity for the new servovalve is 2.3 in/sec (0.059 m/sec) and that for the conventional servovalve is 2.06 in/sec (0.0528 m/sec).

ii) the new servovalve offers higher damping than the conventional under same input conditions.

iii) the conventional servovalve has lower rise time (approx. 4 ms) than the new servovalve (approx. 9 ms)

iv) the damped natural frequency of the system with the conventional servovalve is 250 rad/sec whereas that with

the new servovalve is 150 rad/sec.

The two servovalve configuration were also tested for square wave input under conditions as stated in Table 4.2.

Figs.4.6 and 4.7 respectively show the effect of orifice area and the back pressure and Fig 4.8 shows the comparison of the conventional and the new servovalves for square wave input.

Fig. 4.6 shows the effect of reduction of orifice size from $3.2*10^{-2} in^2$ ($2.066*10^{-5}$ m^2) to $8.77*10^{-3}$ in^2 ($5.66*10^{-6}$ m^2). It can be concluded that as the orifice area is reduced,

i) the rise time does not change considerably (and is approx. equal to 17 ms).

ii) the damped natural frequency of the system also independent of the orifice size (and is approx. equal to 136 rad/sec).

iii) the damping is increased and therefore the settling time is reduced.

iv) the steady state velocity is reduced from 2.84 in/sec (0.073 m/sec) to 2.8 in/sec (0.072 m/sec). As already explained, this confirms with the equation 3.26.

From Fig. 4.7, we can say that as the back pressure is increased form 80 psi ($4.83*10^5$ N/m^2) to 180 psi ($1.24*10^6$ N/m^2),

i) the % overshoot is reduced from 59% to 57% and the

Type	V_i	K_a	M	A_0	P_r
	V	mA/V	Slugs	in^2 (m^2)	psi (N/m^2)
Conventional	2.1	7.09	792	--	--
New	2.1	7.09	792	$3.2*10^{-2}$ ($2.066*10^{-5}$)	80 ($4.83*10^5$)
					180 ($1.24*10^6$)
				$8.77*10^{-3}$ ($5.66*10^{-6}$)	80 ($4.83*10^5$)
					180 ($1.24*10^6$)
				$4.38*10^{-3}$ ($2.83*10^{-6}$)	80 ($4.83*10^5$)
					180 ($1.24*10^6$)

Table 4.2 Input and Test Conditions: square wave input.

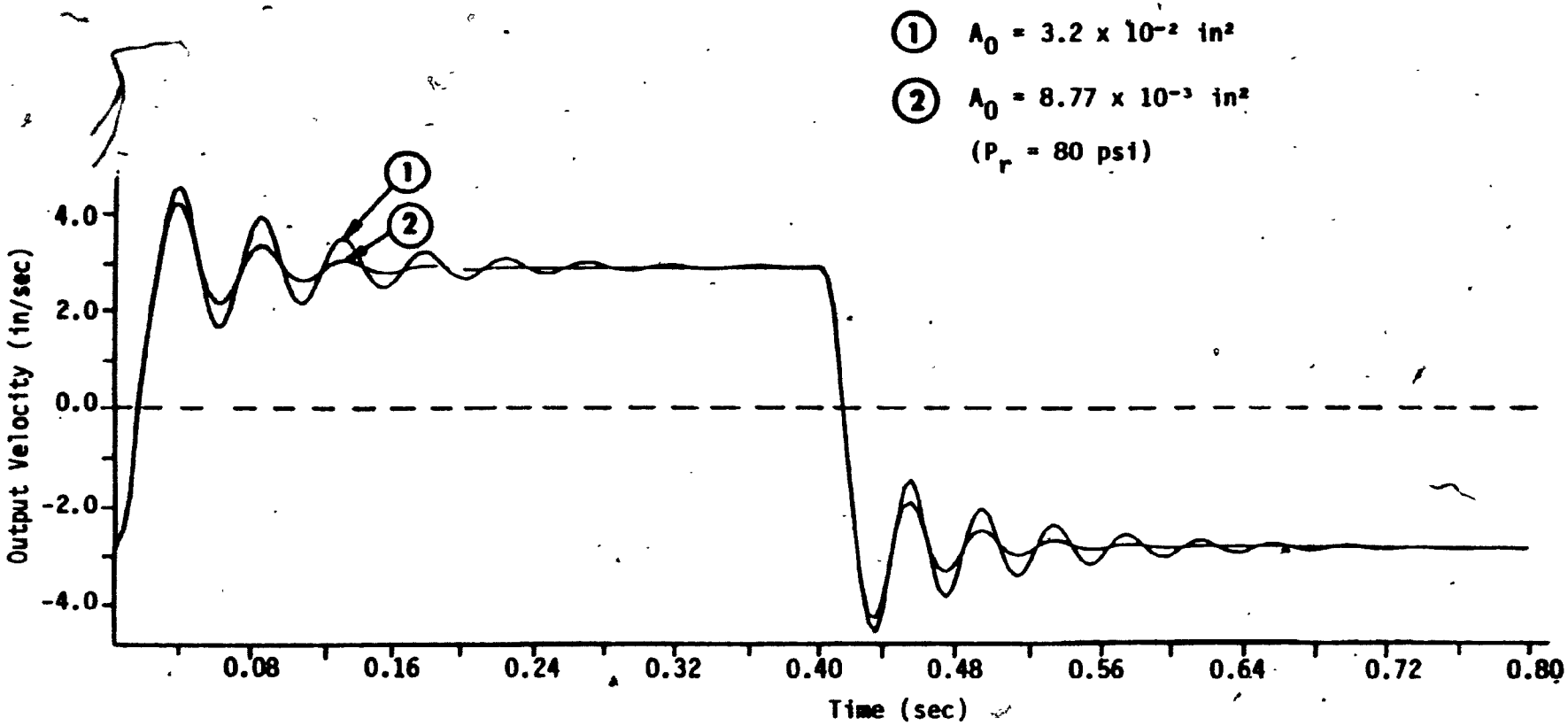

Fig. 4.6: Transient Response of New Servovalve for Different Orifice Sizes: square wave input. (Simulation)

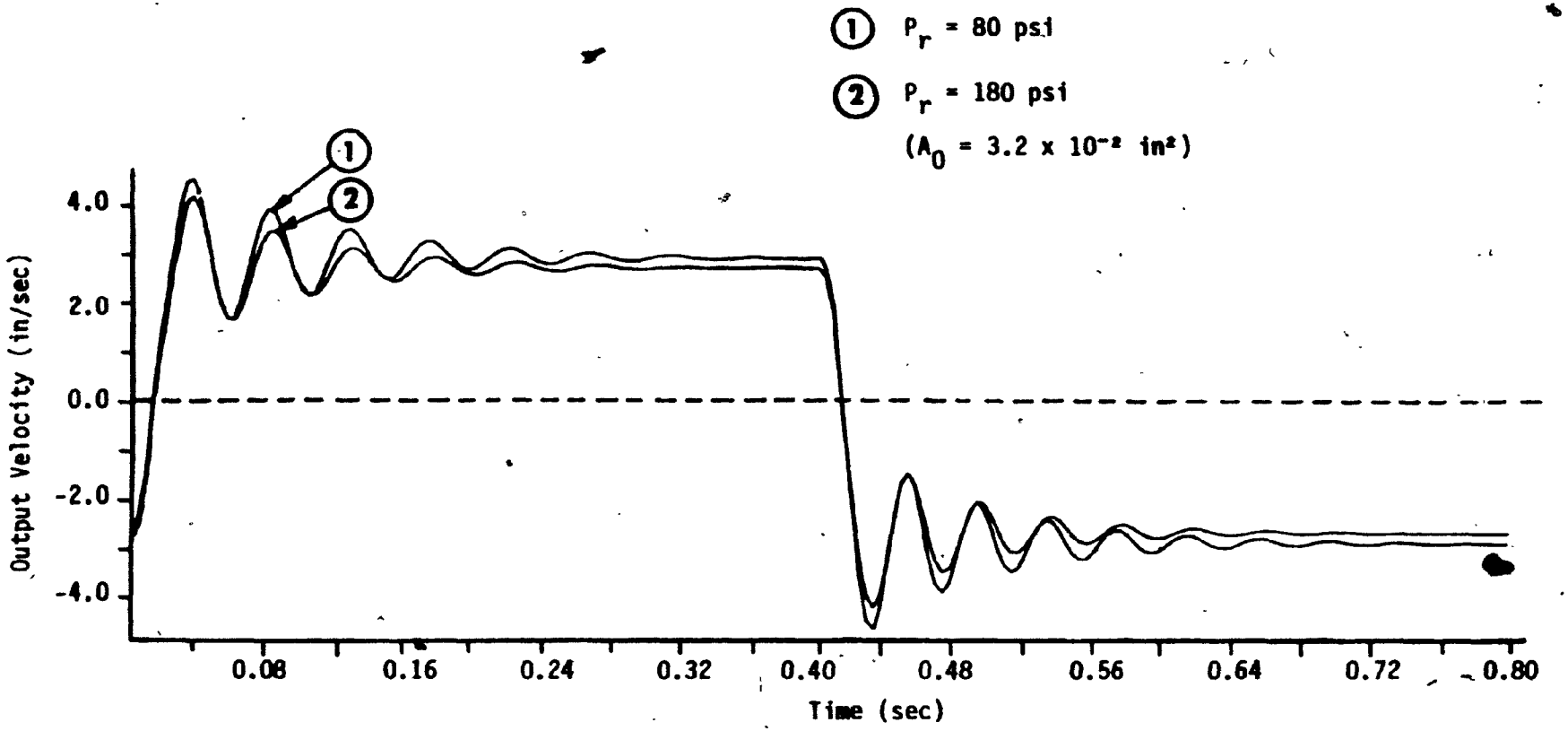

Fig. 4.7: Transient Response of New Servovalve for Different Back Pressures: square wave input. (Simulation)

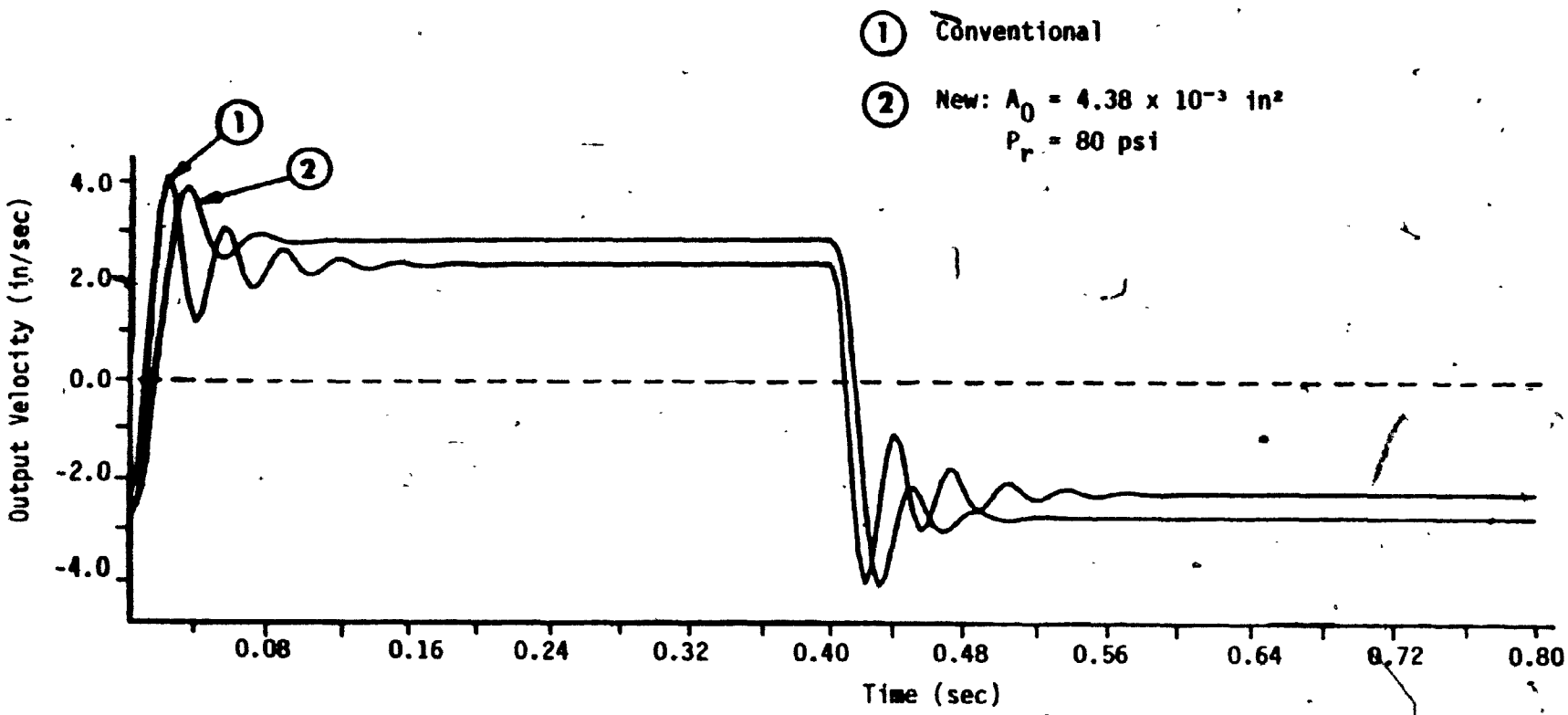

Fig. 4.8: Comparison of Conventional and New Servovalve: square wave input (Simulation).

settling time is reduced marginally.

ii) the steady state velocity is reduced from 2.6 in/sec (0.067 m/sec) to 2.5 in/sec (0.064 m/sec). Again, this also confirms with the equation 3.26.

Fig. 4.8 shows the comparison of the conventional and the new servovalve under same input conditions. The response of the new servovalve with $A_0=4.38*10^{-3}$ in^2 ($2.83*10^{-6}$ m^2) and P_r=80 psi ($4.83*10^6$ N/m^2) is chosen for comparison. Following deductions can be drawn form the comparison.

i) the steady state velocity for new servovalve is 2.69 in/sec (0.069 m/sec) whereas that for conventional servovalve is 2.28 in/sec (0.058 m/sec).

ii) the new servovalve also offers higher damping than the conventional servovalve.

iii) the rise time for the conventional servovalve is 9 ms and that for the new servovalve is 17 ms.

iv) the damped natural frequency for the conventional servovalve is 192 rad/sec whereas that for the new servovalve is 136 rad/sec.

4.5 SUMMARY

In this chapter, the two systems with the conventional and the new servovalve are modelled and simulated on a digital computer. The transient and steady

state response of both the servovalves is tested under identical two-step and square wave input conditions. From these simulation results the conclusions are drawn which are summarized below.

For the new servovalve configuration,

a) as the orifice size is reduced,

i) the damping is increased and the steady state velocity is reduced.

ii) there is no appreciable change in the rise time and the damped natural frequency.

b) as the back pressure is increased,

i) the % overshoot is reduced and there is some reduction in settling time.

ii) the steady state velocity is reduced.

The comparison of the conventional and the new servovalve shows that,

i) the new servovalve offers a higher steady state velocity and higher damping under similar input conditions.

ii) the damping of the system depends on the size of the orifice and the back pressure.

iii) the system with conventional servovalve has lower rise time and higher damped natural frequency than that with the new servovalve.

CHAPTER 5

EXPERIMENTAL INVESTIGATION OF THE TWO SERVOVALVE CONFIGURATIONS

5.1 INTRODUCTION

In Chapter 3, steady state analysis of servosystems with two servo configurations has been done. This analysis showed that the new servovalve gives higher steady state velocity under certain conditions. The two configurations have been modelled and simulated and their transient responses have been studied in Chapter 4. The transient analysis was based on simplified mathematical representation of individual components. This chapter describes the experimental evaluation of the two servo configurations.

Section (5.2) describes the test set up used for experiments. In section (5.3), operation of the test rig is explained. The selection and special features of the components used in the test set up are discussed in section (5.4). Section (5.5) includes results of various experiments carried on the two servovalve configurations. Finally in section (5.6), the results are compared and conclusions are drawn.

5.2 DESIGN AND DESCRIPTION OF THE TEST STAND

The design of the test stand was based on the operational and functional requirements. From the operational point of view, space, ease of operation, and ease of changing from the conventional to the new servovalve configuration were of the prime importance. In order to reduce the space requirement, most of the components were mounted on a plate which was fixed to the base vertically. To facilitate quick change from the conventional to the new configuration, seven quick change manual on-off valves were installed at the appropriate locations. From the functional requirement servovalve, direction control valve etc. were selected [section 5.4] and the servo controller, on-off controller were designed.

Fig. 5.1 shows the pictorial view of the experimental set up. The hydraulic power supply consists of a tank (1), a variable displacement non-compensated piston pump (2), an electric motor (3), a direct operated relief valve (4), a check valve (5), and an accumulator (6). The electric motor drives the pump whose delivery could be varied by changing the pump displacement. The pressure developed by the pump depends upon the relief valve setting (4). Once the pump displacement is set, the pump delivery is constant. This delivery has to be always greater than the load flow requirement at any time in order to achieve constant pressure. The relief valve maintains constant pressure by

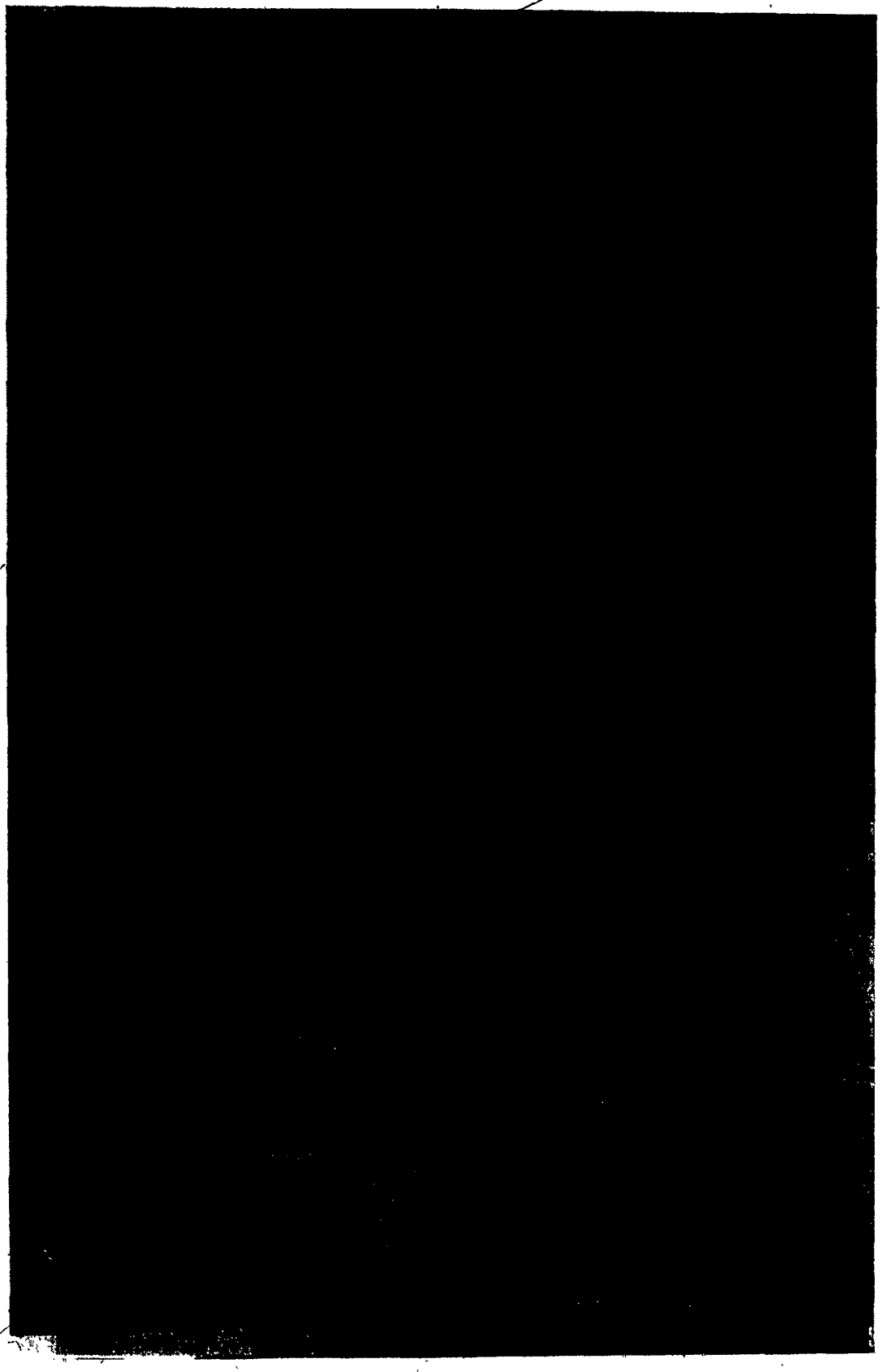

Fig. 5.1 Pictorial View of the Experimental Set Up

dumping the excess quantity of the oil back to the tank. The accumulator (6), helps to reduce pressure ripple caused by discontinuous pump delivery and change in load flow requirement. The check valve (5) installed between the pump and the accumulator prevents back flow from the accumulator to the pump. A fine high pressure filter (7) is placed between the accumulator and the servovalve to keep the contamination level to a prescribed limit.

Since the excess quantity of oil is always dumped to the tank at high pressure, oil temperature is raised. In order to keep this temperature at the permissible level, a heat exchanger, a low pressure pump and a low pressure filter is used to form an independent pumping and cooling system (8). The oil from the tank is passed through the low pressure filter and the heat exchanger where it is cooled by circulating water.

A two stage flow control servovalve (9) is used to control the flow to the actuator. In order to drive the servovalve, a proportional type servovalve controller (10) is used. The controller output is connected to the first stage of the servovalve viz. the torque motor which displaces the spool and controls the flow to the linear actuator (11). A double ended piston is selected so as to obtain symmetrical characteristics in either directions. One end of the piston is connected to a loading table (12) on which inertial load could be mounted. A heim joint is used

to couple the loading table and the piston so as to take some misalignment. The table is mounted on two sets of linear roller bearings and shaft assemblies which offer negligible frictional resistance and also takes some misalignment. Two external stops are installed outside the cylinder so that cylinder damage due to piston impact is avoided. A 4 way 3 position direction control valve (13) is installed between the servovalve and the actuator which is required to switch the pressure and drain ports in case of the new servovalve configuration. An on-off controller (14) is used to drive the appropriate solenoid of the direction control valve depending upon the sign of the error. A fine metering valve is placed (15) in the drain line which can be adjusted to give accurate orifice by means of a calibrated vernier handle. A pilot operated relief valve (16) is installed in the downstream of the metering valve to adjust the back pressure. In order to change the servovalve configuration quickly, seven (7) manual on-off valves are installed in appropriate locations.

Diaphragm type pressure tranducers are used to record pressures in the actuator chambers. A moving magnet type velocity transducer is used to measure the velocity of the load and also to use it as a feedback device.

5.3 OPERATION OF THE TEST STAND

The hydraulic pump, which is coupled to the electric motor, pumps oil from the tank and gives a constant displacement. The relief valve and accumulator combination provides a constant pressure to the servovalve. The spool of the servovalve is displaced proportional to current in the torque motor coils. This current can be varied by varying the input voltage and the forward loop gain. The controller can be used in either open or closed loop mode and the type of input can be selected by function generator. In order to test the system with the conventional servovalve, manual valves (3) and (6) are closed and the rest are kept open. [Fig. 5.2]. The flow path in this case is shown by arrows drawn adjacent to the pipe lines in Fig. 5.2 e.g. in the forward stroke, the pump supplies oil which passes through valve (1), and the servovalve, to the valve (5). Since the valve (5) is open, the oil is supplied to the actuator. The return line is connected to the tank through valves (7) and (4), the servovalve and valve (2). For return stroke, valves (4) and (7) are on pressure side whereas valves (2) and (5) are on return side.

The actuator drives the load which is mounted on the loading table. The output velocity is sensed by the velocity transducer attached to the table. The velocity transducer gives output voltage proportional to the table velocity.

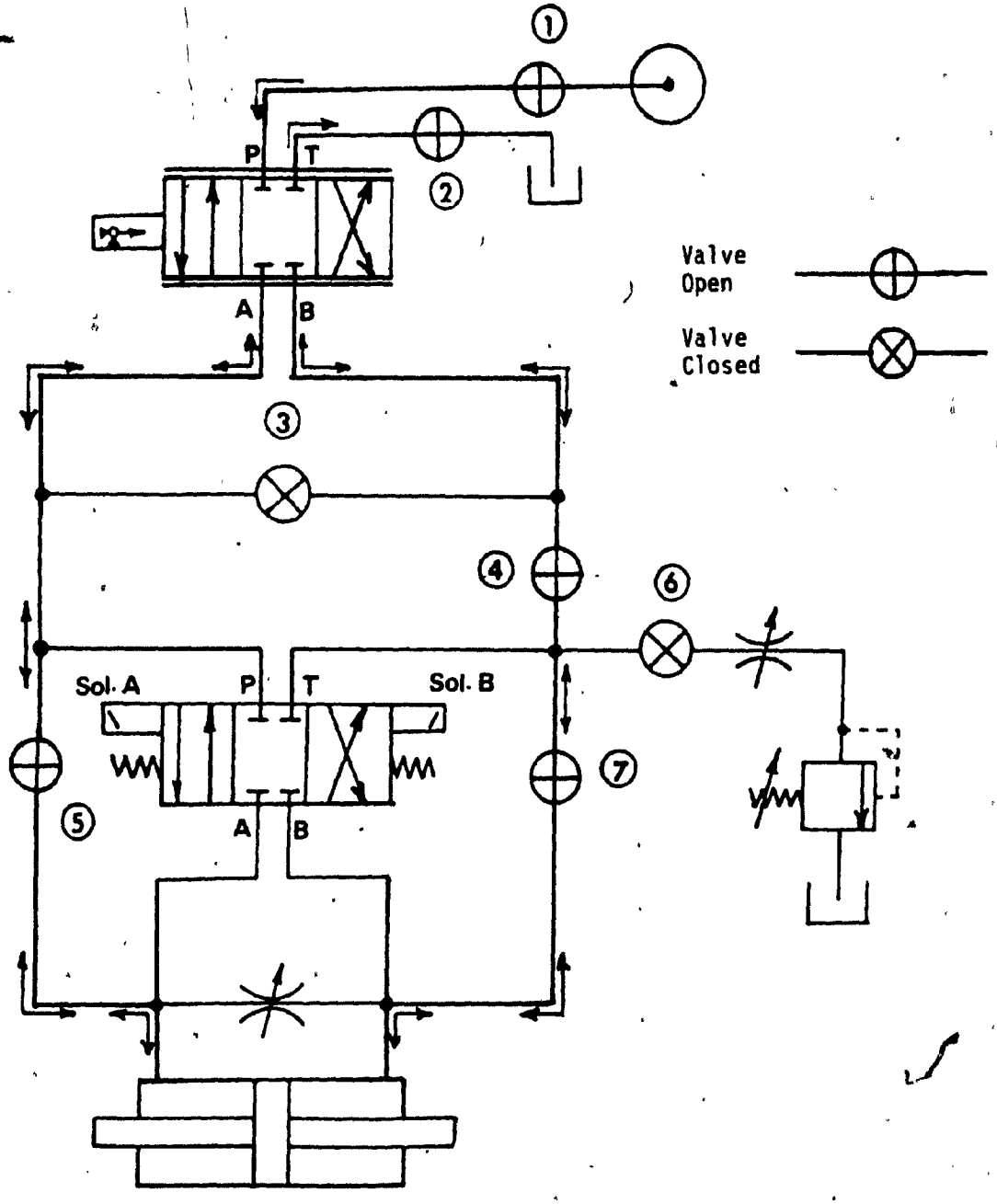

Fig. 5.2 Flow Path for Conventional Servovalve Configuration

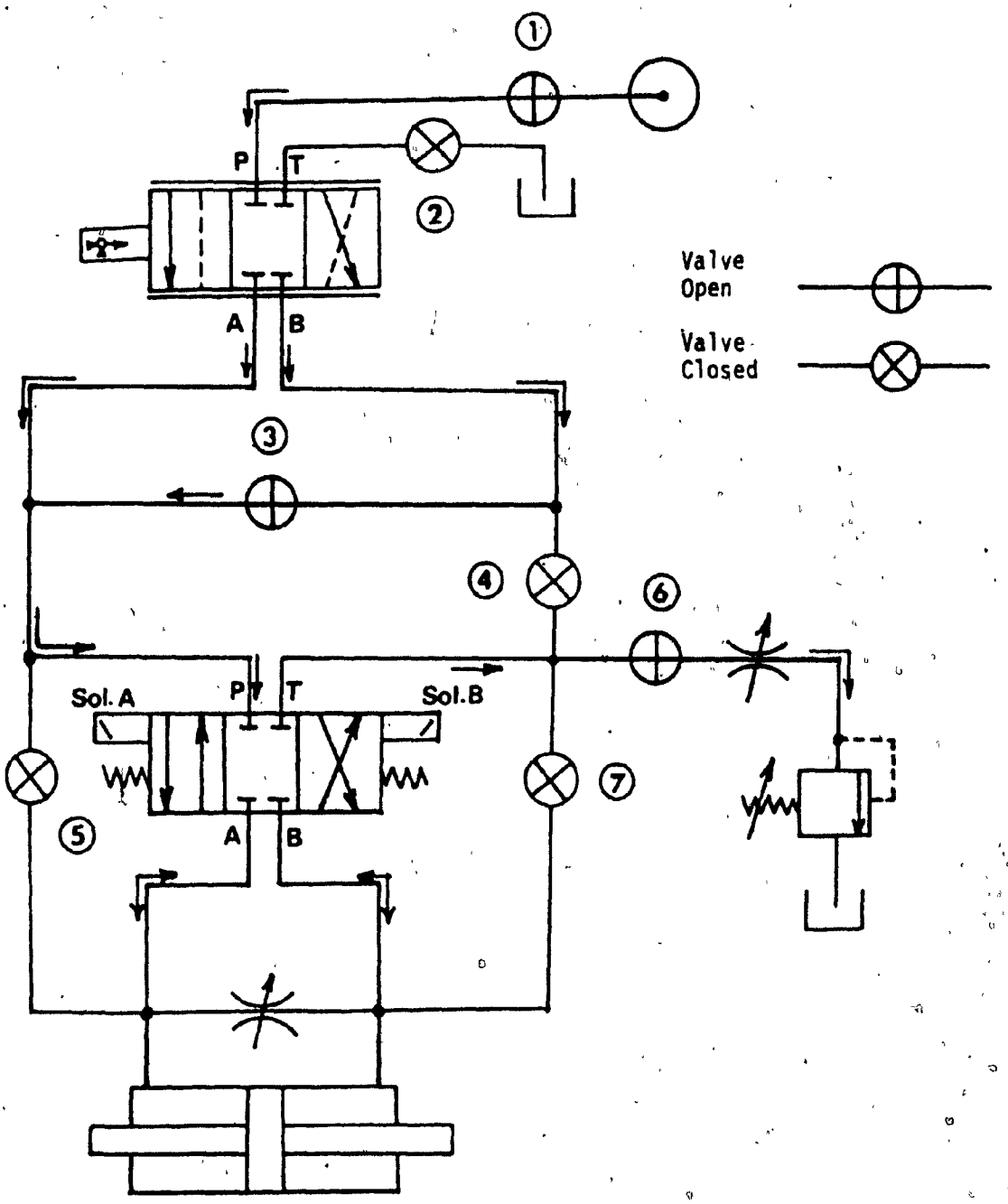

Fig. 5.3. Flow Path for New Servovalve Configuration

This voltage is fed back to the summing junction on the servovalve controller to complete the loop.

For testing the new servovalve configuration, valves (2),(4),(5) and (7) are closed and rest of them are kept open [Fig. 5.3]. In this case, for either stroke, the direction control valve receives a common pressure line since the output ports of the conventional servovalve are joined together. For forward stroke, port A of the direction control valve is connected to the pressure side and port B is connected to the drain side. Similarly, for return stroke, B is connected to the pressure side and A is connected to the tank through the valve (6), the metering valve and the relief valve.

As explained in section 2.5, for the new servovalve configuration, the function of switching the pressure and drain ports is done by the direction control valve. The sign of the error voltage $(V_i - V_f)$ is used as an input to the on-off controller which drives the direction control valve. Depending upon this sign, either solenoid A or solenoid B is activated. A fine needle type metering valve and pilot operated relief valve are installed in the drain line. The needle valve is fitted with a calibrated vernier handle so that the drain orifice can be adjusted accurately and repetetively. The relief valve is also calibrated so as to set the back pressure accurately.

5.4 SELECTION OF COMPONENTS

Table 5.1 describes the special features of important components and the reasons for their selection. As a common selection criterion, the hydraulic components were selected in such a way that the pressure rating is at least 3 times the operating pressure (1000 psi). The specifications of all the components are given in Appendix D.

Components	Special features	Reasons for selection
Servovalve	.Aircraft quality .Flatfrequency upto 35 Hz	.Good linearity and low threshold. .Canbe represented by byfirstorder transfer function for this application
Actuator	.Double ended .5 inch stroke .No cushioning	.Similar characteristics in both directions. .Compact .Full stroke can be used for testing
Needle valve	.Ratio of orifice size to servovalve opening at rated current = 16	.Extremely accurate .Different area ratios available

Table 5.1 Special Features of Components used in Test Set Up.

Table 5.1 (Continued)

Direction control valve	.Rated flow 7 gpm .120 V AC solenoid .4way,3position spring centered, center blocked	.Low pressure losses in the valve .Faster switching time than DC solenoid .Replacethe servovalve vaive to perform the function of switching pressure and drain ports
Relief valve	.Pilot operated .50-1000 psi pressure settings	.Low pressure override .Different pressure level settings (P_r/P_s) possible
Velocity transducer	.Moving magnet type	.Linear .No external excitation required, output voltage proportional to the velocity

5.5 EXPERIMENTAL RESULTS AND COMPARISON

As explained in the Chapter 4, the two servovalve configurations are tested for two types of inputs viz. two-step and square wave. The input and the test conditions for the two-step and the square wave input are respectively given in Table 4.1 and 4.2. In order to verify the results obtained from the simulation, tests are carried out on the two servovalve configurations under same conditions.

The Table 5.2 gives the input conditions for two-step input which is same as Table 4.1. Fig. 5.4 and 5.5 respectively show the effect of system gain K_a and mass M on the transient and steady state response of the conventional servovalve. It can be seen as the gain is increased from 6.67 mA/V to 7.46 mA/V (Fig. 5.4), the steady state velocity is increased from 2.0 in/sec (0.051 m/sec) to 2.5 in/sec (0.064 m/sec) and there is no change in damped natural frequency of the system. Also, as the mass is increased, from 653 to 938 Slugs (Fig. 5.5), the damped natural frequency of the system is reduced and there is reduction in the steady state velocity (2.5 in/sec to 2.35 in/sec). The effect on damping, or % overshoot is not significant.

Fig. 5.6 and 5.7 respectively show the effect of metering orifice A_0 and back pressure P_r on the response of the new servovalve which can be stated as follows. As the

Type	V_{i1} V	V_{i2} V	K_a mA/V	M Slugs	A_0 in^2 (m^2)	P_r psi (N/m^2)
Conventional	0.8	1.2	6.67	653	--	--
				938	--	--
			7.46	653	--	--
				938	--	--
New	0.8	1.2	6.67	938	$3.2*10^{-2}$ ($2.066*10^{-5}$)	80 ($4.83*10^5$)
						180 ($1.24*10^6$)
					$8.77*10^{-3}$ ($5.66*10^{-6}$)	80 ($4.83*10^5$)
						180 ($1.24*10^6$)
					$4.38*10^{-3}$ ($2.83*10^{-6}$)	80 ($4.83*10^5$)
						180 ($1.24*10^6$)
			7.46	653	$3.2*10^{-2}$ ($2.066*10^{-5}$)	80 ($4.83*10^5$)
						180 ($1.24*10^6$)
					$8.77*10^{-3}$ ($5.66*10^{-6}$)	80 ($4.83*10^5$)
						180 ($1.24*10^6$)
					$4.38*10^{-3}$ ($2.83*10^{-6}$)	80 ($4.83*10^5$)
						180 ($1.24*10^6$)

Table 5.2 Input and Test Conditions: 2-Step Input

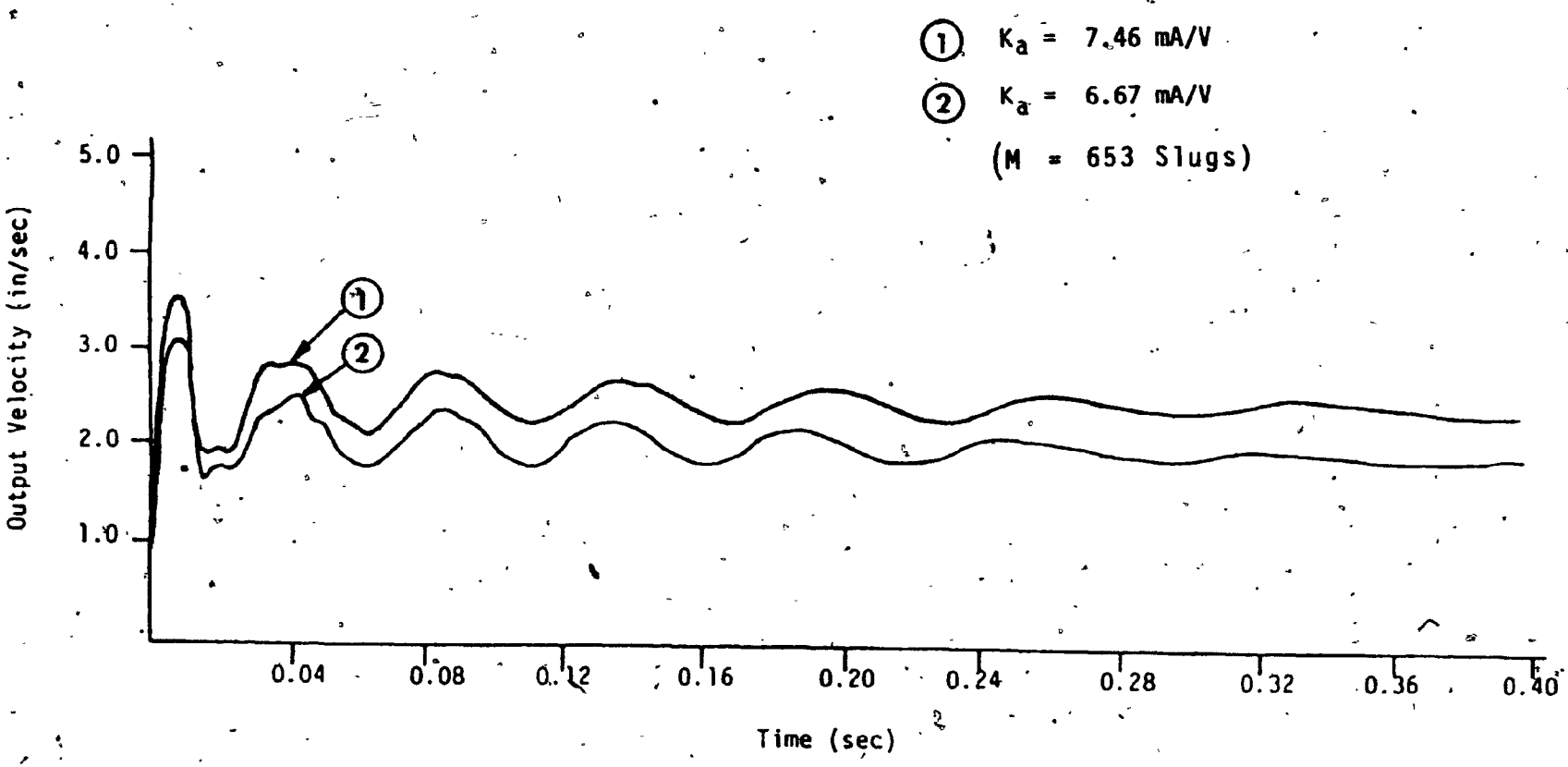

Fig. 5.4. Effect of Gain on Conventional Servovalve: 2-Step Input (Experimental)

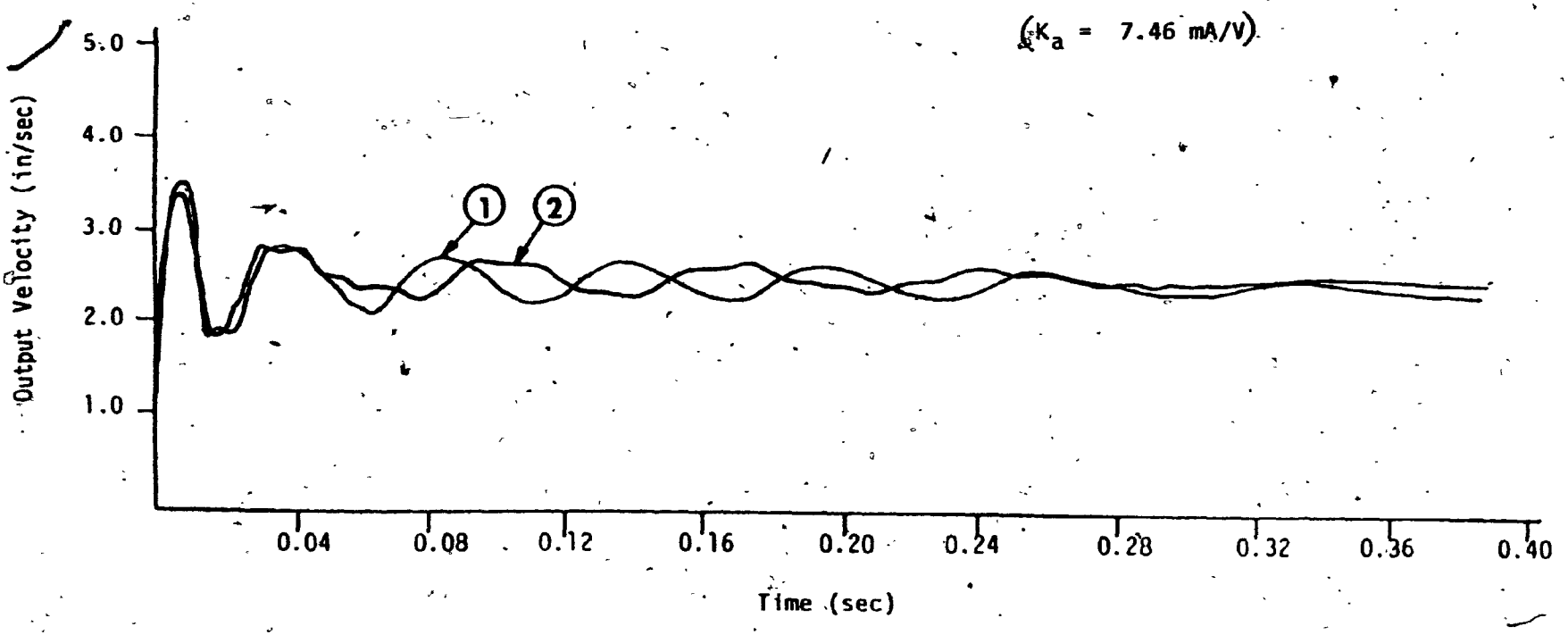

Fig. 5.5. Effect of Mass on Conventional Servovalve: 2-Step Input (Experimental)

orifice size A_0 is reduced (Fig. 5.6), the steady state velocity is reduced from 3 in/sec (0.076 m/sec) to 2.2 in/sec (0.07 m/sec) to 2.2 in/sec (0.056 m/sec). Also the settling time is seen to be reduced (especially for curves 1 and 3 in Fig. 5.6). As the back pressure is increased, the steady state velocity is reduced from 3.0 in/sec (0.076 m/sec) to 2.8 in/sec (0.071 m/sec).

In Fig. 5.8, the response of the conventional and the new servovalve is compared. For the new servovalve, $A_0=8.77*10^{-3}$ in^2 and $P_r=80$ psi is chosen which is seen to give best response out of the different test conditions. It can be seen that the under identical input conditions,

i) the new servovalve gives 2.6 in/sec (0.066 m/sec) and the conventional servovalve gives 2.43 in/sec (0.061 m/sec)

ii) the new servovalve offers higher damping than the conventional servovalve.

iii) the conventional servovalve shows a rise time of approx. 3 ms whereas that for new servovalve is approx. 5 ms.

The two servovalve configurations are then subjected to square wave input under the input conditions as given in Table 5.3 (which is same as Table 4.2).

Fig. 5.9 and 5.10 respectively show the effect of orifice area and back pressure on the new servovalve under cyclic input.

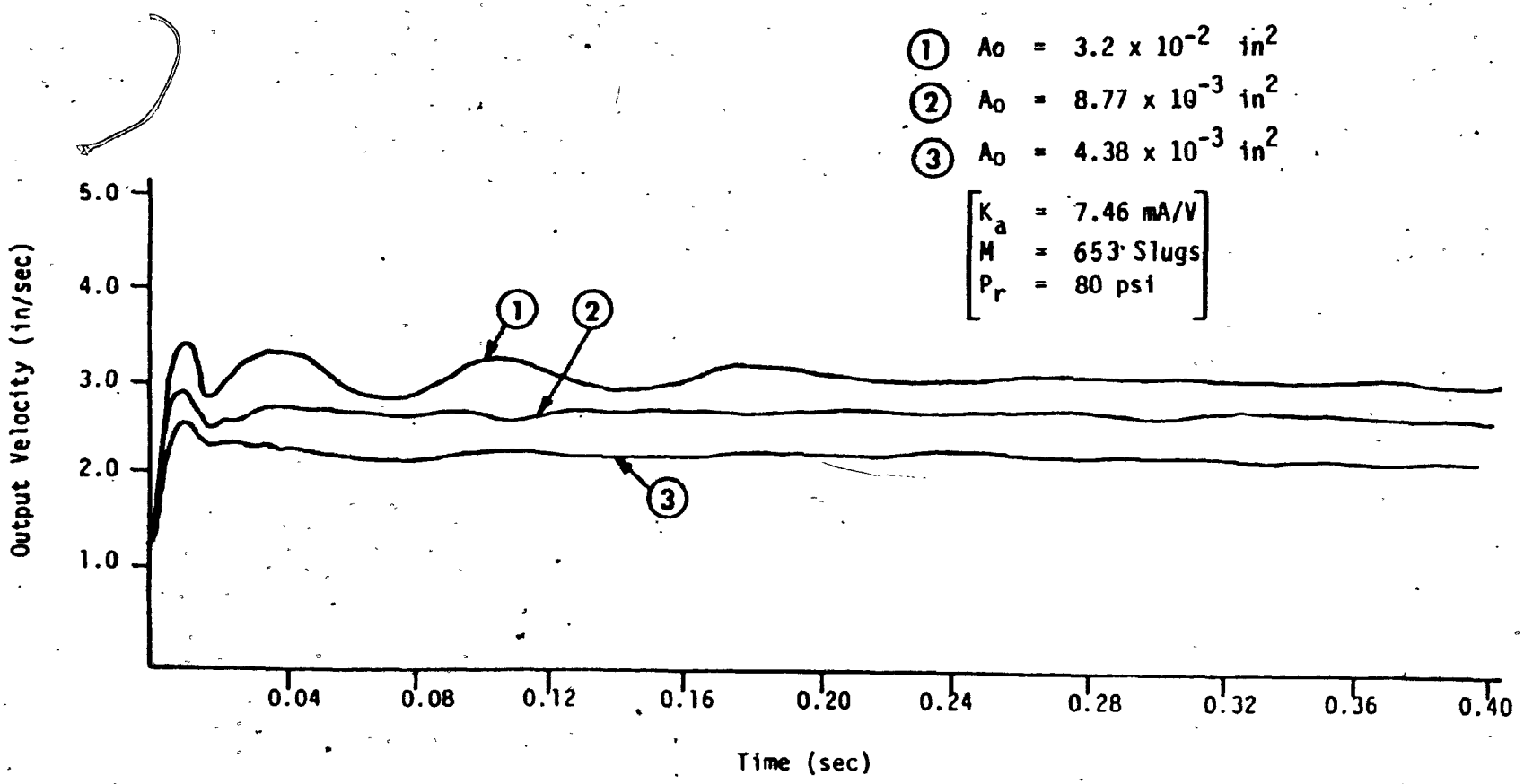

Fig. 5.6. Effect of Metering Orifice on New Servovalve: 2-Step Input (Experimental)

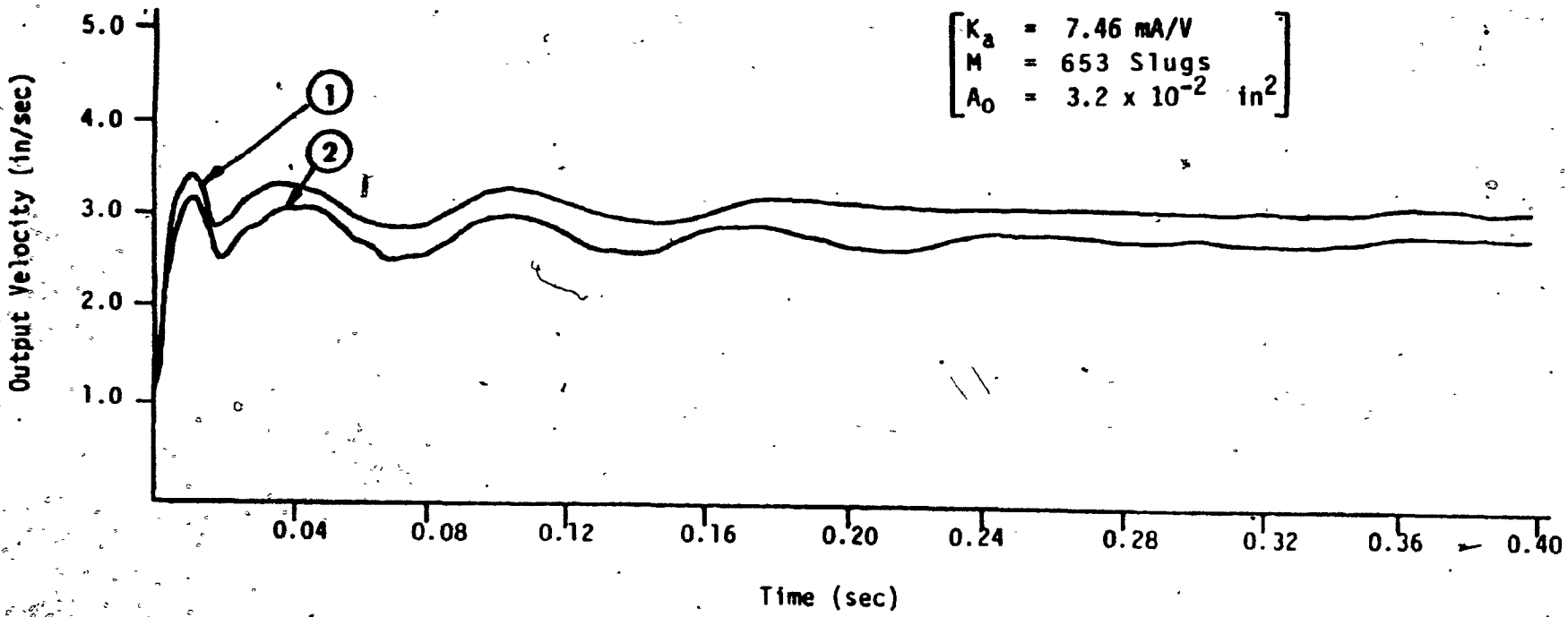

Fig. 5.7. Effect of Back Pressure on New Servovalve: 2-Step Input (Experimental)

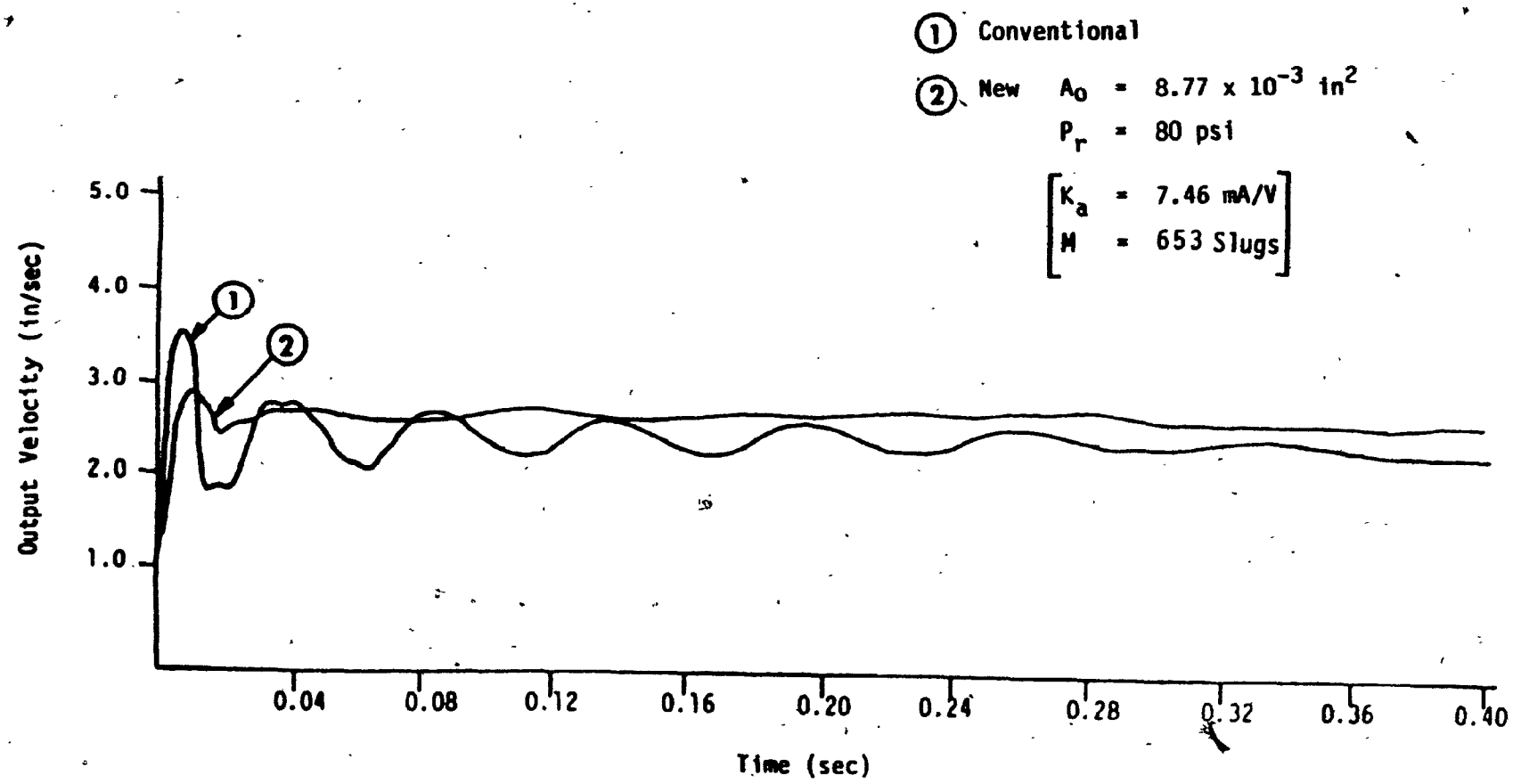

Fig. 5.8. Comparison of Conventional and New Servovalves: 2-Step Input (Experimental)

Type	V_i	K_a	M	A_0	P_r
	V	mA/V	Slugs	in^2 (m^2)	psi (N/m^2)
Conventional	2.1	7.09	792	--	--
New	2.1	7.09	792	$3.2*10^{-2}$ ($2.066*10^{-5}$)	80 ($4.83*10^5$)
					180 ($1.24*10^6$)
				$8.77*10^{-3}$ ($5.66*10^{-6}$)	80 ($4.83*10^5$)
					180 ($1.24*10^6$)
				$4.38*10^{-3}$ ($2.83*10^{-6}$)	80 ($4.83*10^5$)
					180 ($1.24*10^6$)

Table 5.3 Input and Test Conditions: square wave input.

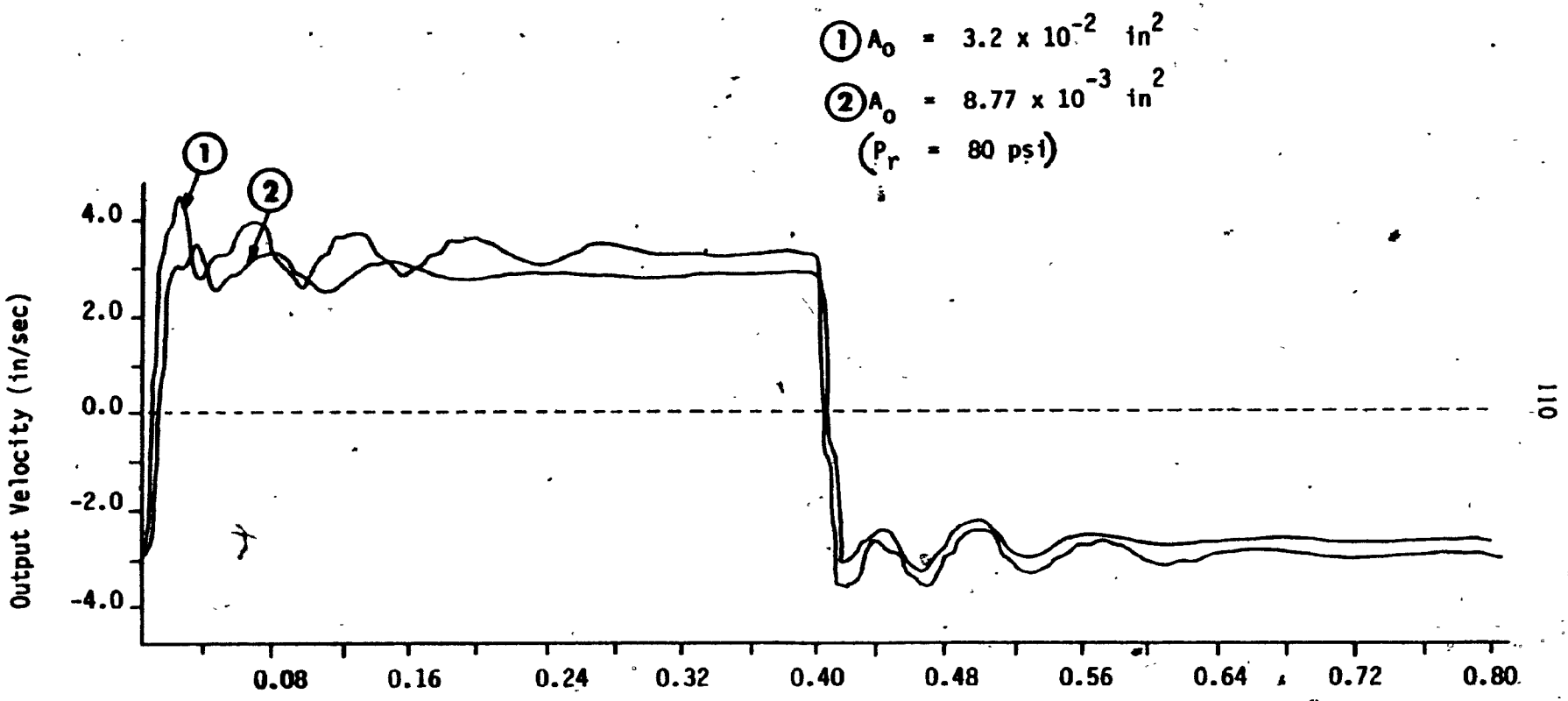

Fig. 5.9. Transient Response of New Servovalve for Different Orifice Sizes: square wave input. (Experimental)

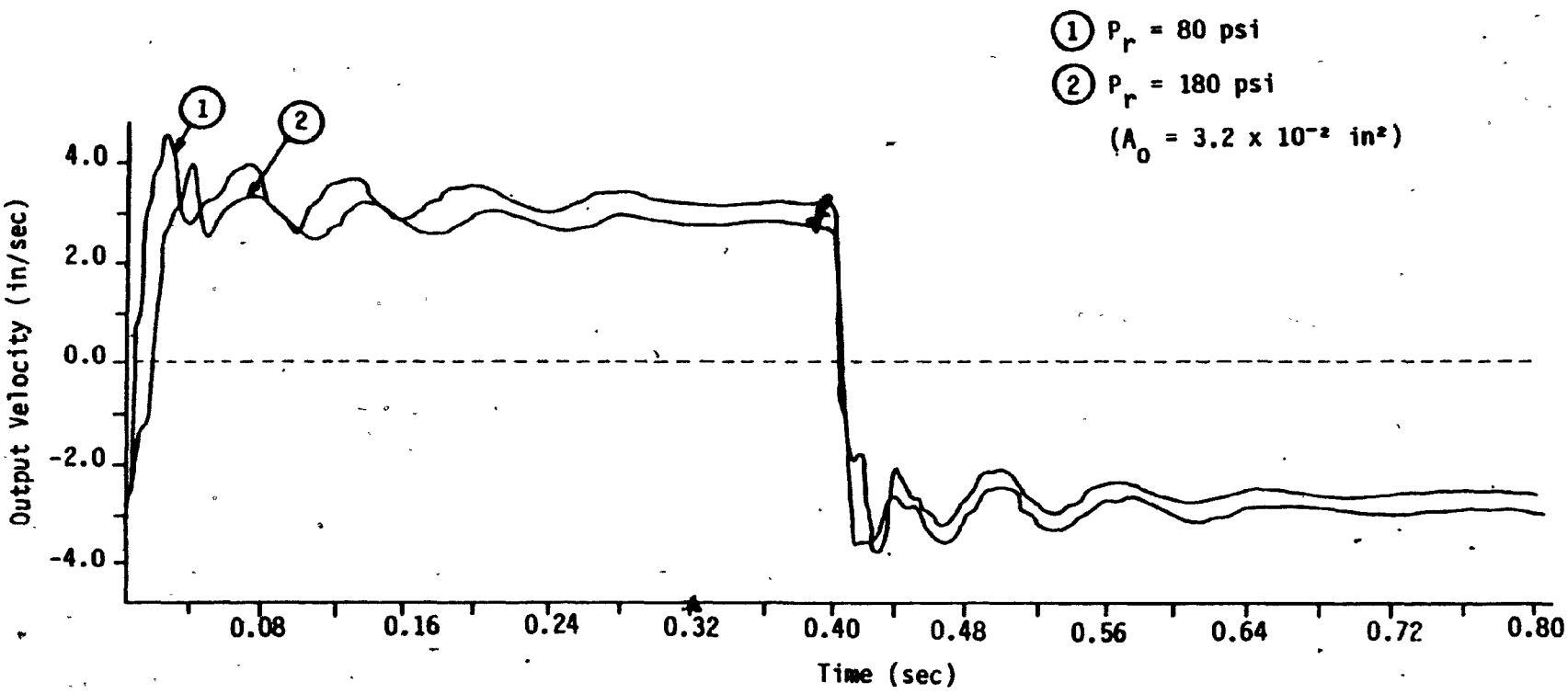

Fig. 5.10: Transient Response of New Servovalve for Different Back Pressures: square wave input (Experimental).

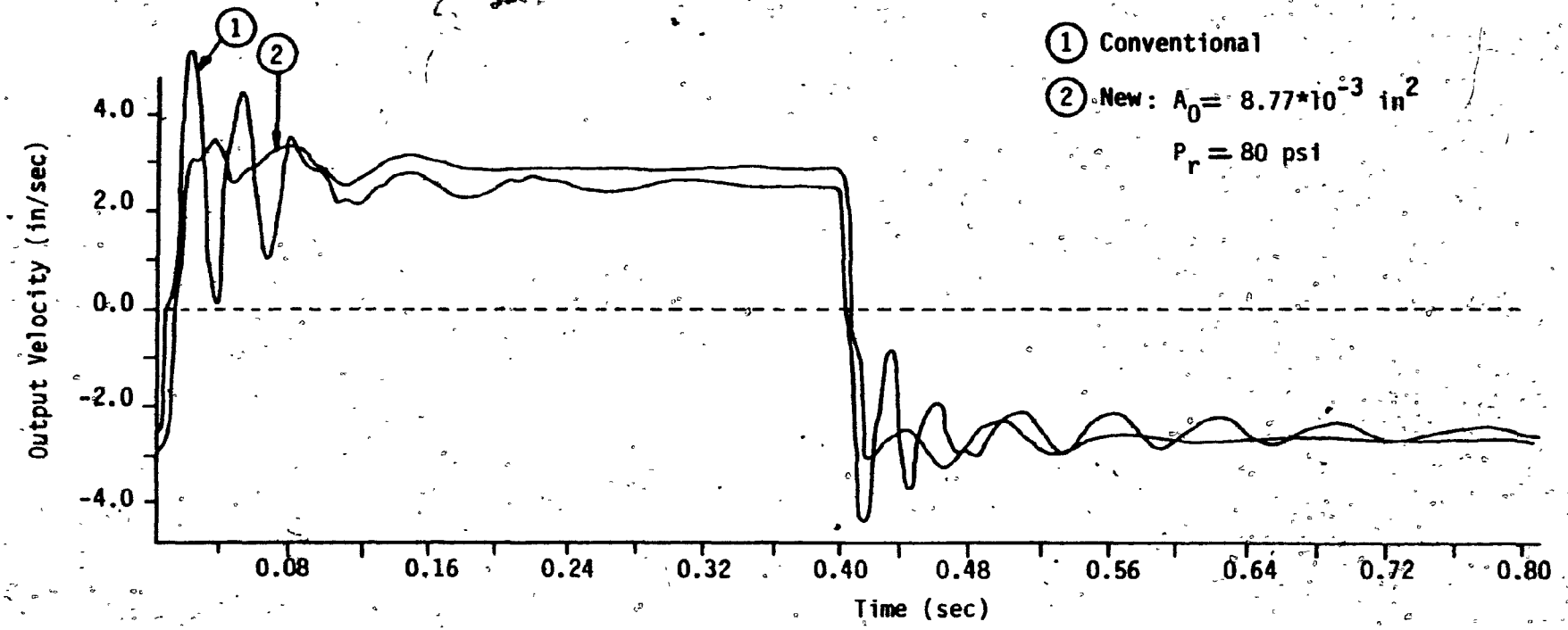

Fig. 5.11: Comparison of Conventional and New Servovalve: square wave input (Experimental).

From Fig. 5.9, it can be seen that as the orifice is reduced,

i) steady state velocity is reduced from 3.21 in/sec (0.083 m/sec) to 2.93 in/sec (0.075 m/sec).

ii) there is no appreciable change in the rise time or the damped natural frequency.

iii) the damping is increased.

In case of negative voltage input (return stroke), the transient response was seen to be inconsistent.

Some nonlinearity is seen for about 60 ms after the direction of the step has been changed. This can be explained by the fact that immediately after the step change the velocity and hence the flow is changing, causing the relief valve opening to adjust for the flow.

Fig. 5.10 shows the effect of increase in back pressure from 80 psi ($4.83*10^5$ N/m^2) to 180 psi ($1.24*10^6$ N/m^2). It can be seen that as the back pressure is increased,

i) the steady state velocity reduces from 3.26 in/sec (0.083 m/sec) to 2.82 in/sec (0.072 m/sec).

ii) the nonlinearity viz. the dead zone is seen to be more prominent in initial (approx.) 60 ms. This can be explained by the fact that as the back pressure is increased, the force required to move the relief valve spool to another position is increased.

iii) the damped natural frequency is not affected.

In Fig. 5.11, the conventional and new servovalve are compared. From the comparison, following conclusions can be drawn.

i) the system with conventional servovalve shows some nonlinearity close to zero velocity. This may be due to change in the coulomb friction as the direction of motion is changed.

ii) the new servovalve gives steady state velocity of 3.26 in/sec (0.0083 m/sec) whereas the conventional servovalve gives 2.8 in/sec (0.072 m/sec).

iii) the new servovalve offers higher damping than the conventional servovalve.

5.6 SUMMARY

In this chapter, conventional and new servovalves are tested under 2- step and square wave inputs on the experimental test rig. From the experimental results, the following conclusions can be drawn.

For the new servovalve configuration,

a) as the orifice size is reduced,

i) the damping is increased and the steady state velocity is reduced.

ii) there is no significant change in the rise time and the damped natural frequency of the system.

b) as the back pressure is increased,

i) the effect of relief valve dynamics is more

significant.

ii) the steady state velocity is reduced.

The comparison of the conventional and the new servovalve shows that,

i) the new servovalve offers a higher steady state velocity and higher damping under similar input conditions.

ii) the damping of the system depends on the size of the orifice. Increase in back pressure reduces the % overshoot.

iii) the system with conventional servovalve has lower rise time.

CHAPTER 6

COMPARISON OF SIMULATION AND EXPERIMENTAL RESULTS

6.1 INTRODUCTION

In chapter 4, the systems with the conventional and the new servovalve are modelled and simulated for 2-step and square wave inputs. In chapter 5, experimental response of both the servovalves is analysed for the same set of input and test conditions used in chapter 4.

In this chapter, section 6.2 covers the comparison of experimental and simulation results for two-step and square wave inputs and in section 6.3 conclusions are drawn based on this comparison.

6.2 COMPARISON

As explained in section 4.3, the mathematical model is developed based on some assumptions. Some of these assumptions are, that the actuator coulomb friction is as described by equation 4.10, that the switching of direction control valve is described only by a pure time delay, that the relief valve offers a constant back pressure etc. Even though the simulation and the experimental results, in general, show the same trend, it is necessary to compare the two sets of results in order to check the mathematical

model.

Figs. 6.1 and 6.2 respectively show the comparison of experimental and simulation response for conventional servovalve. Figs. 6.3, 6.4 and 6.5 show the comparison of experimental and simulation results for new servovalve.

Individually, the simulation and experimental results have been already included in sections 4.4 and 5.5 respectively.

From Fig. 6.1, it can be seen that the discrepancy between the two sets of results in steady state velocity is only 3%. The experimental response is seen to be more oscillatory than the simulation. The discrepancy in damped natural frequency is seen to be high (approx. 27%).

From Fig. 6.2, it can be seen that the discrepancy in steady state velocity is 6%. In this case also the experimental response is found to be more oscillatory. Some nonlinearity in experimental response is observed near zero velocity. This may be due to the change in coulomb friction, as the direction of piston movement changes.

In Fig. 6.3, simulation and experimental response of new servovalve for 2-step input is compared. It is seen that the initial transient in experimental response does not

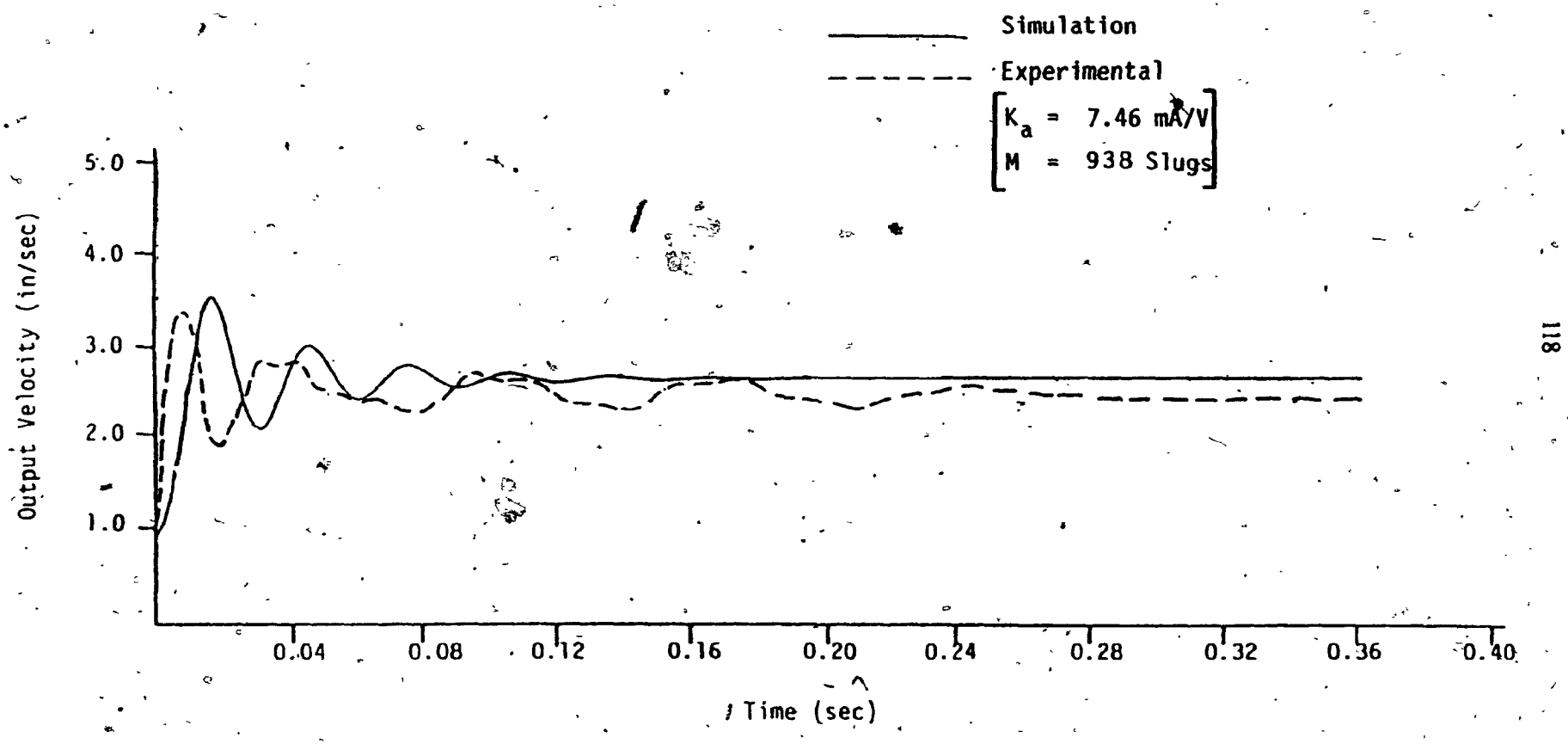

Fig. 6.1. Comparison of Simulation and Experimental Response: 2-Step Input (Conventional Servovalve)

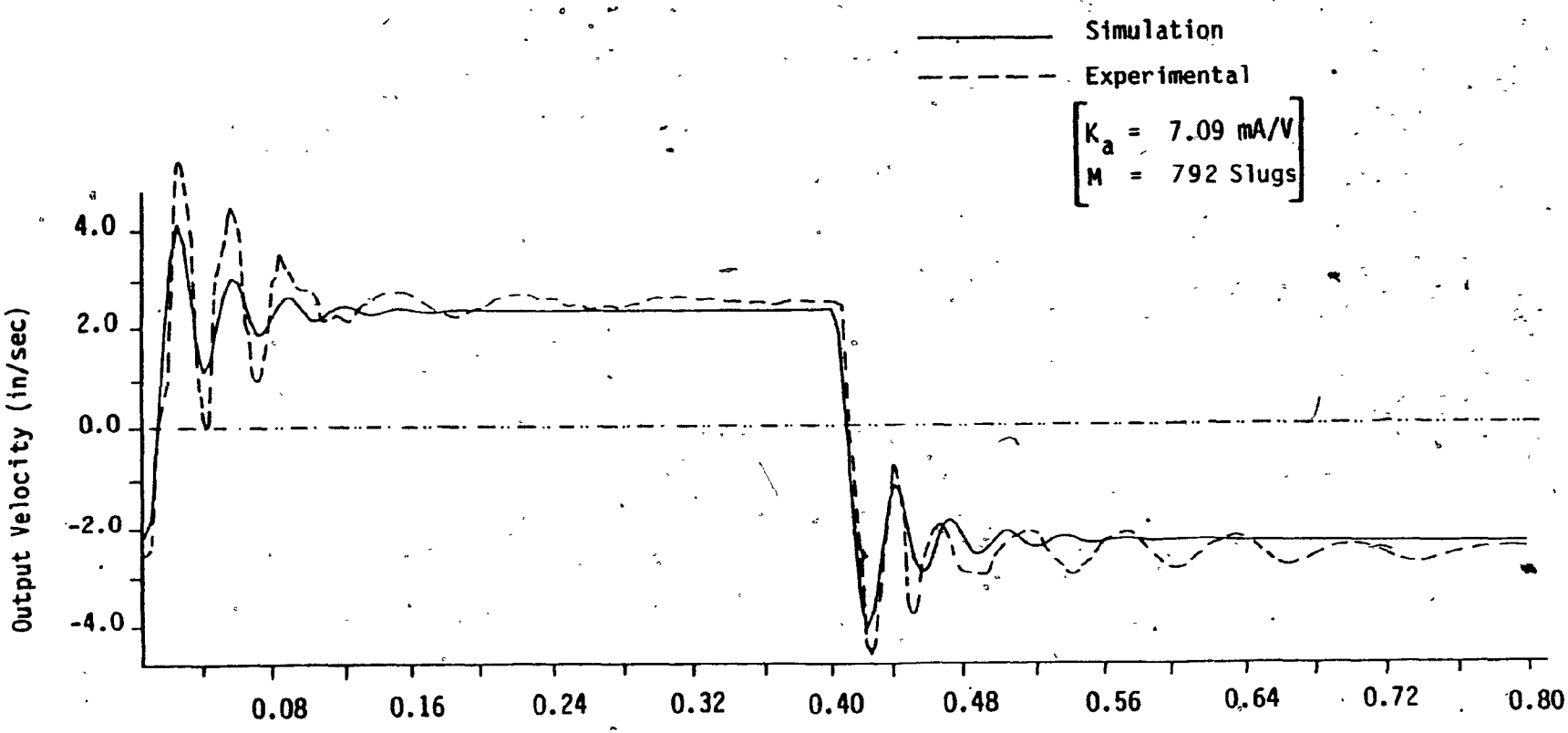

Fig. 6.2. Comparison of Simulation and Experimental Response: square wave input. (Conventional Servovalve)

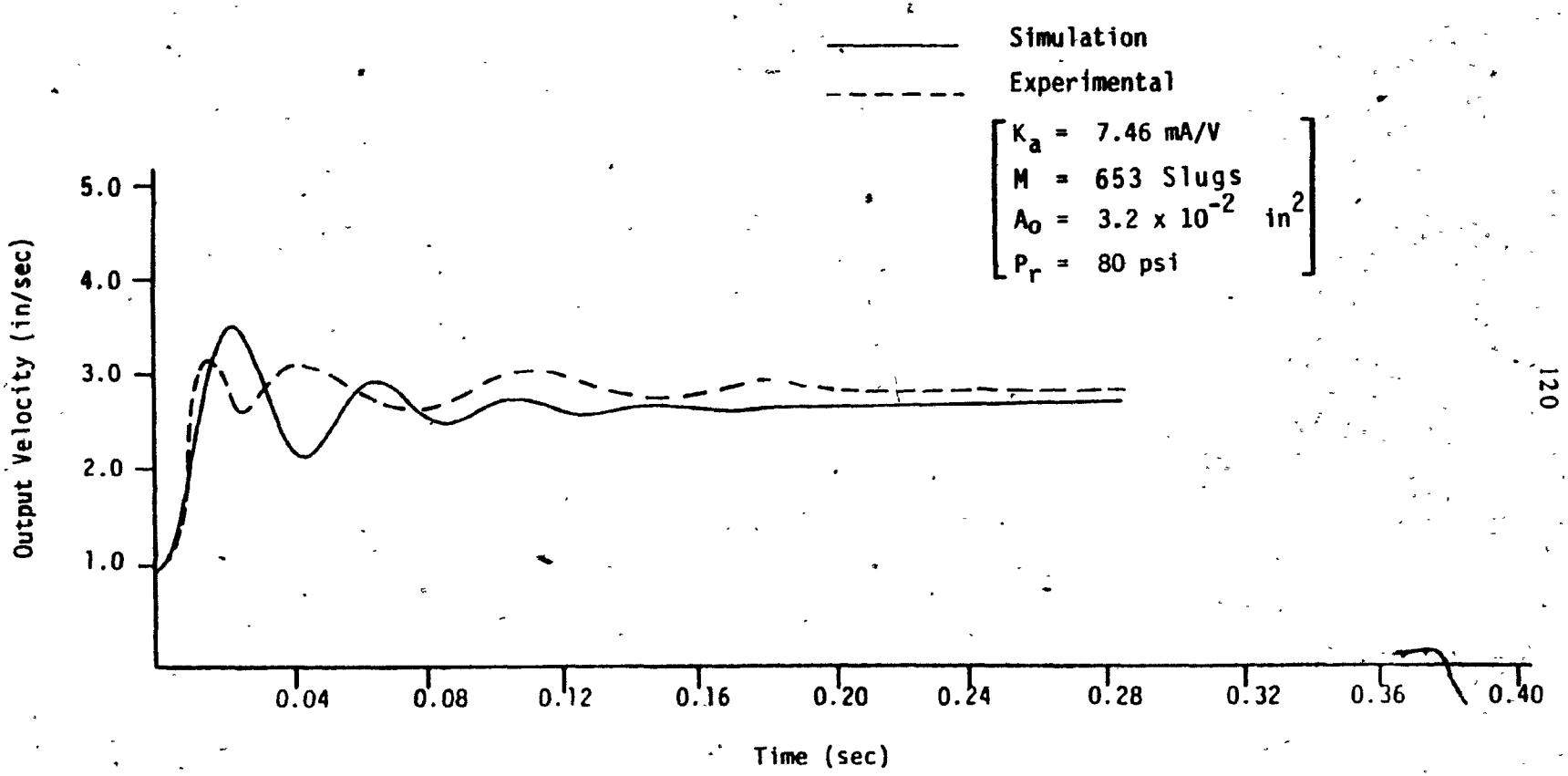

Fig. 6.3. Comparison of Simulation and Experimental Response: 2-Step Input (New Servovalve)

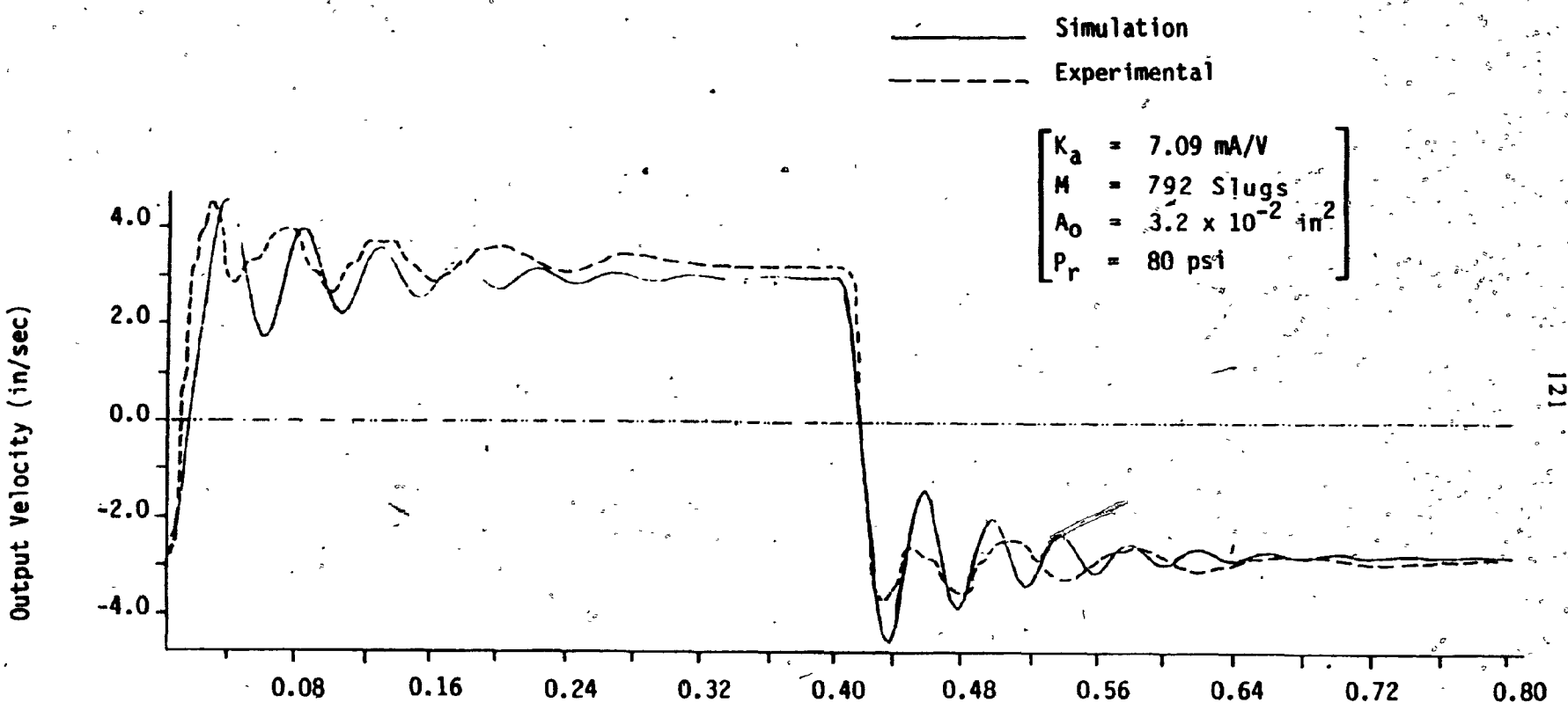

Fig. 6.4. Comparison of Simulation and Experimental Response, Orifice Size: square wave input, (New Servovalve)

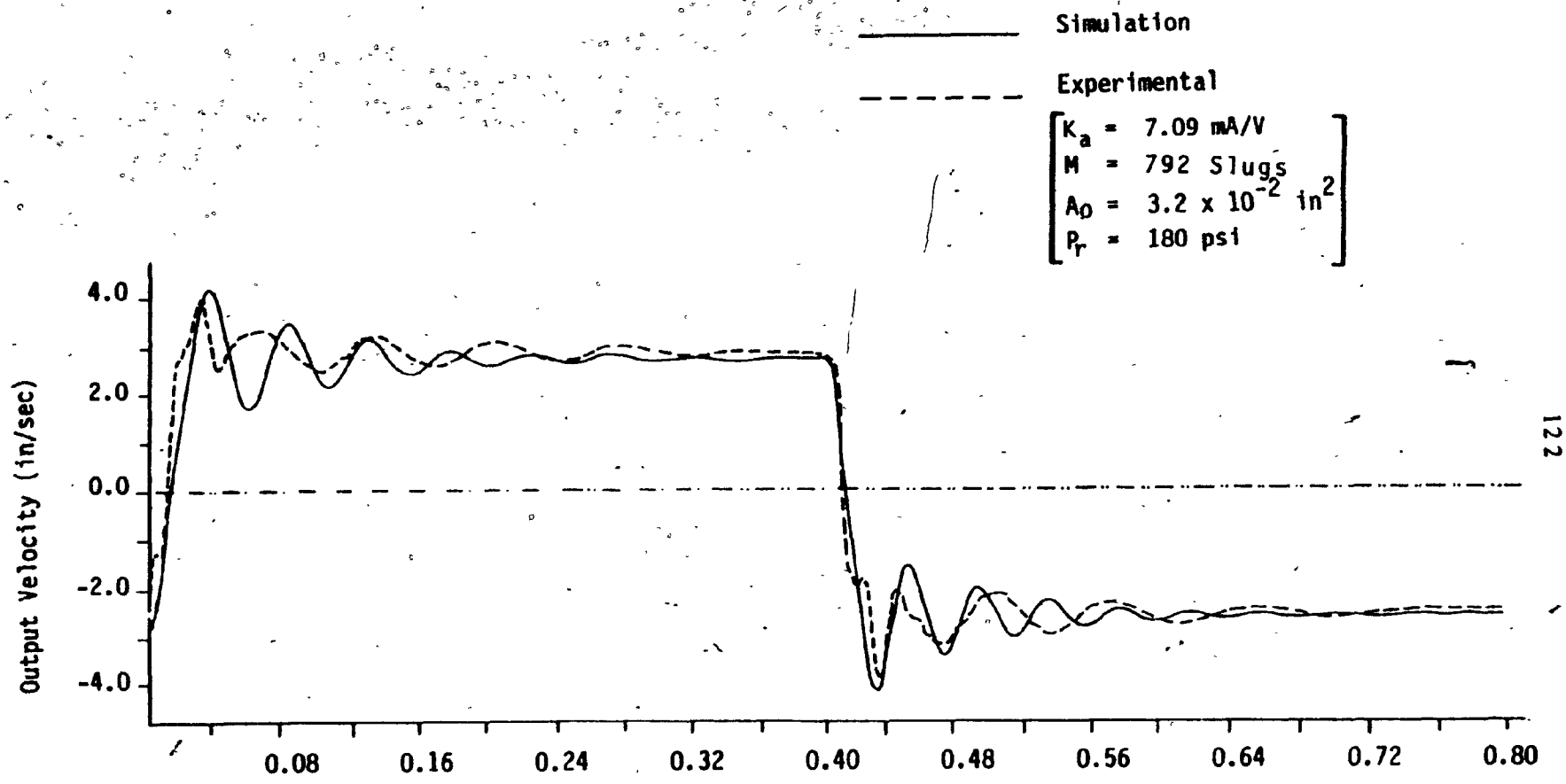

Fig. 6.5. Comparison of Simulation and Experimental Response, Back Pressure: square wave input (New Servovalve)

match favourably with the simulation. This can be explained by the following fact. When a second step is given, flow going through the relief valve is increased. During the transient flow condition, relief valve opening is changing and trying to adjust to the changing flow. Since the mathematical model does not take into account this phenomenon, discrepancy is seen between the experimental and simulation response during this period.

In Fig. 6.4, the effect of orifice size on the new servovalve is compared. The discrepancy in steady state velocity is seen to be 4% and also the correlation in transient response is close.

In Fig. 6.5, the simulation and experimental results for P_r=180 psi is compared. The discrepancy in steady state velocity is seen to be ±1%. The effect of relief valve dynamics is seen to be more because of the increase in back pressure.

6.3 CONCLUSIONS

Based on the comparison of the experimental and the simulation results, the following conclusions could be drawn.

- The mathematical model for servosystem with conventional servovalve is a sound guide to predict its performance when controlling an inertial load on

frictionless bearings.

- The mathematical model for servosystem with new servovalve is good to predict the transient response for different metering orifice areas and back pressure except in initial transient at high pressure setting. This model does not take into account the pressure transient due to sudden opening of the direction control valve when the actuator starts its motion.

CHAPTER 7

DESIGN PROCEDURE

7.1 INTRODUCTION

From the steady state analysis (Chapter 3) and transient analysis (Chapters 4 and 5), it has been proved that the new servovalve configuration offers higher steady state velocity and higher damping if the orifice size and the back pressure are properly tuned. In Chapter 6, the correlation between the simulation and the experimental results is shown.

This chapter describes a general design procedure. In section (7.2), an operating zone is established based on results from 4 different sets of system parameters, in which the new servovalve gives a higher steady state velocity, lower % overshoot and lower settling time. Section (7.3) provides a procedure to determine the orifice size and back pressure for the new servovalve knowing the system parameters. Finally, in section (7.4), the results are summarized.

7.2 DETERMINATION OF OPERATING ZONE

In order to determine the operating zone, the systems with the conventional and the new servovalve are tested for 4 different sets of system parameters. These 4 sets are given in the Table 7.1.

Values	Set 1	Set 2	Set 3	Set 4
P_s	700.0	700.0	700.0	700.0
v_1	26.0	26.0	26.0	26.0
v_2	19.5	19.5	19.5	19.5
β	$11.63*10^4$	$11.63*10^4$	$11.63*10^4$	$11.63*10^4$
ρ	0.03	0.03	0.03	0.03
K_f	0.23	0.23	0.23	0.23
F_s	101.0	101.0	101.0	101.0
F_d	39.1	39.1	39.1	39.1
V_i	2.15	2.15	2.15	3.5
K_a	7.09	7.09	10.0	10.0
C_l	$6.31*10^{-3}$	$8.21*10^{-3}$	$8.21*10^{-3}$	$8.21*10^{-3}$
M	820.0	1230.0	1230.0	1230.0

Table 7.1 System Parameters for 4 Different Sets

The values of the parameters which are underlined are different than the values shown in set 1 i.e., basically, the leakage coefficient (C_l), amplifier gain (K_a), mass (M) and the voltage input (V_i) have been changed.

First, the system with the conventional servovalve is simulated for the 4 sets of values and the steady state opening of the servovalve (A_v) is determined. Then, the new servovalve is tested for various area ratios (A_O/A_v) and relief valve setting (P_r/P_s) as tabulated in Table 7.2.

A_O/A_v	P_r/P_s
0.5	0.00
0.8	0.08
2.0	0.20
3.0	0.30
5.0	0.40
8.0	—

Table 7.2 Test Conditions for the New Servovalve

Each value of area ratio is simulated for all the five values of relief valve setting. Thus in all 120 combinations are simulated. For all the cases, the %-overshoot, the steady state velocity and the settling time

are determined.

In order to compare these values with the conventional servovalve, following normalized quantities are defined.

- Normalized % overshoot δ^*

$$\delta^* = \left.\frac{\delta_n}{\delta_c}\right|_{\text{set } i} \qquad i=1,4 \qquad (7.1)$$

- Normalized settling time T*

$$T^* = \left.\frac{T_n}{T_c}\right|_{\text{set } i} \qquad i=1,4 \qquad (7.2)$$

- Normalized steady state velocity V*

$$V^* = \left.\frac{V_n}{V_c}\right|_{\text{set } i} \qquad i=1,4 \qquad (7.3)$$

- Normalised area ratio A*

$$A^* = \left.\frac{A_0}{A_v}\right|_{\text{set } i} \qquad i=1,4 \qquad (7.4)$$

where, the settling time T_n is the time required to reach $\pm$ 5% of the steady state value. The subscripts n and c represent the corresponding value for the new and the conventional servovalve respectively.

Figs. 7.1 to 7.6 show the variation of the normalized settling time T^*, normalized % overshoot δ^* and normalized steady state velocity V^* for different area ratios (A_0/A_v), as the relief valve setting (P_r/P_s) is changed from 0.0 to 0.4. In each figure, the different curves are marked as,

Number	P_r/P_s
1	0.00
2	0.08
3	0.20
4	0.30
5	0.40

From the Figs. 7.1 to 7.6, following conclusions can be drawn. The effect of area ratio and back pressure can be stated as follows.

a) As the area ratio A_0/A_v is increased from 0.5 to 8.0,

i) the settling time T^* is reduced (Figs. 7.1 and 7.2) till A_0/A_v = 2.5 and then starts increasing. For sets 1 and 2, the settling time T^* is less than 1.0 upto A_0/A_v = 5.5 whereas for the sets 3 and 4, the settling time T^* is less than 1.0 upto 3.5. This is valid for all the pressure ratios for 0.0 to 0.4.

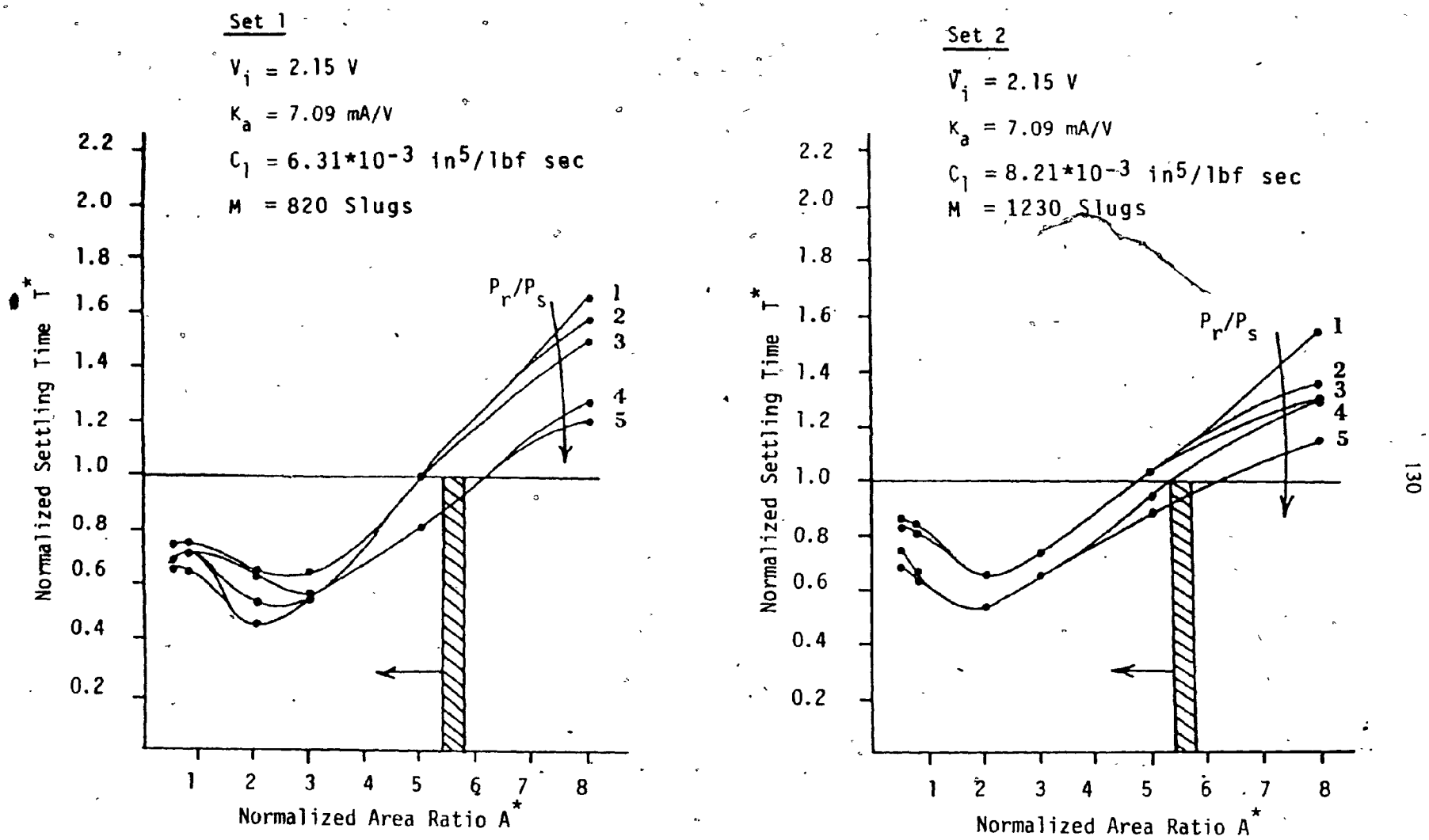

Fig. 7.1 Influence on the Settling Time : (Sets 1 and 2)

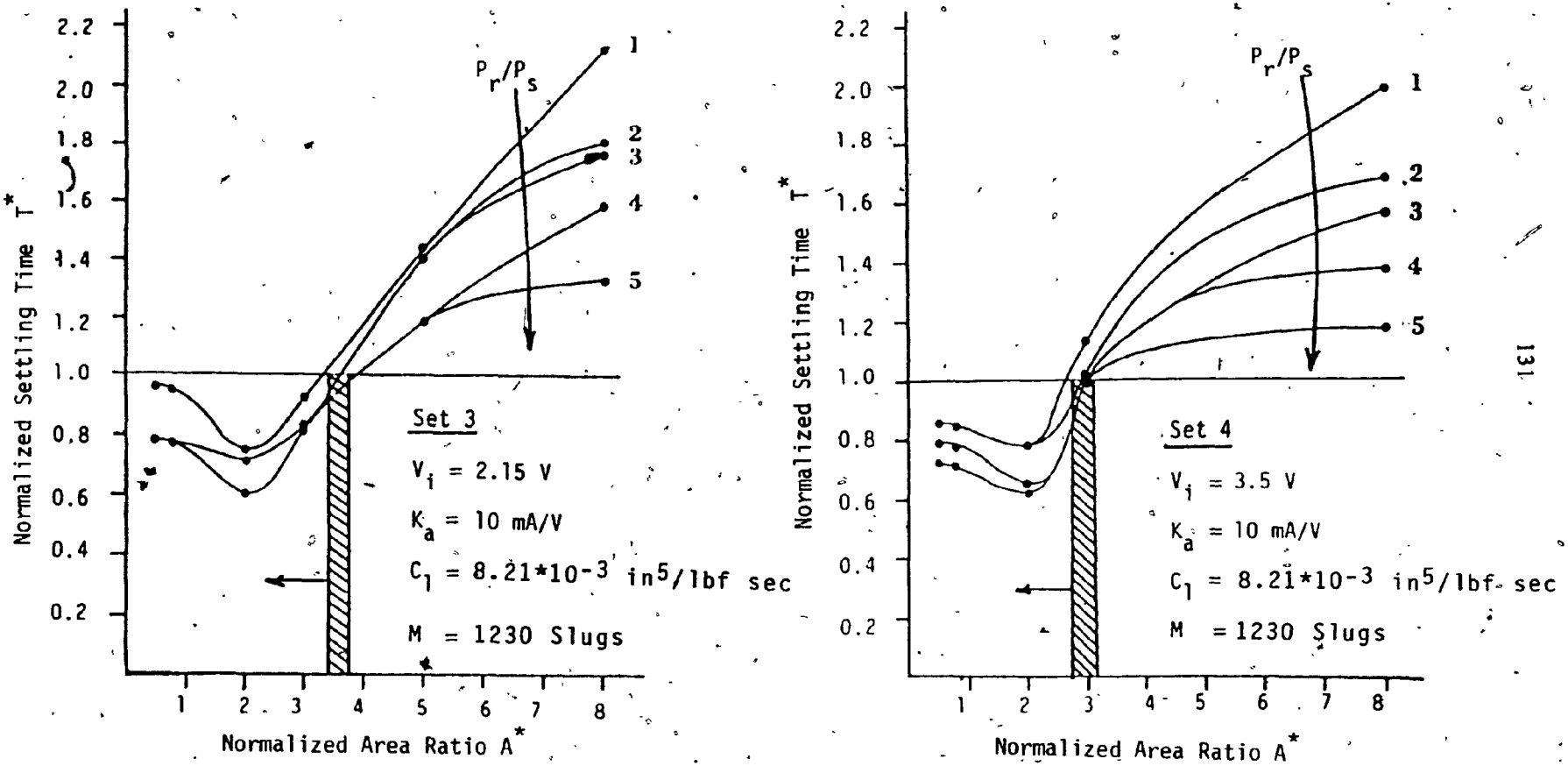

Fig. 7.2 Influence on the Settling Time : (Sets 3 and 4)

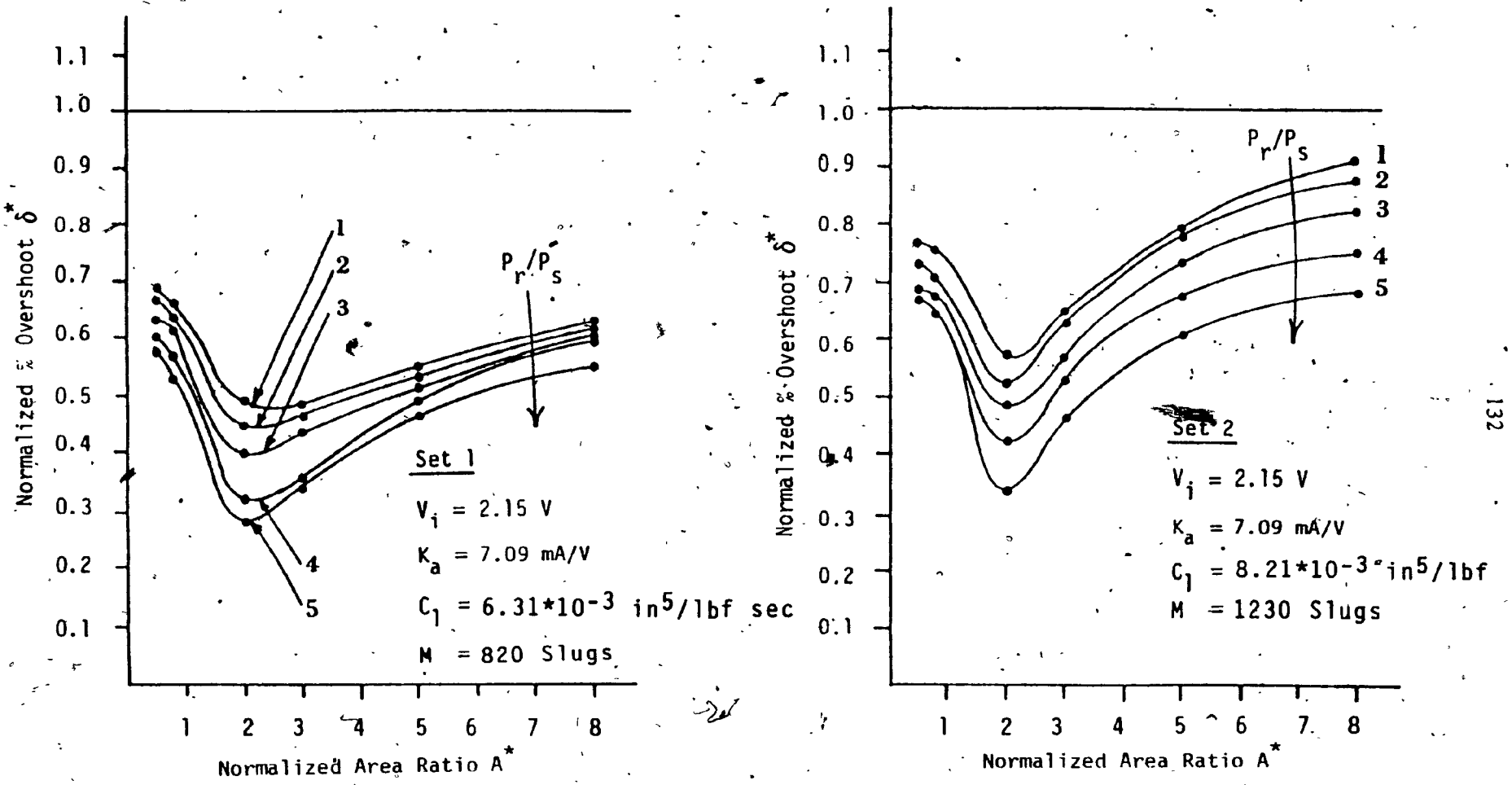

Fig. 7.3 Influence on the % Overshoot : (Sets 1 and 2)

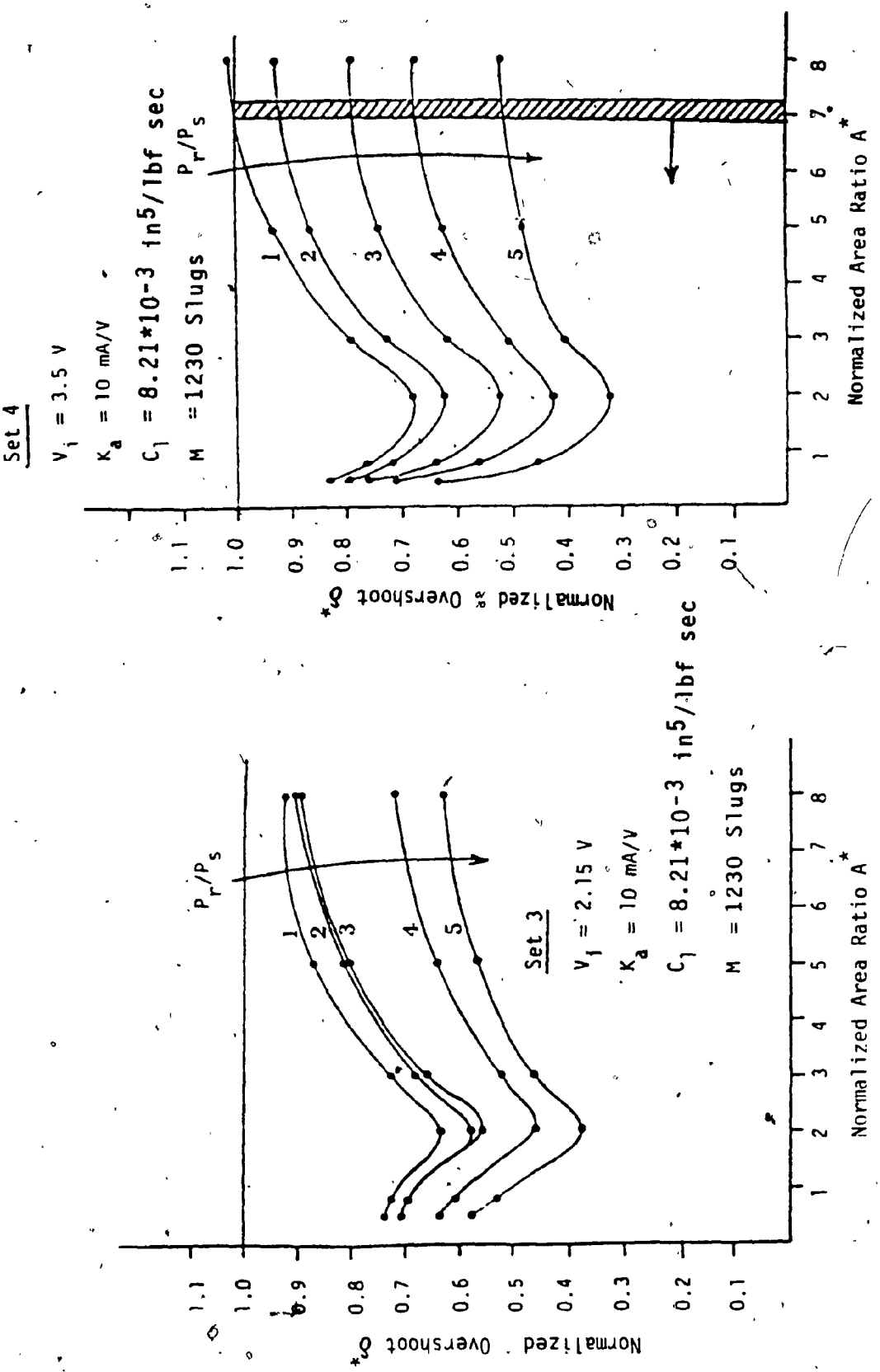

Fig. 7.4 Influence on the % Overshoot : (Sets 3 and 4)

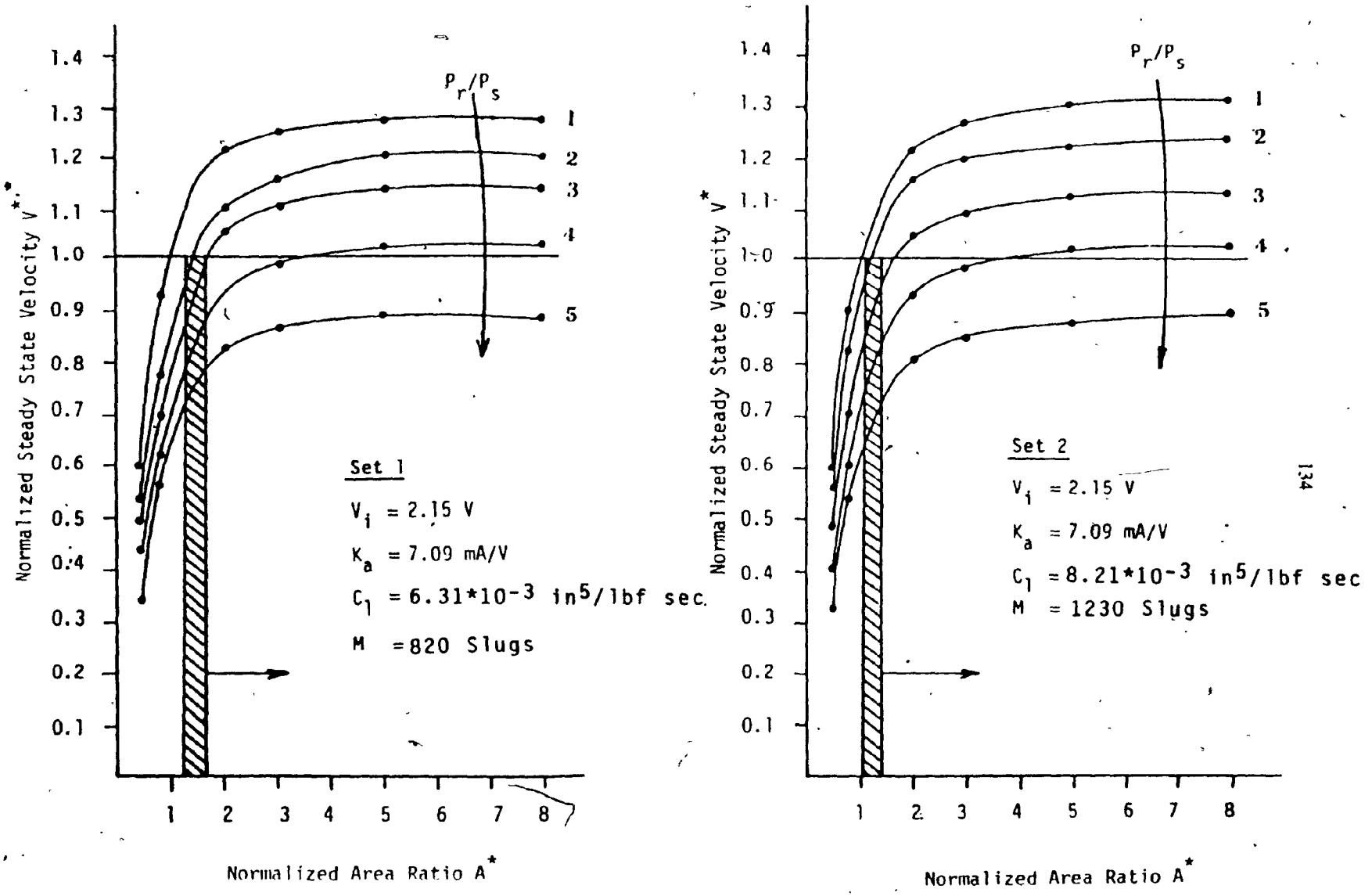

Fig. 7.5 Influence on the Steady State Velocity: (Sets 1 and 2)

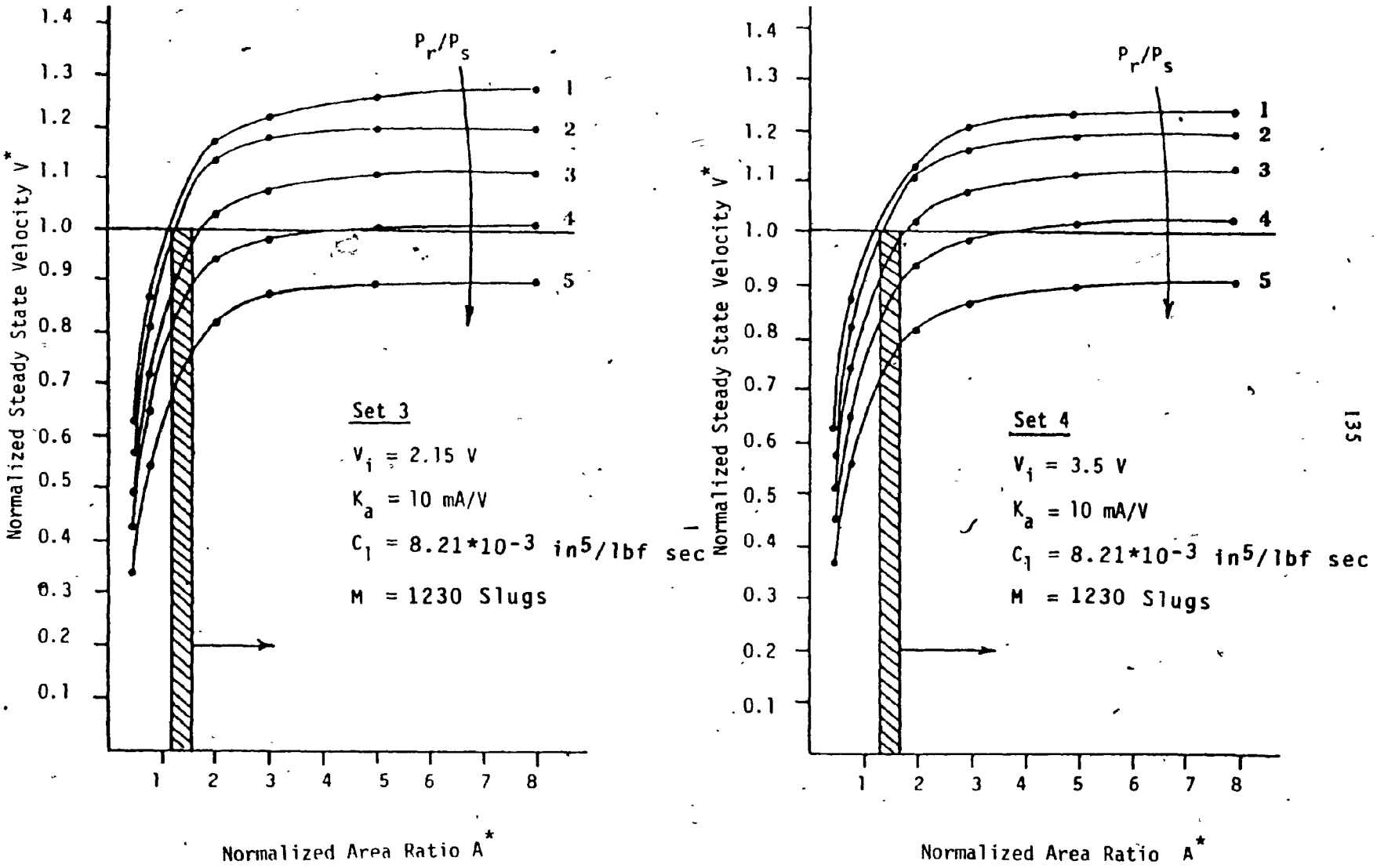

Fig. 7.6 Influence on the Steady State Velocity: (Sets 3 and 4)

ii) the % overshoot δ^* is seen (Fig. 7.3 and 7.4) to be less than 1.0 for all the pressure ratios except for set 4 (Fig. 7.4) at $P_r/P_s = 0.0$ and $A_0/A_v > 7.0$.

iii) the velocity V^* is increased (Fig. 7.5 and 7.6) and for all the sets, it is greater than 1.0 for $A_0/A_v > 1.5$ and $P_r/P_s < 0.2$. The velocity V^* is less than 1.0 for all the sets for $P_r/P_s = 0.4$ and is seen to be saturating beyond $A_0/A_v > 4.0$ for all values of P_r/P_s.

b) The effect of back pressure P_r/P_s, as it is increased from 0.0 to 0.4 is seen to be as follows.

i) there is a reduction in settling time T^* which is seen to be more for sets 3 and 4 (Fig. 7.2) for $A_0/A_v > 4.5$.

ii) the % overshoot δ^* is also reduced e.g. for set 2 (Fig. 7.3), at $A_0/A_v = 0.5$; increase in P_r/P_s from 0.0 to 0.4 results in reduction in % overshoot from 0.76 to 0.67.

iii) the velocity V^* is reduced e.g. for set 1 (Fig. 7.5); at $A_0/A_v = 0.5$, increase in P_r/P_s from 0.0 to 0.4 results in reduction in V^* from 0.61 to 0.35.

Based on the the settling time T^*, the % overshoot δ^* and the steady state velocity V^*, the new servovalve will be better if it gives higher velocity, lower settling time and lower % overshoot than the conventional.

On the individual plot, a region is marked beyond (or upto) which the new servovalve gives better performance e.g. in Fig. 7.5 and 7.6, the steady state velocity V^* will be greater than 1.0 for $A_O/A_V > 1.5$ for $P_r/P_s < 0.2$.

A common region for all the sets, which may be termed as an 'operating zone' is seen between $A_O/A_V = 1.5$ to 3.0 for $P_r/P_s < 0.2$. In this zone, the new servovalve gives better performance than the conventional i.e. it gives higher steady state velocity V_n, lower settling time T_n and lower % overshoot δ_n. It should be noted that this region is common to all the four sets of system parameters and such zone is not seen for $P_r/P_s = 0.3$ or 0.4.

7.3 DETERMINATION OF ORIFICE SIZE AND BACK PRESSURE

In order to determine the orifice size A_O and the back pressure P_r so that the system is operating in the 'operating zone', the designer should know the opening A_V of the conventional servovalve at the steady state. The value of A_V could be determined by knowing the system parameters and the operating velocity as follows.

The actuator flows Q_1 and Q_2 in the steady state are given as follows.

$$Q_1 = C_d A_v \sqrt{\frac{2}{\rho}(P_s - P_1)} \qquad (7.5)$$

$$Q_2 = C_d A_v \sqrt{\frac{2}{\rho}(P_2)} \qquad (7.6)$$

$A_v > 0.0$

(same as 4.6)

Also,

$$Q_1 - C_l(P_1 - P_2) = AV \qquad (7.7)$$

$$Q_2 - C_l(P_1 - P_2) = AV \qquad (7.8)$$

Also in steady state, the force eqn.(4.9) reduces to

$$(P_1 - P_2)A = F_d \qquad (7.9)$$

where F_d is the magnitude of coulomb friction when the piston is in motion. In steady state, the relationship between the supply pressure P_s and the actuator pressures P_1 and P_2 is given [37] as

$$P_1 + P_2 = P_s \qquad (7.10)$$

The values of F_d, A, P_s, C_d, C_l, ρ, and V are assumed to be known. Therefore, from eqns. (7.9) and (7.10), directly P_1 and P_2 can be found out. Substituting eqn. (7.5) in (7.7),

$$C_d A_v \sqrt{\frac{2}{\rho}(P_s - P_1)} - C_l(P_1 - P_2) = AV \qquad (7.11)$$

Therefore, from eqn. (7.11), the steady state value of A_v could be determined. Then, based on the conclusions drawn in section (7.2), the orifice size and the back pressure could be selected (A_0/A_v=1.5 to 3.0 and $P_r < 0.2$) which will give higher steady state velocity, lower % overshoot and lower settling time than the conventional servovalve.

7.4 SUMMARY

In this chapter, simulation results of the conventional and the new servovalve, for 4 different sets of system parameters are studied. It is seen from these results that there exists a region, which is termed as an 'operating zone', in which the new servovalve gives higher velocity, lower settling time and lower % overshoot than the conventional servovalve. Later, a procedure is described to determine the tuning parameters for the new servovalve so that the system could be run in the operating zone.

CHAPTER 8

CONCLUSIONS AND EXTENSIONS

In this thesis, a novel electrohydraulic servovalve configuration was proposed and was followed by simulation and experimental investigations into its characteristics. The simulation and experimental results were compared and it was shown that the mathematical models are good to predict the performance of the two servovalve configurations. Therefore, the simulation technique was used as a basis for further comparison.

The advantage of this new servovalve is that if the orifice size and the back pressure are properly tuned, it gives higher steady state velocity, lower settling time and lower % overshoot than the conventional servovalve. It was shown (based on 4 different of system parameters that there exists an operating zone in which this advantage is observed.

An apparent disadvantage of this new servovalve must be mentioned. The direction control part of the new servovalve introduces a pure time delay which may cause limit cycle oscillations in some cases.

Further extensions on this research work could include the following.

1) A servosystem with the new servovalve configuration could be used in CNC machines, robots etc. Therefore, its response to load disturbance should be studied.

2) Expermentally, it was found that the servosystem with the new servovalve configuration exibits limit cycle oscillations at high back pressure and low flow. Therefore, the role of relief valve should be studied in more detail by including the relief valve dynamics in the mathematical model and also by carrying out experiments.

3) Based on some criteria such as rise time, settling time etc., an optimization program should be developed to determine the orifice size and the back pressure for the desired operating velocity.

4) A tuneable controller should be designed so as to adjust the metering orifice and the back pressure of the new servovalve configuraton based on the current operating conditions of the system.

5) The mathematical model should be used to study the effects of the pure time delay of the direction control

valve on the transient response of the system.

6) Mathematical analysis of the new servovalve should be done so as to obtain a third order or a second order transfer function which would help in predicting frequency response, effect of orifice size and back pressure on the damping and the gain etc.

REFERENCES

1 Maskrey R.H. and Thayer W.J., " A Brief History of Electrohydraulic Servomechanisms",Transactions of ASME, Journal of Dynamic Systems, Measurement and Control, Vol. 100 June 1978, pp 110-116.

2 Thayer W.J., "Transfer Functions for Moog Servovalves", Moog Inc. Controls Division , East Aurora, N.Y., Technical Bulletin 103, 1965.

3 Martin H.A. and McCloy D.,"Some aspects of Bistable Hydraulic Servos", Second Fluid Power Symposium, Guildford, England, January, 1971.

4 Kearney R.E., Hunter W.I, Weiss P.L. and Spring K., "Tilt-table/Ankle-actuator System for the Study of Vertibulospinal reflexes", Medical and Biological Engeneering, Vol. 21, May 1983.

5 Lourigan P.M., "Servovalve, Solid State Controls Steer Farm Tractor Selectively", Hydraulics and Pneumatics, Oct. 1981.

6 Stikeleather L.F. and Suggs C.W., "An Active Seat Suspension System for Off Road Vehicles", Transactions of ASAE, 1970, pp 99-106.

7 Broome D.R., "The Effect of Flexibly Coupled Loads on the Dynamics of Hydraulic Servomechanisms in Arm Prostheses", Journal of Mechanical Engineering Science, Vol. 21, No. 2, 1979.

8 Lu T.D., Miller V.G. and Fischer J.A., "Cycle Pile Load

Testing-Loading System and Instrumentation", Behavior of Deep Foundations, Raymond Lundrgren, ASTM, 1979, pp 435-450.

9 Vinayagalingam T., "Acceleration Detection and Inertia Compensation of Pentograph Head using a Constant Flow Hydraulic Servo", Trans. of ASME, Journal of Engineering for Industry, Vol. 104, Feb. 1982.

10 Vilenius M.J. and Vivalvdo T.K., "The Effect of Nonlinearities on the Dynamic Characteristics of an Electrohydraulic Servovalve", Simulation, Nov.1976

11 Martin D.J. and Burrows C.R., "The Dynamic Characteristics of an Electrohydraulic Servovalve", Trans. of ASME, Journal of Dynamic Systems, Measurement and Controls, Dec. 1976

12 Montgomery J. and Lichtarowicz A., "The Effect of Assymmetrical Lap on the Performance of the Hydraulic Servomechanism", Second Fluid Power Symposium, Guildford, England, January, 1971

13 Kaneko T., "A research on Electrohydraulic Pressure Control Servovalve", Bulletin of JSME, Vol. 21, No. 155, May 1978.

14 LeQuoc S., Cheng R.M.H. and Limaye A., "A Tuneable Electrohydraulic Servovalve Configuration to Achieve High Actuator Velocity, Fast Response and High Damping", ASME paper 84-WA/DSC, New Orleans, U.S.A., Dec. 1984.

15 Cheng R.M.H., LeQuoc S. and Limaye A., "A New Tuneable

Electrohydraulic Servovalve Configuration to Achieve High Gain and High Damping," Canadian Patent Application No. 265-8003-1, File No. 84- 001, 1984.

16 Watton J., "The Generalised Response of Servovalve-Controlled, Single Rod, Linear Actuator and the Influence on Transmission Line Dynamics", Trans. of ASME, Journal of Dynamic Systems, Measurement and Control, Vol 106, June 1984.

17 Leburn M. and Scavarda S., "Simulation of Nonlinear Behaviour of an Electrohydraulic exciter", Simulation, Oct. 1979.

18 Shearer J.L., "Digital Simulation of a Coulomb Damped Hydraulic Servosystem", Trans. of ASME, Journal of Dynamic Systems and Control, Vol. 105, Dec. 1983.

19 Parnaby J., "Instability Due to Static and Coulomb Friction in Autonomous Control Systems", Second Fluid Power Symposium, Guildford, England, Jan. 1971.

20 Vilenius M.J., "The Application of Sensitivity Analysis to Position Control Servos", Trans. of ASME, Journal of Dynamics Systems, Measurement and Control, Vol. 105, June 1983.

21 Young Y.R. and Saggs C.W., "Seat Suspension System for Isolation of Roll and Pitch in Off-Road Vehicles", Trans. of ASAE, Oct. 1973.

22 Houzong J., "On the Stability of the Electrohydraulic Servo Systems of the Revolving Arm of an Industrial Robot", Robots 8, Conference Proc., Robotics International of SME, Detroit, MI, June 1984.

23 Bowns D.E, Tomlinson S.P and Dugdale S.K., "Progress Towards a General Purpose Hydraulic System Simulation Language", Sixth International Fluid Power Symposium, Cambridge, England, 1981.

24 Bowns D.E, "Computer Simulation as a First Step Towards Computer Aided Design of Fluid Power Systems", Fifth International Fluid Power Symposium, Durham, England, Sept. 1978.

25 Kinoglu F. Riley D. Donath M. and Torok D., "Streamlining Hydraulic Circuit Design with Computer Aid", Computers in Mechanical Engineering, Oct. 1982.

26 Leucht P.M. and Mandley D.J., "Computer Aided Design of Electrohydraulic Control Systems", SAE Technical Paper Series NO. 820097, International Congress and Exposition, Detroit, MI.,Feb. 1982.

27 Maskrey R.H., "Possible Uses of Microprocessors for Fluid Power", Hydraulics and Pneumatics, June 1974.

28 Shetty D. and Copeland B., "A Computer Controlled Fluid Power System for Shaping and Planing Machine Tools", ASME Winter Annual Meeting, New Orleans, Dec. 1984.

29 Bell R. and Cowan P., "The Performance of a High Speed Servomotor", Second Fluid Power Symposium, Guildford, England, Jan. 1971.

30 Steber G.R., "Simulation of a Pressure Relief Valve", Simulation, May 1969.

31 Iyengar S.K.R., "Static and Dynamic Performance of Compound Relief Valve due to Contaminent Exposure",

Fifth International Fluid Power Symposium, Sept. 1978.

32 Chong F.K. and Dransfield P., "The Effect of Choice of Relief Valve on the Response of a hydraulic Control System", Conference on Control Engineering, Melbourne, Australia, June 1979.

33 Tumarkin M.B., " Hydraulic Servomechanisms : Structure and Kinematics ", British Library Lending Division, U.K., 1975.

34 U.S.Patent 4,170,214, Double A Products Co., Filed on Jan. 23, 1978, Issued Oct. 9, 1979.

35 U.S.Patent 4,342,256, Danfoss A.S. Filed on May 22, 1979, Issued in Aug. 3, 1982.

36 Funke M.F. and Pecan L.K., "The Design, Fabrication and Test of an Electrofluidic Servovalve", Applied Tech. Lab, U.S.Army Research and Tech. Lab, AVRADCOM TR-80-D-2, 1982.

37 Meritt H.E., "Hydraulic Control Systems", John Wiley and Sons Inc., N.Y., 1967.

38 Stringer J., "Hydraulic Systems Analysis: An Introduction", The Macmillan Press Ltd., London, 1976.

39 Gullian M., "Hydraulic Servosystems: Analysis and Design", Plenum Press, London, 1969.

40 Viersma T.J., "Analysis, Synthesis and Design of Hydraulic Servosystems and Pipelines", Elsevier Scientific Publishing Co., Elsevier-North Holland Inc., N.Y., 1980.

APPENDIX A

APPENDIX A

A.1 SERVOVALVE CONSTANTS

The equivalent transfer function of the servovalve is given as

$$\frac{A_v}{I} = \frac{K_x K_v}{\tau_v S + 1} \qquad (A.1)$$

(Same as eqn. 4.5)

The constant $K_x K_v$ is a product of the servovalve torque motor gain K_x and the servovalve area constant K_v. In steady state, the flow through the servovalve is given as

$$Q_2 = C_d A_v \sqrt{\frac{2}{\rho} P_2} \qquad (A.2)$$

(Same as eqn. 4.6)

Therefore, from equation A.1, in steady state,

$$Q_2 = C_d K_x K_v I \sqrt{\frac{2}{\rho} P_2} \qquad (A.3)$$

This equation was used to determine the constant $K_x K_v$.

For different values of the input currents I, the supply pressure P_s was adjusted such that the pressure P_2 is 520 psi ($3.44*10^6$ N/m^2). The output flow Q_2 was measured for each value of input current. The graph of the current I

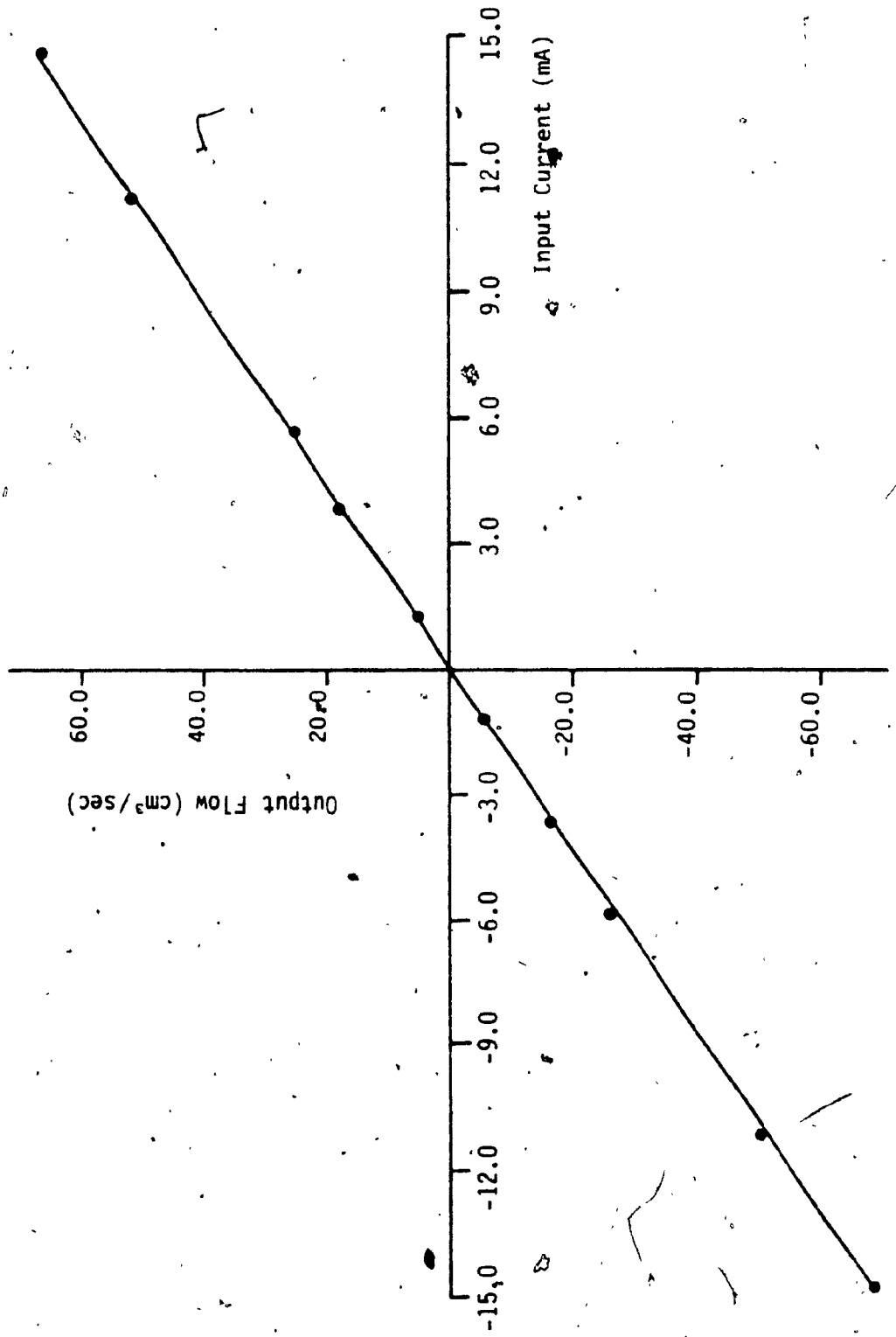

Fig. A.1. Flow Characteristics of 73-207 Servovalve

versus flow Q_2 was plotted Fig. A.1 and the constant K_xK_v was determined as follows.

Slope of the graph = 4.57 $cm^3/sec/mA$

Therefore,

$$K_xK_v = \frac{4.57}{0.6\sqrt{\frac{2}{860}}*520*6894.57}$$

$$K_xK_v = 0.08334\ cm^3/mA$$

$$= 0.051\ in^3/mA$$

A.2 NEEDLE VALVE

For the experimental purpose, a 1RF4 needle valve with regulating stem was used . The characteristics of this valve have been provided by the manufacturer as shown in Fig. A.2 (Courtsey Whitey Valves).

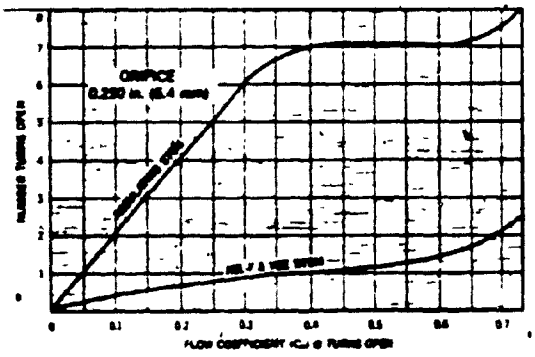

Fig. A.2 Flow Characteristics of the Needle Valve

The relationship between flow rate and the flow coefficient is given as

$$Q_0 = C_v \sqrt{\frac{\Delta P}{G}} \qquad (A.4)$$

where ΔP is the pressure drop across the valve in psi, G is the specific gravity of the fluid and Q_0 is the flow rate through the needle valve. By using Equation A.4, the flow coefficients of the valve for different openings were determined.

The flow rate through the valve is also given as

$$Q_0 = C_d A_0 \sqrt{\frac{2}{\rho} P_s} \qquad (A.5)$$

Using equations (A.4) and (A.5), various orifice diameters were calculated. The calibration curve for the needle valve is shown in Fig. A.3

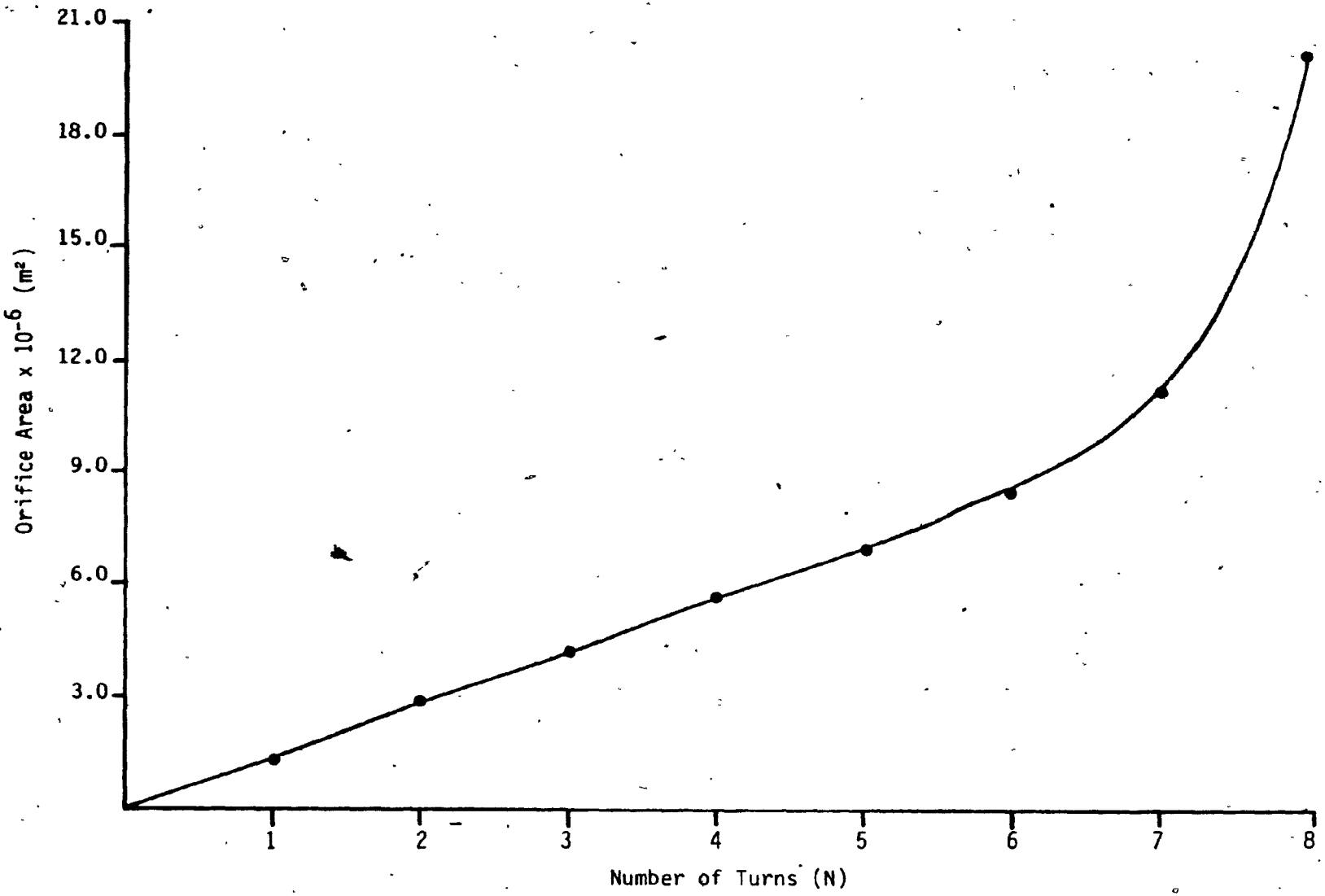

Fig. A.3. Calibration Curve for the Metering Valve

A.3 VELOCITY TRANSDUCER

A moving magnet type velocity transducer was used as a velocity measuring and feedback device. It is a self generating device that provides a DC voltage output. The voltage is generated across the induction coils as the magnet moves with respect to the coils and is directly proportional to the velocity of the magnet.

This velocity transducer was calibrated by mounting it on a precision lathe. The rod which holds the magnet was connected to the moving carriage and the body was fixed on the guideways. The voltage across the coils was measured for both the strokes and for different velocities. Fig. A.4 shows the calibration curve for the velocity transducer. The transducer is seen to be linear over the range of velocity selected for measurement.

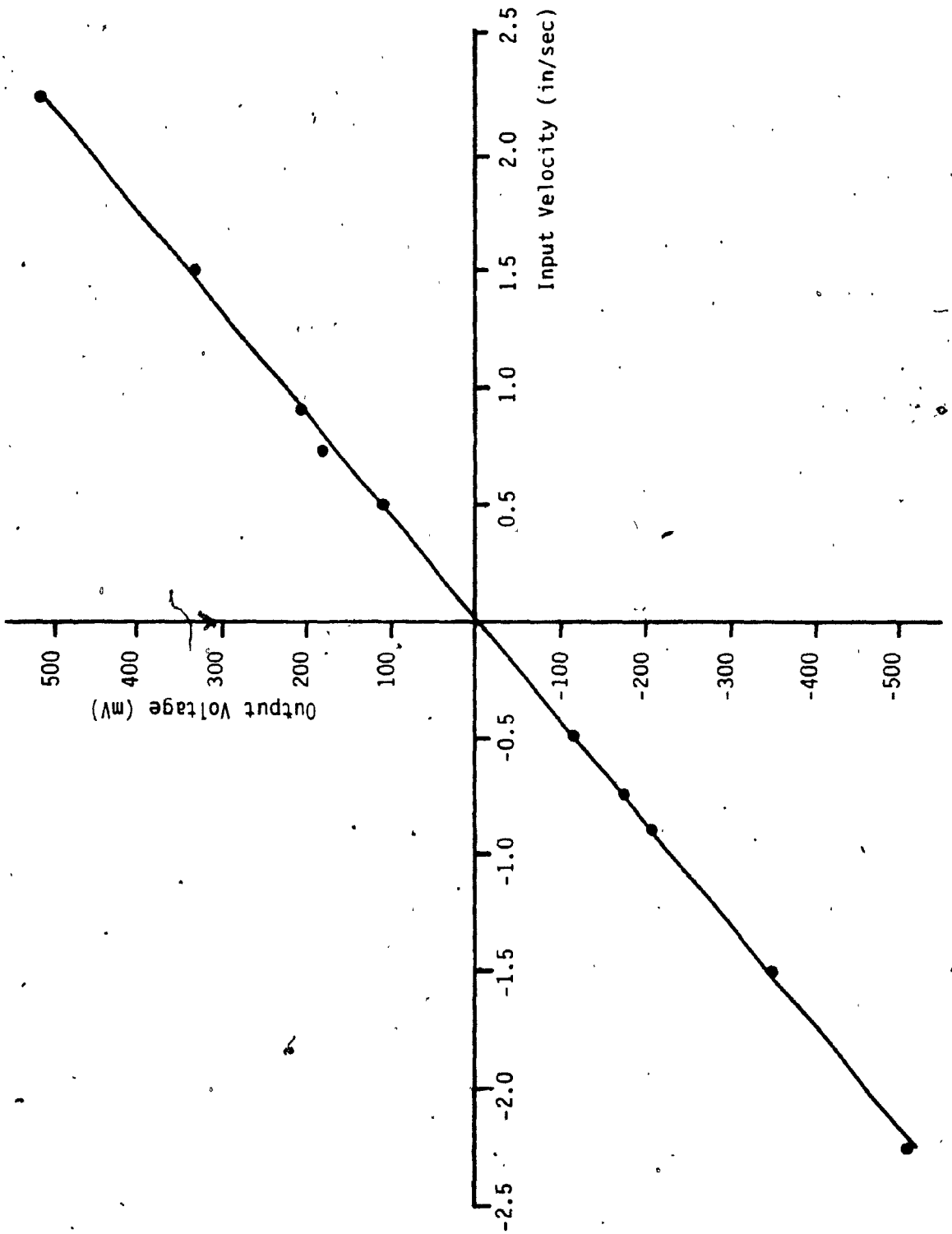

Fig. A.4. Calibration Curve for Velocity Transducer

A.4 VISCOUS AND COULOMB FRICTION

Friction is present whenever one mechanical part moves on another part. The friction present in linear actuator can be divided in two parts viz. viscous and coulomb. Therefore,

$$F_f = F_v + F_c \tag{A.6}$$

Viscous friction is present when a film of lubricant is sheared as the mechanical parts move and is directly proportional to the relative velocity between the moving parts. Coulomb friction is present when there is incomplete or no effective lubrication. The coulomb friction can be further divided in two parts viz. starting and running friction. Starting friction is the force required to start the motion. Once the motion starts, the coulomb friction force between the moving parts is called as the running friction.

For the linear actuator used in the experimental set up, the net force developed can be written as

$$(P_1 - P_2)A = M \frac{d^2X}{dt^2} + B \frac{dX}{dt} + F_c \tag{A.7}$$

When the actuator is stationary, the net force is used only to overcome the starting friction. Whereas, when a

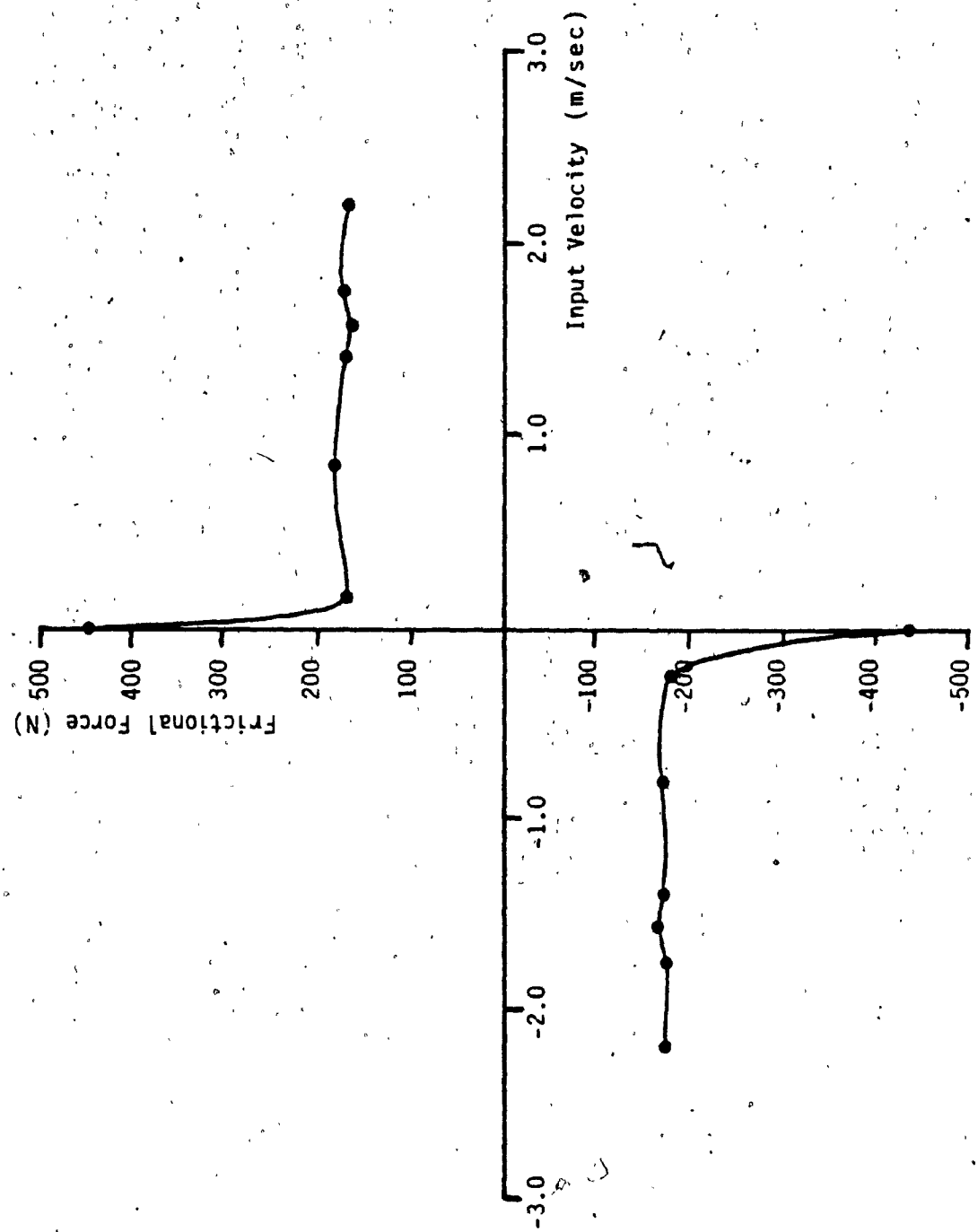

Fig. A.5. Friction Characteristics of Linear Actuator

steady state velocity is achieved, it is used to overcome running and viscous friction. In order to determine these parameters, following tests were carried out.

The supply pressure was increased slowly from zero till the actuator was in motion. The actuator velocity V and the two pressures P_1 and P_2 were recorded. The same procedure was carried out for different velocities. From the two pressure readings at $V=0$ and $V=0^+$, the static and dynamic values of coulomb friction were determined. It was seen that the viscous friction force is negligible. The coulomb friction characteristics of the actuator are given in Fig. A.5.

A.5 LEAKAGE COEFFICIENT

All the moving parts have some clearance which acts as a leakage path under high pressure. For the test stand as shown in Fig. 5.1, the combined leakage through the small flow control valve installed across the actuator ports and through the cylinder was measured in order to determine the leakage coefficient. Fig. A.6 gives the variation of the leakage flow with the pressure differential.

As seen from the graph, the variation of the leakage flow is directly proportional to the pressure difference across the piston. Therefore, the slope of the graph gives the valve of the leakage coefficient.

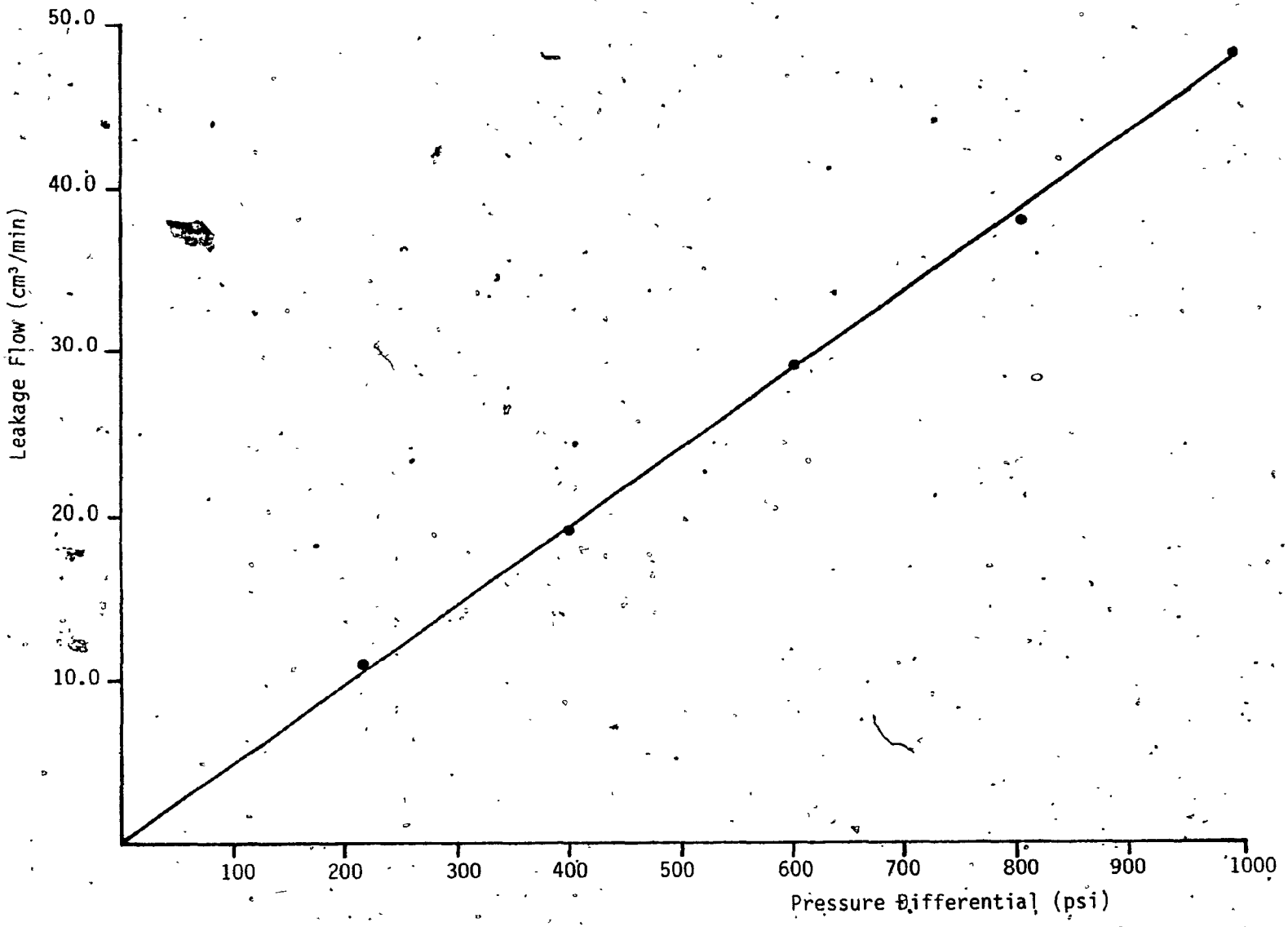

Fig. A.6. Leakage Characteristics of Linear Actuator

Slope of the graph = 0.04839 cm^3/min psi

= $5.05*10^{-3}$ in^5/lbf sec

A.6 RELIEF VALVE

A pilot operated relief valve is installed in the drain line of the new servovalve. Following procedure was used to calibrate the relief valve. Fig. A.7 shows the schematic of the set up used to calibrate the relief valve. The pilot relief valve (2) to be tested was installed in line with another relief valve (1), a calibrated pressure gauge and a pump as shown in the Fig. A.7.

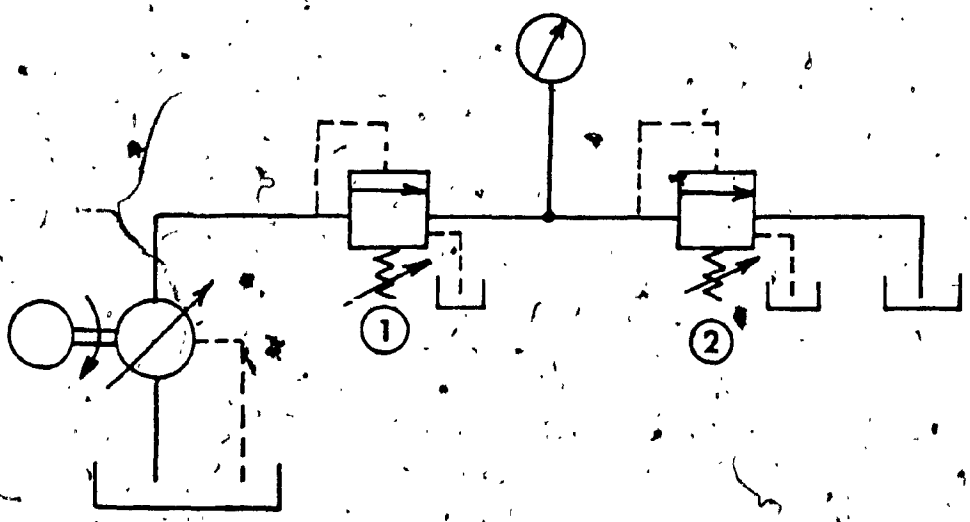

Fig. A.7 Schematic of the Test Set Up for Calibration of Relief Valve

Initially both the valves were kept completely open

and no flow was observed through the drain line. This is because the direct operated relief valve (1) was set at negligible pressure (initial setting of the spring) whereas the pilot operated valve was set at certain initial pressure (50 psi approx.) and therefore all the pump output was dumped to the tank through the valve (1). The pressure in the line was slowly increased by adjusting the pressure setting knob of the valve (1) till some flow was observed through the drain line. This pressure at which the valve 2 cracked open was noted. Then the pressure in the line was reduced slowly till the flow was stopped. The pressure was also noted. The pressure setting knob of the valve 2 was then closed by 1, 1.5, 2 and 2.5 turns successively and the same procedure was repeated. Fig. A.8 gives the calibration curve for the relief valve. Some difference in closing and opening pressure was observed (approx. 30-40 psi) indicating hysteresis of the valve. For simplicity, this is not shown on the calibration curve.

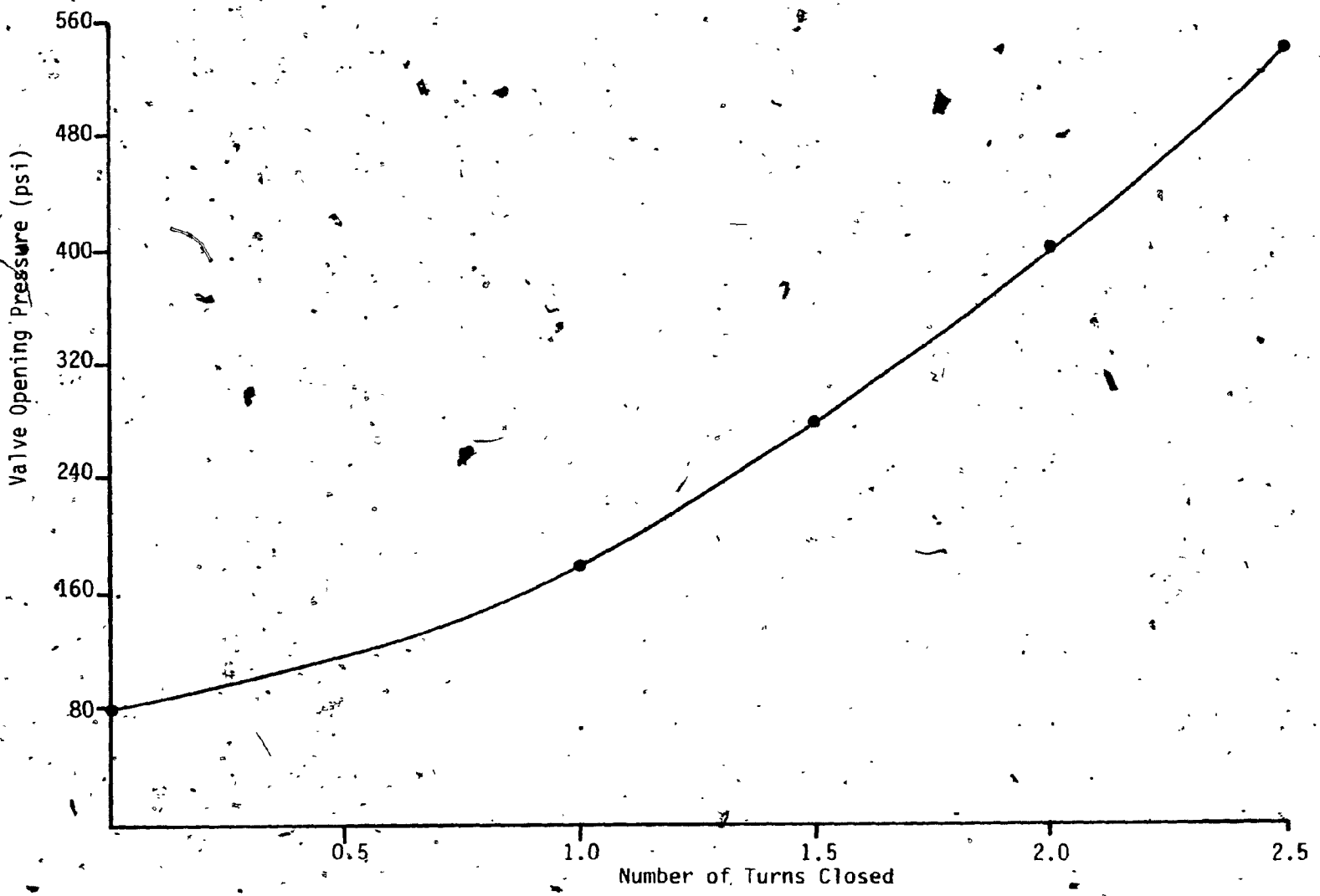

Fig. A.8. Calibration of Reliefvalve

A.7 PRESSURE TRANSDUCERS

A calibration curve for the pressure transducer-indicator combination was obtained by using a dead weight tester as follows. The positive port of the transducer was connected to the output of the dead weight tester and the negative port was kept open to the atmosphere. Various pressure levels from 0-1000 psi with 100 psi steps were obtained by mounting appropriate dead weights on the dead weight tester. The pressure was then lowered back to zero in steps of 100 psi. The corresponding output voltages given by the transducer indicator were recorded. Same procedure was used for the second transducer-indicator combination. No considerable hysteresis was observed (<20 psi). Figs A.9 and A.10 show the calibration curves for the two pressure transducers.

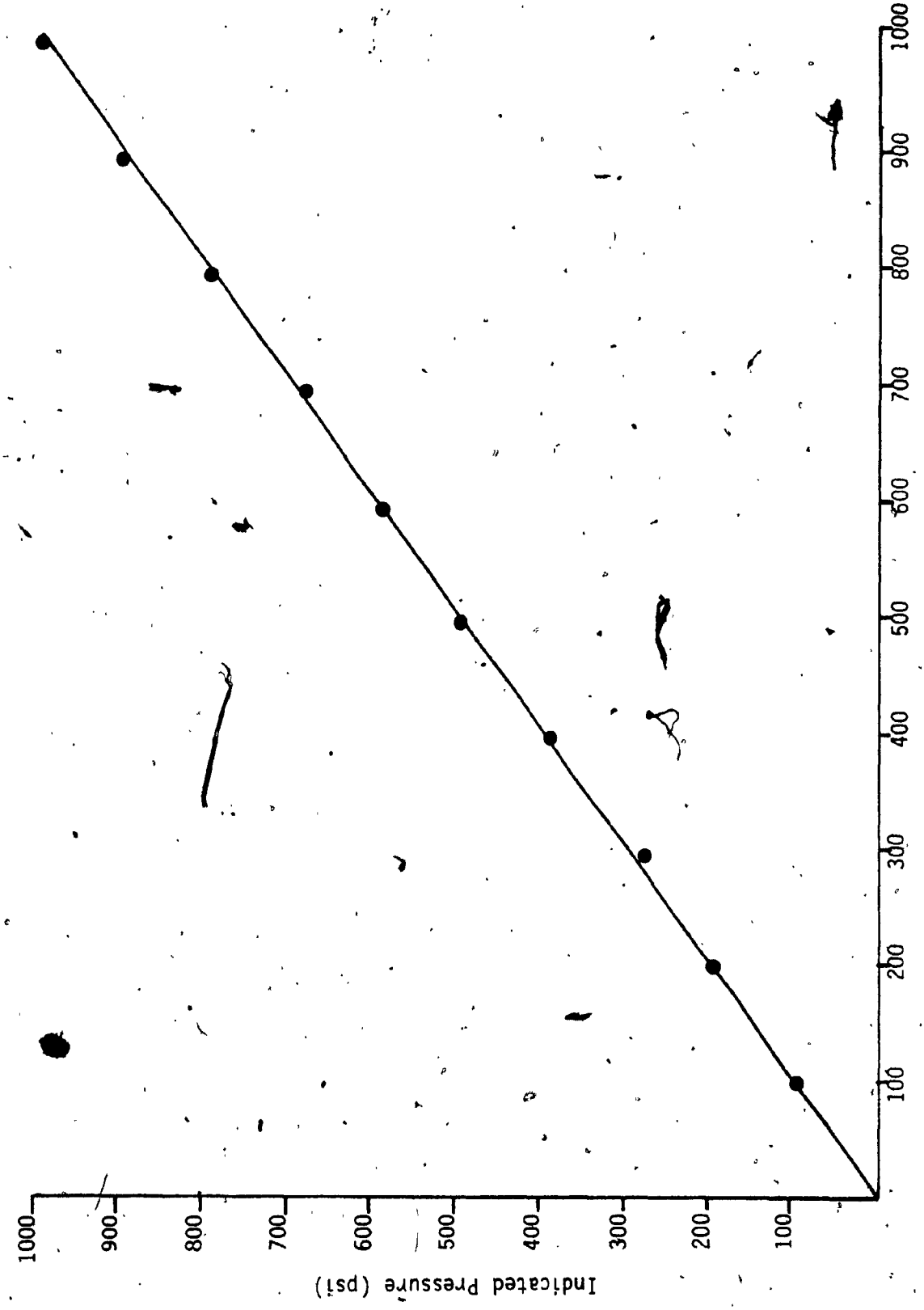

Fig. A.9. Calibration of Pressure Transducer (Transducer #1)

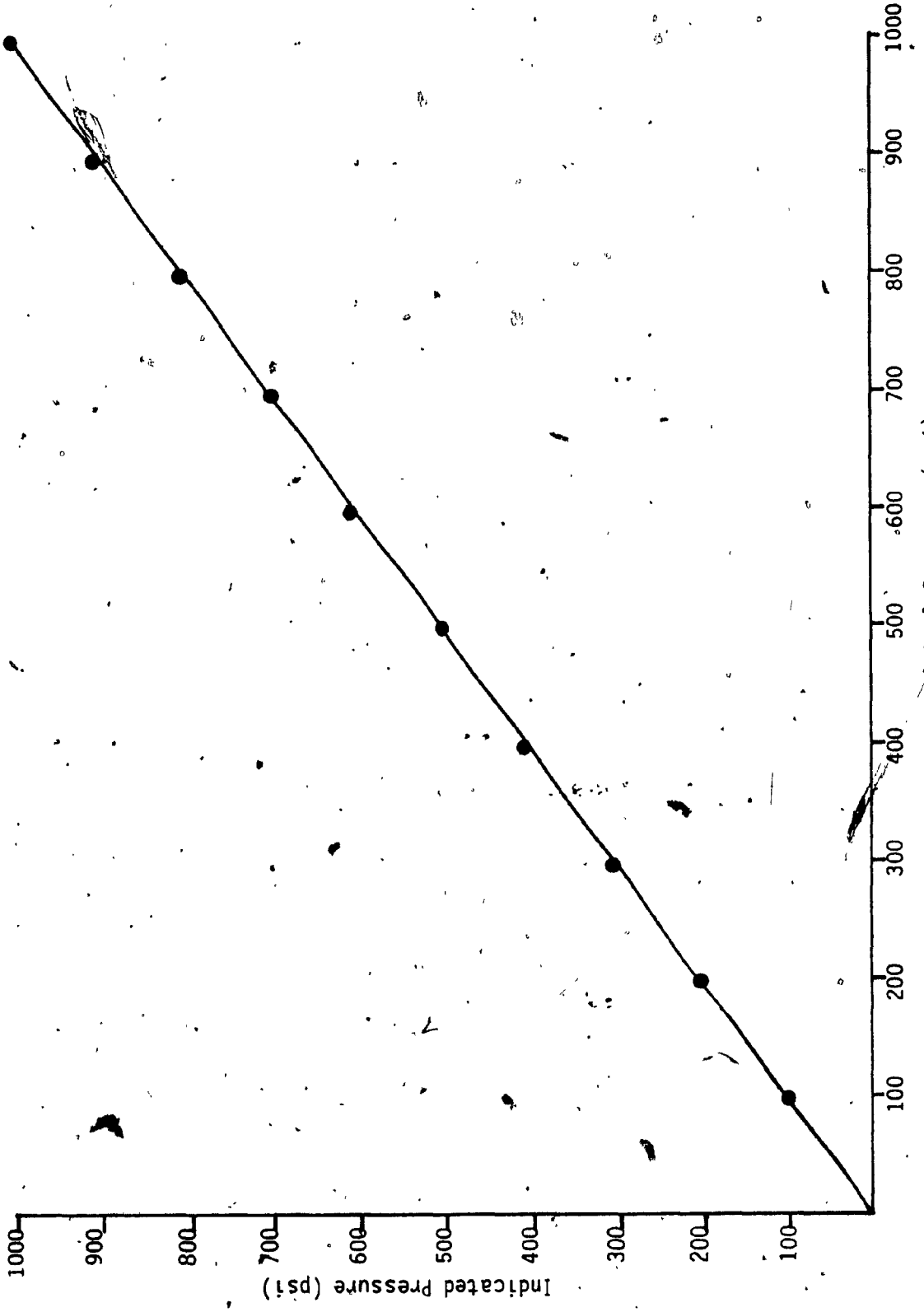

Fig. A.10 Calibration of Pressure Transducer (Transducer #2)

APPENDIX B

APPENDIX B

B.1 SERVOVALVE CONTROLLER

Fig. B.1 shows the circuit diagram for the servocontroller used to drive the servovalve. The controller is proportional i.e the output voltage of the controller is directly proportional to the sum of the input voltage signals.

The controller consists of a preamplifier stage (op-amps A_1 and A_2), a feedback stage (op-amp A_3) and a current amplifier stage (op-amp A_4 and transistors T_1 and T_2). The torque motor coils of the servovalve are connected to the output of the controller.

The preamplifier stage is provided with summing junction at the amplifier A_1 and adjustment for bias and gain at amplifier A_2. The feedback stage provides operational stability and linear response characteristics. The two transistors used in the current amplifier stage are PNP and NPN type and therefore provide sufficient current in positive as well as negative voltage input.

Fig. B.2 shows the input-output relationship of the controller for a gain of 7 mA/V. The controller was also tested for 4 mA/V and 6 mA/V and a linear relationship was observed in all the cases.

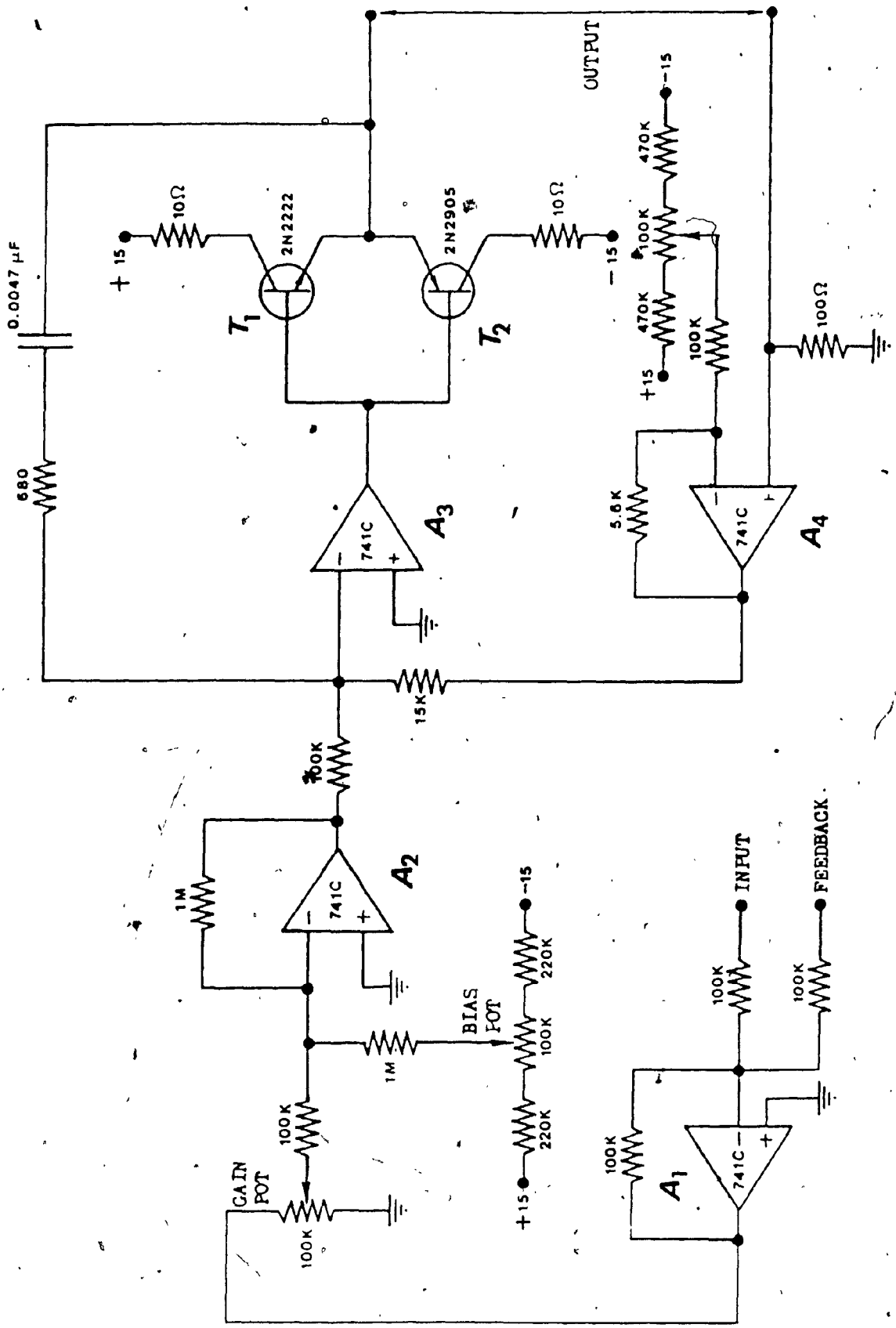

Fig. B.1 Schematic of the Servocontroller

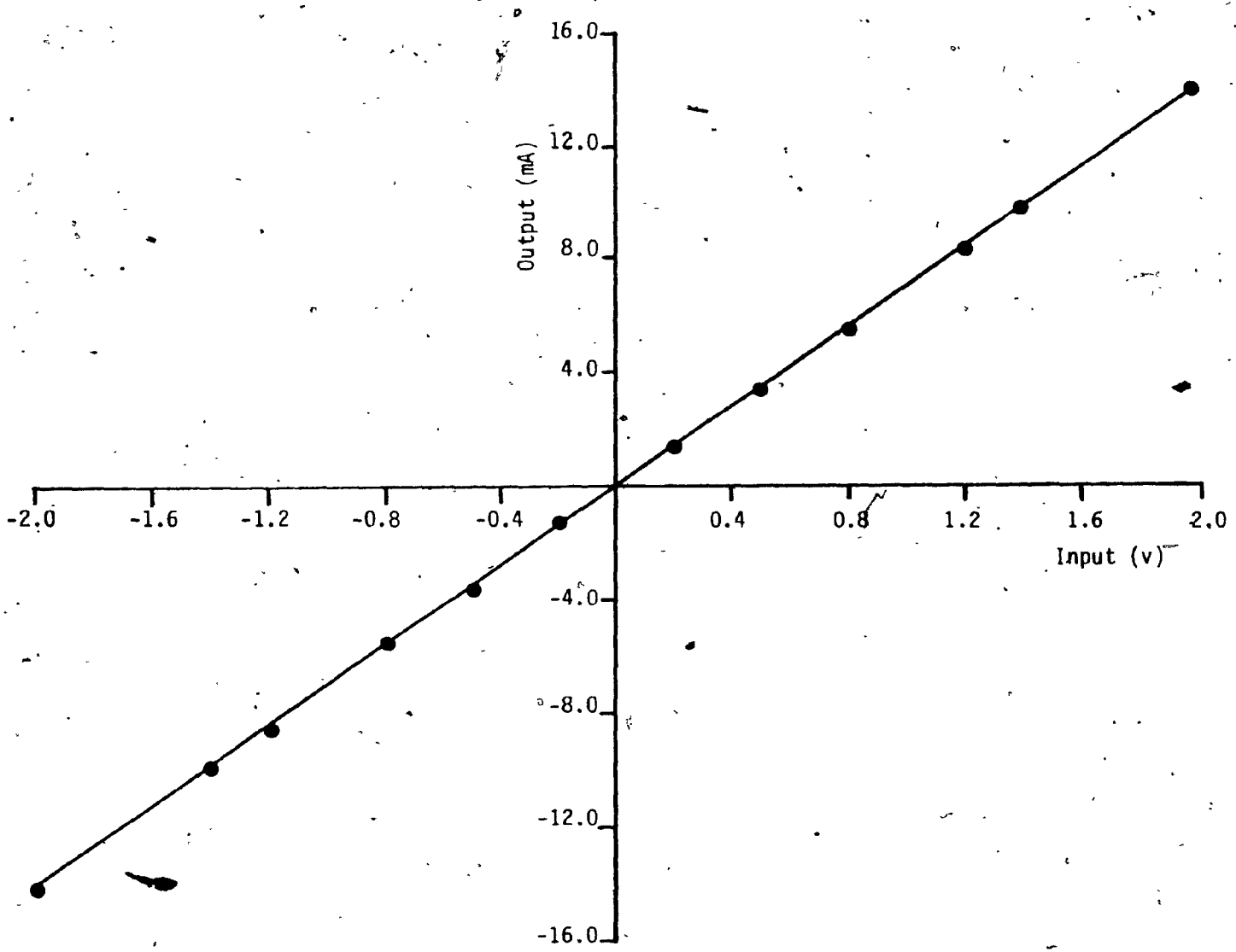

Fig. B.2. Servocontroller Characteristics

B.2 ON-OFF CONTROLLER

In order to drive the solenoids of the direction control valve, an on-off controller was designed and built. Fig. B.3 shows the schematic of the on-off controller.

Depending upon the sign of the input, the output of the op-amp A_1 is + 15 V. The amplifier A_2 inverts the signal and feeds it amplifier A_3. A set of opto coupler-triac driver and triac is provided for each of the amplifiers A_3 and A_4. The output of triac T_1 is connected to solenoid A and that of T_2 is connected to solenoid B of the direction control valve. An additional circuit is provided at the amplifier A_1 to adjust the offset (swithching level) and to introduce intentional hysteresis if required.

Thus, depending on the sign of the input, appropriate solenoid is activated and switching of the supply and drain port is achieved.

The on-off controller and the direction control valve together introduce a pure time delay in actuation. This delay was seen to be 8 ms but sometimes varying from 3 to 10 ms.

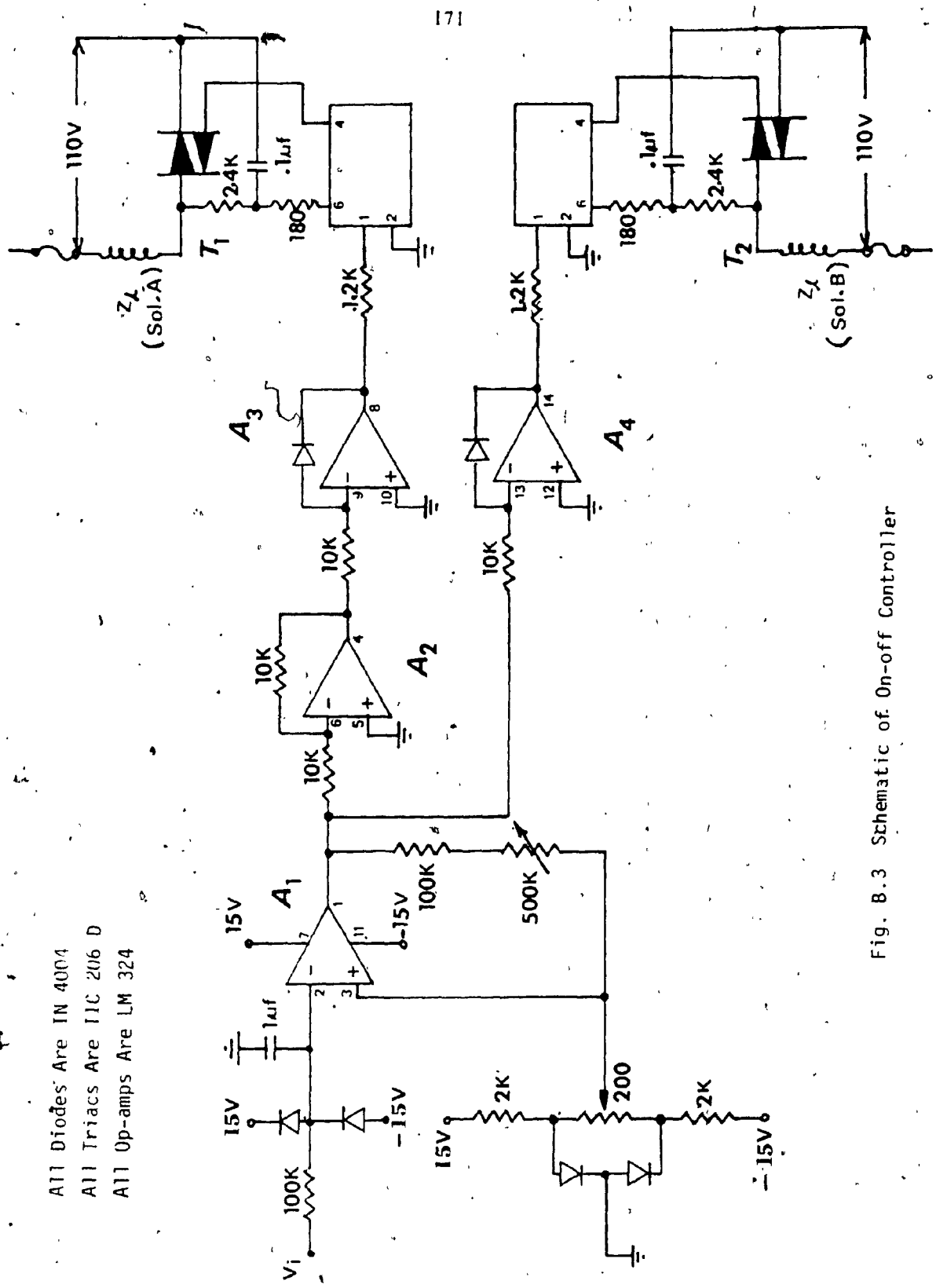

All Diodes Are IN 4004
All Triacs Are IIC 206 D
All Op-amps Are LM 324

Fig. B.3 Schematic of On-off Controller

B.3 CIRCUIT FOR TWO-STEP INPUT

In order to get a two-step input, a circuit which will add 2 signals was designed. Fig. B.4 shows a schematic of this circuit.

It was seen that the switches S_1 and S_2 introduce a short (15 ms) but high transient output when switched on. Therefore, a monostable and OR gate combination was used to eliminate this transient. In order to add two signals or get a two step, the switch S_1 should be closed i.e. pin 3 of OR gate should be high. When S_2 is closed, V_1 (positive voltage) is added to the signal from the function generator and when S_2 is open, V_2 (negative voltage)is added to the signal from the function generator. Thus the position of swith S_2 decides whether V_1 or V_2 is added. The magnitude of the second step can be adjusted by varying the supply voltage (V_1 or V_2)

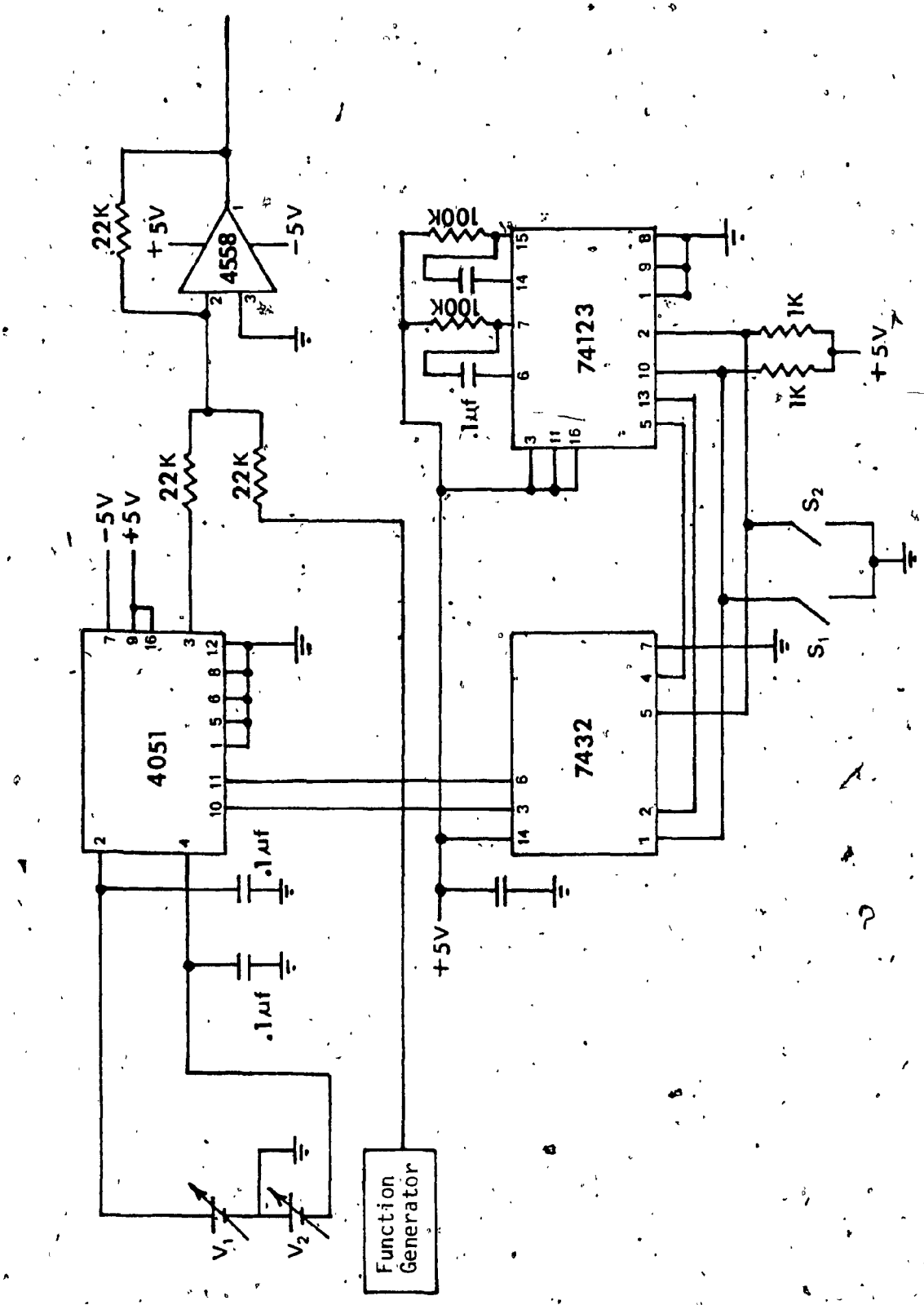

Fig. B.4 . Schematic of the Circuit for 2 Step Input

APPENDIX C

LISTING OF THE COMPUTER PROGRAM

```
C
C   THIS PROGRAM CALLS ON THE FUNCTION RUNGE TO SOLVE FOR THE
C   SYSTEMS OF DIFFERENTIAL EQUATIONS FOR THE CONVENTIONAL AND NEW
C   SERVOVALVE CONFIGURATIONS.  THE EQUATIONS WITH THE GIVEN INITIAL
C   CONDITIONS DESCRIBE THE VELOCITY RESPONSE SUBJECTED TO
C   STEP INPUT VOLTAGE COMMAND
C     THEY ALSO GIVE THE TRANSIENT RESPONSES FROM SUDDEN ADJUSTMENT OF
C     RESTRICTOR AREA OR BACK PRESSURE.  K IS THE VALUE RETURNED
C     BY THE FUNCTION RUNGE.  IT EQUALS 1 WHEN THE DERIVATIVES
C     ARE TO BE CALCULATED AND 0 WHEN INTEGRATION ACROSS ONE STEP
C     IS COMPLETED.
C
      INTEGER RUNGE
      REAL KA,KXKV,KF,MASS
      DIMENSION F(4),Y(4)
      DIMENSION XARRAY(20000),YARRAY(20000)
      OPEN (FILE='CALCOMP',STATUS='OLD',UNIT=20)
C
C   READ AND PRINT OUT THE INPUT DATA
C
      READ (18,10) PS,PR,AO,VINPUT
   10 FORMAT (8E10.4)
      READ (18,20) V1,V2,CL,CF,CD,BETA,RHO,MASS
   20 FORMAT (8E10.4)
      READ (18,30) KA,KF,KXKV,TAUV,AREA,FS,FD
   30 FORMAT (7E10.4)
      READ (18,40) DXMO,M,LOOP
   40 FORMAT (2E10.4,I2)
      READ (18,50) DELAY
   50 FORMAT (F10.4)
C
C   INITIALISATION OF VALUES
C
      T = 0.0
      THETAF = DXMO*KF
      ICOUNT = 0
      M = 0
C
C     Y(1)= SERVOVALVE OPENING
C     Y(2)= PRESSURE P1
C     Y(3)= PRESSURE P2
C     Y(4)= OUTPUT VELOCITY
C
      Y(1) = 0.0
      Y(2) = 0.0
      Y(3) = 0.0
      Y(4) = 0.0
      WRITE (8,220) T,(Y(I),I=1,3),Q1,Q2,QL,FF,THETAF
      NO = 0
C
C   CALL ON THE FOURTH-ORDER RUNGE-KUTTA FUNCTION
C
  200 M = M+1
      K = RUNGE(4,Y,F,T,H,M)
C
C   WHENEVER K=1, COMPUTE DERIVATIVE VALUES FROM THE SYSTEM OF
C   DIFFERENTIAL EQUATIONS FOR BOTH AV BEING GREATER THAN OR
C   LESS THAN ZERO.  THE STATEMENT 205 GIVES THE ALTERNATIVE
C   EQUATION FOR AV<0.
C
      IF (M .EQ. 5) M = 0
      IF (K .NE. 1) GOTO 210
C
C     MODEL OF THE INPUT
C
```

```
      W = SIN(7.854*T)
      IF (W .GE. 0.0) VINS = VINPUT
      IF (W .LT. 0.0) VINS = -VINPUT
C
C     MODEL OF THE SERVOVALVE CONTROLLER
C
      DELTAI = KA*(VINS-KF*Y(4))
C
C     MODEL OF THE NEW SERVOVALVE
C
      F(1) = (KXKV*DELTAI-Y(1))/TAUV
      Y1 = Y(1)
      IF (T .LT. 0.4+DELAY  .OR.  (T .GE. 0.8+DELAY  .AND.
     #    T .LT. 1.2+DELAY)) THEN
      Y(1) = ABS(Y(1))
      GOTO 203
      ENDIF
      IF (Y(1) .EQ. 0.0) GOTO 202
      IF ((T .GE. 0.4+DELAY  .AND.  T .LT. 0.8+DELAY)  .OR.
     #    T .GE. 1.2+DELAY) THEN
      Y(1) = -ABS(Y(1))
      GOTO 201
      ENDIF
  201 IF (Y(2) .LE. PR) THEN
      Q1 = 0.0
      ELSE
      Q1 = -CD*AO*SQRT(2.0*(Y(2)-PR)/RHO)
      ENDIF
      Q2 = CD*Y(1)*SQRT(2.0*(PS-Y(3))/RHO)
      GOTO 204
  202 Q1 = 0.0
      Q2 = 0.0
      GOTO 204
  203 Q1 = CD*Y(1)*SQRT(2.0*(PS-Y(2))/RHO)
      IF (Y(3) .LE. PR) THEN
      Q2 = 0.0
      ELSE
      Q2 = CD*AO*SQRT(2.0*(Y(3)-PR)/RHO)
      ENDIF
  204 CONTINUE
C
C     MODEL OF THE CONDUITS
C
      F(2) = BETA/V1*(Q1-AREA*Y(4)-CL*(Y(2)-Y(3)))
      F(3) = BETA/V2*(-Q2+AREA*Y(4)+CL*(Y(2)-Y(3)))
C
C     MODEL OF THE ACTUATOR
C
      QL = CL*(Y(2)-Y(3))
C
C     MODEL OF THE COLOUMB FRICTION IN THE ACTUATOR
C
      IF (Y(4) .EQ. 0.0) GOTO 207
      GOTO 208
  207 FRICT =0.0
  208 FSUM = (Y(2)-Y(3))*AREA
      IF (ABS(FSUM) .LT. FS  .AND.  ABS(Y(4)) .LE. 0.0001)
     #   FF = FSUM
      IF (FSUM .EQ. 0.0) THEN
      FF = 0.0
      GOTO 209
      ENDIF
      IF (ABS(FSUM) .GE. FS  .AND.  ABS(Y(4)) .LE. 0.0001)
     #   FF = FS*FSUM/ABS(FSUM)
  209 IF (ABS(Y(4)) .GT. 0.0001) FF = FD*Y(4)/ABS(Y(4))
```

```
      F(4) = (FSUM-FF)/MASS
      GOTO 200
C
C   FOR T GREATER THAN 0.1, PRINT OUT THE RESULT FOR EVERY 5
C   INTEGRATION TIMESTEPS
C
  210 ICOUNT = ICOUNT+1
      IF (ICOUNT .LT. 4) GOTO 200
C
C   PRINT THE RESULTS
C
      THETAF = Y(4)*KF
      IF (T .GT. TMAX) GOTO 300
      WRITE (8,230) T,Y1,(Y(I),I=2,3),Q1,Q2,QL,FF,THETAF
  230 FORMAT (1X,F6.4,5X,8(E10.4,3X))
      ICOUNT = 0
      TIM = T-0.8
      IF (TIM .GE. 0.0) THEN
      NO = NO + 1
      XARRAY(NO) = TIM
      YARRAY(NO) = THETAF
      ENDIF
C
C   PASS THE PROGRAM TO THE SECOND PART IF THE TIME VARIABLE EXCEEDS
C   THE TIME RANGE
C
      IF (T .LT. TMAX-0.00001) GOTO 200
C
C   CALL THE GRAPH PLOTTING LIBRARY SUBROUTINES TO PLOT THE GRAPH
C   OF THE CONVENTIONAL CONFIGURATION
C
  300 CALL PLOTS(0,0,20)
      CALL PLOT(0.0,0.0,-3)
      CALL SCALE(XARRAY,34.0,NO,1)
      CALL SCALE(YARRAY,14.0,NO,1)
        XARRAY(NO+2)=0.024
        YARRAY(NO+2)=0.190
        YARRAY(NO+1)=-1.125
      CALL AXIS(0.0,0.0,1H ,-1,34.0,0.0,
     $          XARRAY(NO+1),XARRAY(NO+2))
      CALL AXIS(0.0,0.0,1H ,1,14.0,90.0,
     $          YARRAY(NO+1),YARRAY(NO+2))
      CALL LINE(XARRAY,YARRAY,NO,1,0,0)
C      CALL PLOT(13.0,2.0,3)
C      CALL PLOT(14.0,2.0,2)
C      CALL SYMBOL(14.5,1.7,0.6,11HNEW CONFIG.,0.0,11)
      CALL PLOT(0.0,0.0,-3)
      CALL PLOT(0.0,0.0,999)
      STOP
      END
C
C   THE FOURTH-ORDER RUNGE-KUNTA FUNCTION
C
      FUNCTION RUNGE (N,Y,F,X,H,M)
C
C   THE FUNCTION RUNGE EMPLOYS THE FOURTH-ORDER RUNGE-KUTTA METHOD
C   WITH KUTTA'S COEFFICIENTS TO INTEGRATE A SYSTEM OF N SIMULTAN-
C   EOUS FIRST ORDER ORDINARY DIFFERENTIAL EQUATIONS F(J)=DY(J)/DX,
C   (J=1,2,...,N), ACROSS ONE STEP OF LENGTH H IN THE INDEPENDENT
C   VARIABLE X, SUBJECT TO INITIAL CONDITIONS Y(J), (J=1,2,...,N).
C   EACH F(J), THE DERIVATIVE OF Y(J), MUST BE COMPUTER FOUR TIMES
C   PER INTEGRATION STEP BY THE CALLING PROGRAM.  THE FUNCTION MUST
C   BE CALLED FIVE TIMES PER STEP (PASS(1)...PASS(5)) SO THAT THE
C   INDEPENDENT VARIABLE VALUE (X) AND THE SOLUTION VALUES
C   (Y(1)...Y(N)) CAN BE UPDATED USING THE RUNGE-KUTTA ALGORITHM.
```

```
C   M IS THE PASS COUNTER.  RUNGE RETURNS AS ITS VALUE 1 TO
C   SIGNAL THAT ALL DERIVATIVES (THE F(J)) BE EVALUATED OR 0 TO
C   SIGNAL THAT THE INTEGRATION PROCESS FOR THE CURRENT STEP IS
C   FINISHED.  SAVEY(J) IS USED TO SAVE THE INITIAL VALUE OF Y(J)
C   AND PHI(J) IS THE INCREMENT FUNCTION FOR THE J(TH) EQUATION.
C   AS WRITTEN, N MAY BE NO LARGER THAN 50.
C
      INTEGER RUNGE
      DIMENSION PHI(50),SAVEY(50),Y(N),F(N)
C
      GOTO (1,2,3,4,5),M
C
C     ..... PASS 1.....
C
    1 RUNGE = 1
      RETURN
C
C     ..... PASS 2 .....
C
    2 DO 22 J = 1,N
      SAVEY(J) = Y(J)
      PHI(J) = F(J)
   22 Y(J) = SAVEY(J) + 0.5*H*F(J)
      X = X + 0.5*H
      RUNGE = 1
      RETURN
C
C     ..... PASS 3 .....
C
    3 DO 33 J = 1,N
      PHI(J) = PHI(J) + 2.0*F(J)
   33 Y(J) = SAVEY(J) + 0.5*H*F(J)
      RUNGE = 1
      RETURN
C
C     ..... PASS 4 .....
C
    4 DO 44 J = 1,N
      PHI(J) = PHI(J) + 2.0*F(J)
   44 Y(J) = SAVEY(J) + H*F(J)
      X = X + 0.5*H
      RUNGE = 1
      RETURN
C
C     ..... PASS 5 .....
C
    5 DO 55 J = 1,N
   55 Y(J) = SAVEY(J) + (PHI(J) + F(J))*H/6.0
      M = 0
      RUNGE = 0
      RETURN
      END
```

Parameter Values

P_s = 1000 psi

P_r = 100 psi

A_0 = 0.032 in^2

V_i = 2.1 V

V_1 = 26 in^3

V_2 = 19.5 in^3

C_l = $6.31*10^{-5}$

C_d = 0.6

β = $11.6295*10^4$

ρ = 0.03 lb/in^3

M = 820 slugs

K_a = 7.09 mA/V

K_f = 0.23 V/in/sec

τ_v = 0.004 sec

A = 0.98 in^2

F_s = 101 lbf

F_d = 39.1 lbf

t_d = 0.008 sec

APPENDIX D

APPENDIX D

In this appendix, the specifications of the components used in the test set up are included.

-SERVOVALVE

Model	Moog 73-207
Rated current	± 15 mA
Linearity	within ± 5%
Internal leakage	< 0.17 gpm
Coil resistance	200 Ω single coils

Figs. D.1a and D.1b respectively show the frequency and time response of the servovalve.

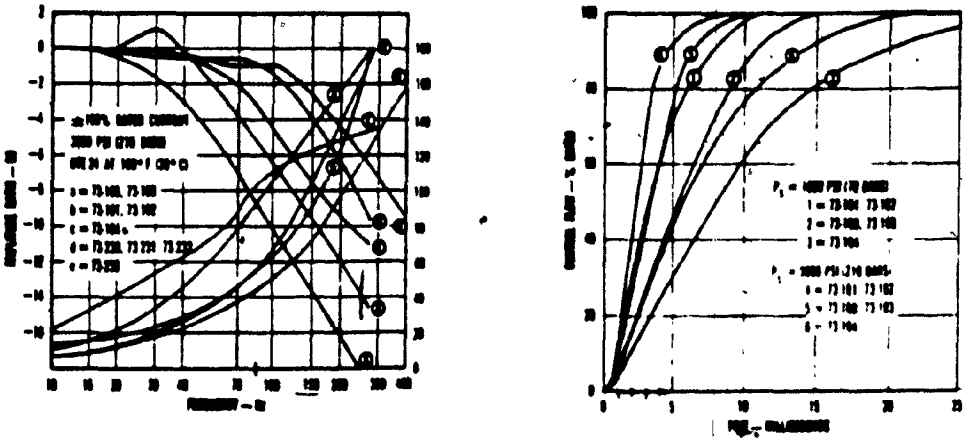

(a) Frequency Response (b) Time Response

Fig. D.1. Frequency and Time Response of 73-207 Servovalve (same as 73-101)

-ACTUATOR

Model	Cowan Dynamics, MCE 845
Rated pressure	3000 psi
Stroke	5 in
Bore size	1.5 in
Rod size	1.0 in, double ended
Cushioning	not present

-NEEDLE VALVE

Model	Whitey 1RF4
Rated pressure	3000 psi
Orifice size	0.25 in (C_V=0.73)

-DIRECTION CONTROL VALVE

Model	Parker Hennifin, D1VW1
Rated pressure	3000 psi
Nominal flow	7 gpm
Type	4 way, 3 position, spring centered, center blocked.
Solenoid	AC 120 V, double

-RELIEF VALVE

Model	Parker Hennifin RP400SM
Rated pressure	3000 psi
Rated flow	6 gpm
Pressure settings	50 to 1000 psi
Type	pilot operated

-VELOCITY TRANSDUCER

Model	Robinson Halpern 240A-4000
Stroke	6 in
Type	moving magnet

-HIGH PRESSURE FILTER

Model	Moog HP 010 A
Rated pressure	3000 psi
Burst pressure	15,000 psi
Element	071-60300, 3 microns

-HYDRAULIC OIL

Make	Shell Tellus 32
Density	860 kg/m^3 (at 15°C)
Viscosity	29.5 mm^2/sec (at 40°C)
Bulk modulus	$2.046*10^8$ N/m^2 (with no air content)